BMR
COMPACTUS

REPORT 178
(PNG 8)

Some Earthquake Focal Mechanisms in the New Guinea/Solomon Islands Region, 1963 - 1968

I. D. RIPPER

BUREAU OF MINERAL RESOURCES
LIBRARY
COPY 3
CANBERRA, A.C.T.

BMR
S55(94)
REP.6
copy3

BMR PUBLICATIONS COMPACTUS
(LENDING SECTION)

DEPARTMENT OF MINERALS AND ENERGY

BUREAU OF MINERAL RESOURCES, GEOLOGY AND GEOPHYSICS

REPORT 178

(PNG 8)

Some Earthquake Focal Mechanisms in the New Guinea/Solomon Islands Region, 1963 - 1968

I. D. RIPPER

AUSTRALIAN GOVERNMENT PUBLISHING SERVICE

CANBERRA 1975

DEPARTMENT OF MINERALS AND ENERGY

MINISTER: THE HON. R.F.X. CONNOR, M.P.

SECRETARY: SIR LENOX HEWITT, O.B.E.

BUREAU OF MINERAL RESOURCES, GEOLOGY AND GEOPHYSICS

ACTING DIRECTOR: L.C. NOAKES

ASSISTANT DIRECTOR, GEOPHYSICAL BRANCH: N.G. CHAMBERLAIN

Published for the Bureau of Mineral Resources, Geology and Geophysics by the Australian Government Publishing Service.

ISBN 0 642 012555

MANUSCRIPT RECEIVED: OCTOBER 1973

REVISED MANUSCRIPT RECEIVED: JULY 1974

ISSUED: AUGUST 1975

Printed in Australia by The Courier-Mail Printing Service, Campbell Street, Bowen Hills, Brisbane

CONTENTS

TABLES

PLATES

FIGURES

SUMMARY

Focal mechanism stereographic projections were plotted for 59 earthquakes that occurred in the New Guinea/Solomon Islands region in the period 1963 to 1968. Graphical solutions have been obtained for 48 of the earthquakes; 33 of these are reasonably good.

The data used were P-wave first arrivals, recorded mainly on the Worldwide Standard Seismograph Network.

Dip-slip overthrust, dip-slip normal, dip-slip with one vertical and one horizontal nodal plane, and strike-slip solutions were defined. Eastern New Guinea appears to be very complex seismically, with the first, third, and fourth earthquake-types occurring. The Bismarck Sea seismic lineation is shown to be a sinistral shear. New Britain, Bougainville, and the north Solomon Sea experience earthquakes with dip-slip overthrust solutions, but a strike-slip solution has also been determined for a north Solomon Sea earthquake.

INTRODUCTION

The seismic zone between the Pacific Plate and the Australian Plate in the New Guinea region is both broad and complex (Denham, 1969). The New Guinea earthquake focal mechanism study reported here was undertaken to assist in the understanding of the seismicity and tectonics of the region enclosed by latitudes 0° and 12°S, and longitudes 130° and 163°E. Localities mentioned in the text are shown in Plate 1.

Before the installation in 1962 of the Worldwide Standard Seismograph Network (WWSSN) stations at Port Moresby (PMG), Rabaul (RAB), and Honiara (HNR), the majority of the focal mechanism solutions computed for New Guinea earthquakes were by Ritsema (e.g. 1957). Ritsema was limited by poor station coverage of the region, and to supplement his data he made extensive use of reflected phases, such as PP. Hodgson & Stevens (1964) found this method unreliable for earthquakes in other regions of the world, but conceded that they had not shown Ritsema's solutions to be unreliable.

Wickens & Hodgson (1967) recomputed all published pre-1962 earthquake focal mechanism solutions for which the data were available; reflected phases were omitted. The New Guinea earthquake hypocentres and origin times are listed in Table 1, and the solutions in Table 2. Of 39 recomputed solutions, 13 were reasonable and involve strike-slip motion. The lack of dip-slip solutions does not indicate that some solutions are wrong or that no earthquakes with such solutions occurred, but, rather, demonstrates that dip-slip solutions cannot be obtained with an inadequate local and regional network of seismograph stations; the determination of at least one of the nodal planes requires several close stations.

More recently, Isacks & Molnar (1971) included the New Guinea region in a study of deep and intermediate-depth earthquakes. The New Guinea earthquakes they examined are listed in Table 3, and the focal mechanism solutions in Table 4.

Johnson & Molnar (1972) also investigated New Guinea earthquake focal mechanisms. Their hypocentres are listed in Table 5, and their solutions in Table 6. Solutions obtained in this Report and by either Isacks & Molnar or Johnson & Molnar are generally similar. One exception is the solution for an earthquake near Wewak on 8 September 1968, which Johnson & Molnar give as strike-slip but which is reported here as dip-slip.

The earthquakes used in this study occurred in the period 1963-1968. In all, 59 earthquakes were examined and 48 graphical solutions were obtained (Figures 2 to 49, and Plates 2 to 4).

TECHNIQUE

Initially, station data were obtained by questionnaire, but this method was found to be unreliable and it was replaced by direct examination of original seismograms or seismogram copies. Copies of 35-mm films of WWSSN seismograms were acquired from the World Data Centre, and these were supplemented by requests for seismograms from non-standard stations.

A focal mechanism solution is obtained from the seismograph station data as follows:

1. The azimuth and epicentral distance of each station from the epicentre are computed.
2. The angle of incidence — that is, the angle between the vertical and the seismic ray as it leaves the earthquake focus — is determined using either the graphs of Bessonova et al. (1960) or the tables of Hodgson & Storey (1953), which relate angle of incidence to epicentral distance. The direction of a P ray as it leaves the focus is thus defined by its azimuth and angle of incidence. If the rays are assumed to travel in straight lines until they pass through a hypothetical sphere (called the focal sphere) centred on the focus, the ray directions can be represented by positions on the sphere. The sphere is, in turn, represented by a Wulff stereographic projection on which points are defined by their azimuth and angle from the vertical.
3. Seismograph station positions are thus represented on the focal sphere by the points at which the seismic rays to the stations pass through the sphere. The standard station codes (Appendix) are used to identify the stations. Different symbols indicate the P-wave polarities, either compression or dilatation, recorded at each seismograph station.
4. Zones of P-wave compression and dilatation on the focal sphere are then separated by two orthogonal planes, which pass through the focus and are represented on the stereographic projection by two arcs. Orthogonality is enforced by ensuring that each arc passes through the pole of the other. The quadrants are alternately compression and dilatation and the planes are called nodal planes.
5. Each nodal plane is defined by the azimuth of its dip direction and the angle of dip, or by the azimuth and plunge of its pole.
6. The lines bisecting the angle between the poles of the orthogonal nodal planes, drawn in the third orthogonal plane, are called the compressional (P) and tensional (T) stress axes of the focal mechanism solution and fall in the P-wave dilatational and compressional quadrants respectively. Each stress axis is defined by the azimuth of its plunge direction and the plunge measured from the horizontal.

The division of the P-wave polarity field into four quadrants by orthogonal nodal planes is widely accepted. Ritsema (1967) conducted a survey of 63 non-orthogonal earthquake solutions in the literature, and obtained an orthogonal solution for every earthquake except one. He suggested that the effect of near-focal crustal inhomogeneities caused the exception. Sykes (1968) stated that he did not know of any earthquake for which the orthogonal P-wave solution was not a reasonable approximation of the observations.

The terminology, 'compressional' and 'tensional' stress axes of the focal mechanism solution, allows these axes to be distinguished from the maximum and minimum principal stresses of the tectonic stress field. McKenzie (1969) notes that if the medium in which the earthquake occurs is already faulted the tectonic stress axes need not coincide with the solution axes, but may fall anywhere within the respective P-wave polarity quadrant, and may differ by up to 90°.

One of the main difficulties in obtaining good focal mechanism solutions is the uneven seismograph station coverage of the focal sphere. For a normal-depth earthquake, the epicentral distance range of 0-22° corresponds to 85 percent of the focal sphere, and 0-90°, 97 percent; distant seismograph stations provide P-wave information for only 3 percent of the focal sphere. Unless there are many stations within about 20° of the epicentre, the coverage of the focal sphere will be limited, and, although an orthogonal nodal plane solution may be obtained, other types of solutions may be possible.

The Wulff projections of the focal mechanism solutions are shown in Figures 2 to 49. The hypocentres of the earthquakes for which solutions have been obtained are listed in Table 7; the station polarities in Table 8; the solutions in Table 9; and the hypocentres of the earthquakes which were examined but which were rejected with no solutions are listed in Table 10. Failure to obtain solutions applied mainly to earthquakes with weak P-wave arrivals and consequently with few station polarities, inconsistent results, and poor coverage of the focal sphere.

A measure of the uncertainty of each solution is provided by the solid angle of uncertainty of the axis of intersection of the orthogonal nodal planes (the B axis). This solid angle is obtained by tracing all possible positions of the ends of the B axis on the focal sphere. The areas thus traced out are shown on the relevant Figures, and the dimensions of the solid angle are given in Table 9 for all earthquakes except those for which an orthogonal solution was not obtained.

A non-orthogonal solution normally does not imply that an orthogonal solution is impossible. Non-orthogonal solutions are generally caused by one or more anomalous readings close to a nodal plane, and these can usually be accounted for by uncertainty in crustal or upper mantle structure at the earthquake focus or along the P-wave path. Hence a non-orthogonal solution usually implies a tight solution.

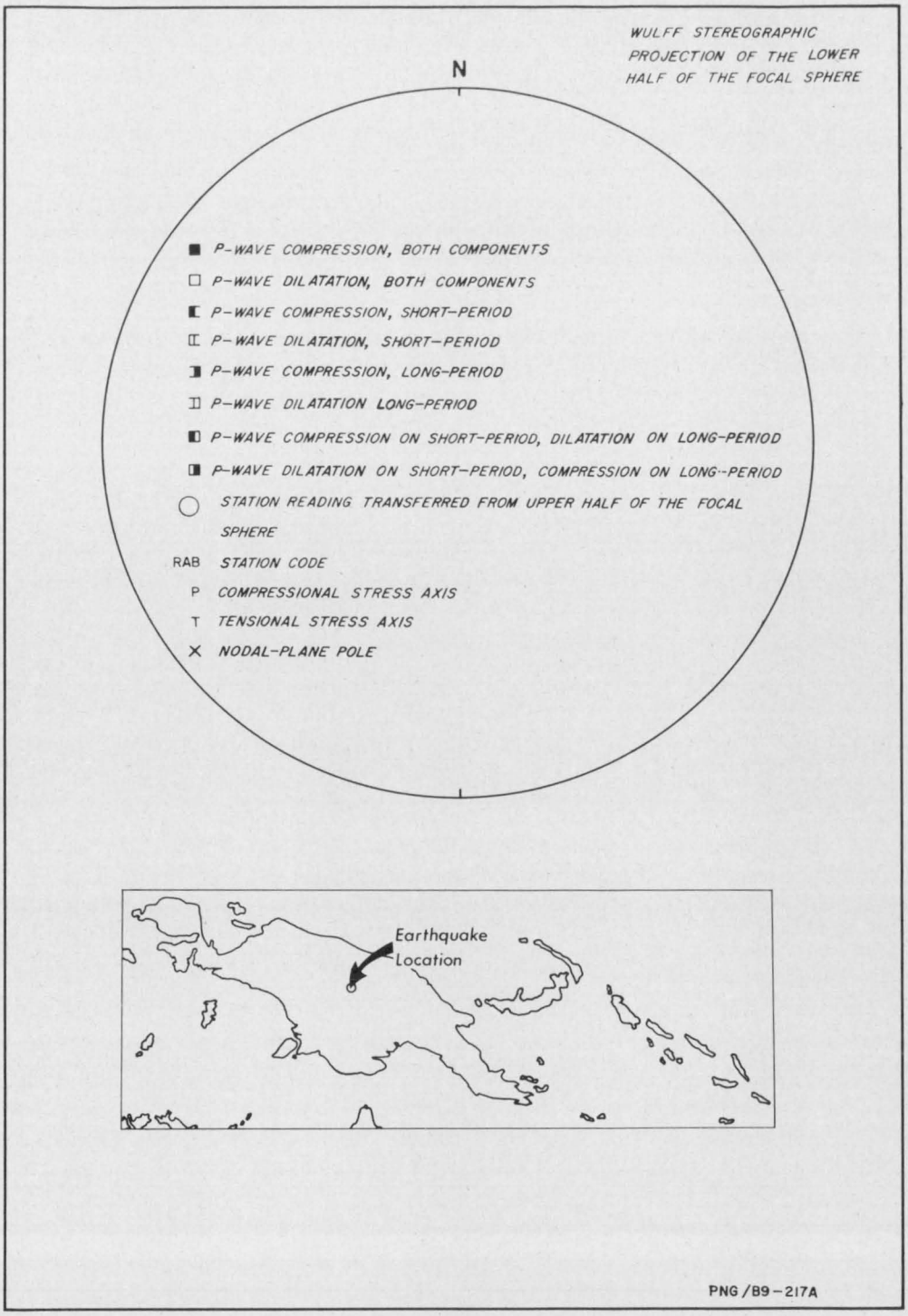

FIGURE 1
Symbols used in Figures 2 to 49

THE SOLUTIONS

The solutions are presented in chronological order, one per page, with the Wulff projection of each solution opposite each description (Figs. 2-49). Figure 1, opposite this page, explains the symbols, except for the B-axis uncertainty, which has been discussed under 'Technique'.

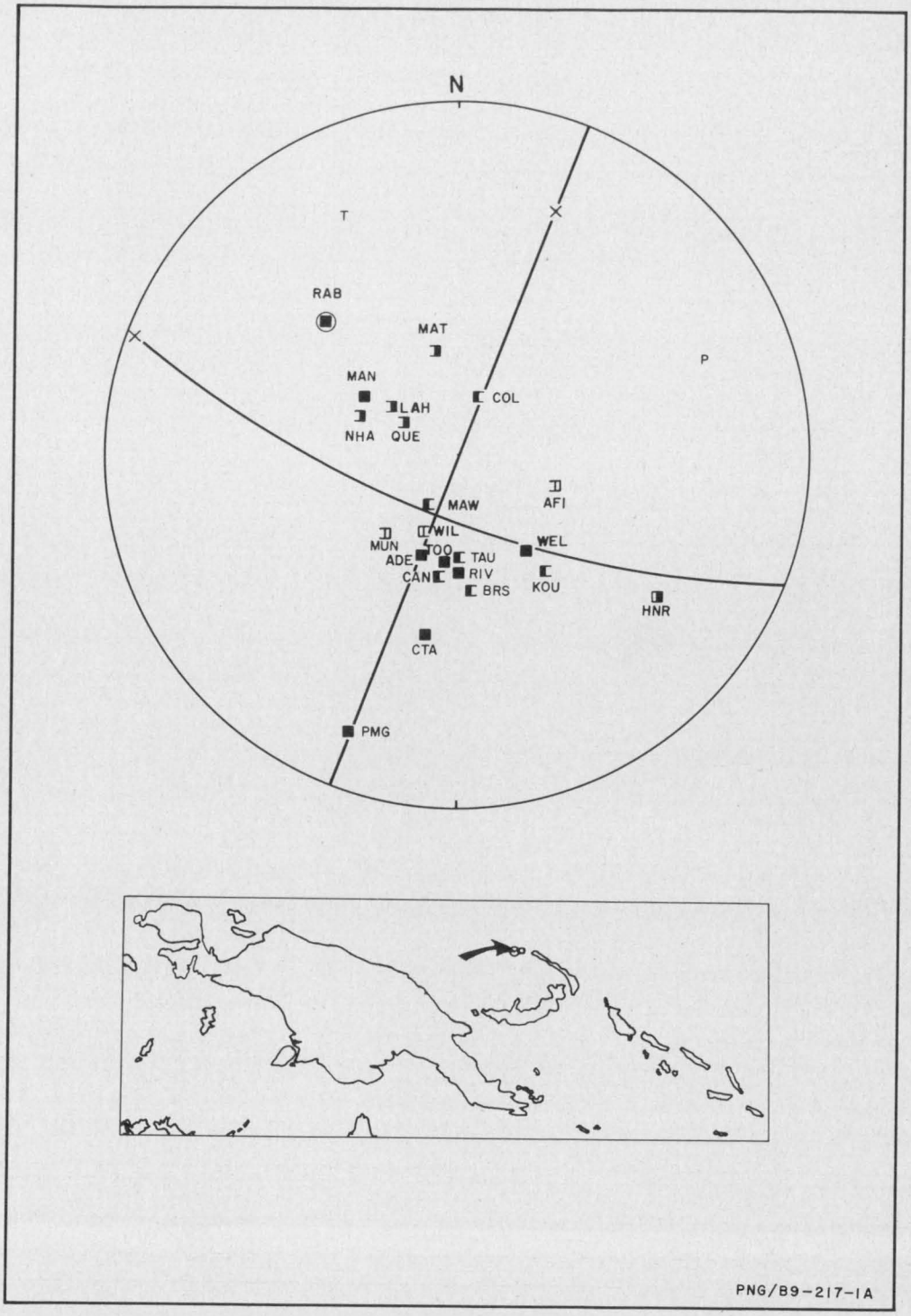
N
T
P
RAB
MAT
MAN
LAH
COL
NHA
QUE
MAW
AFI
WIL
MUN
TOO
WEL
ADE
TAU
CAN
RIV
BRS
KOU
HNR
CTA
PMG
PNG/B9-217-1A

FIGURE 2

Number	: 1			
Location	: 2.8°S, 149.8°E; New Hanover, northwest of New Ireland			
Origin Time	: 28 January 1963 at 12 12 19.0 Universal Time (UT)			
Depth	: 33 km			
Magnitude (M)	: 6.4			
Type	: Strike-slip			
Nodal Planes	:	Azimuth of Dip	Dip	
	:	112	89	
	:	202	69	
Nodal-Plane Poles	:	Azimuth	Plunge	
	:	292	01	
	:	022	21	
P Axis	:	069	15	
T Axis	:	335	15	
		Azimuth	Plunge	Uncertainty
B Axis	:	201	69	1 x 1

The solution is poor because most P-wave first arrivals were weak and the dilatational quadrants are based on three station readings. However, even if the dilatations are ignored, an orthogonal dip-slip solution is impossible.

If the nodal plane which strikes east-southeast (parallel to New Ireland) is the fault plane, the motion is sinistral. The dip of the plane is 69°, which is in fair agreement with that (84°) determined by Johnson & Molnar (1972) considering that it depends on the weak short-period MAW arrival.

Plotted in Plate 2.

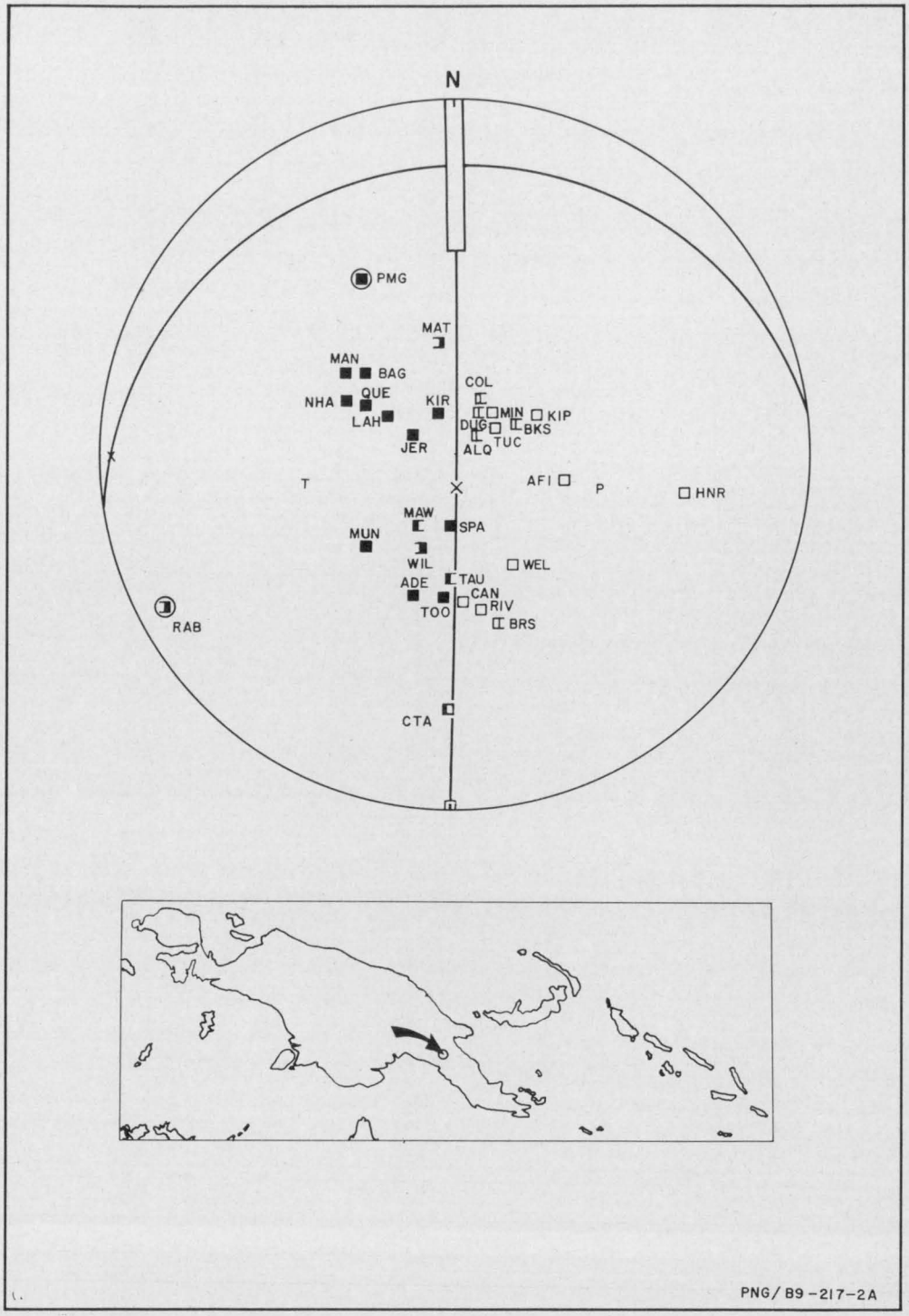
N
PMG
MAT
MAN
BAG
COL
NHA
QUE
KIR
MIN
KIP
LAH
DUG
BKS
JER
ALQ
TUC
T
AFI
P
HNR
MAW
SPA
MUN
WIL
WEL
ADE
TAU
CAN
RIV
TOO
BRS
RAB
CTA
PNG/89-217-2A

FIGURE 3

Number	: 2			
Location	: 7.5°S, 146.2°E; beneath the highlands of New Guinea between Lae and Kerema			
Origin Time	: 26 February 1963 at 20 14 08.7 UT			
Depth	: 171 km			
Magnitude (M)	: 7.2			
Type	: Dip-slip			
Nodal Planes	:	Azimuth of Dip	Dip	
	:	090	88	
	:	348	12	
Nodal-Plane Poles	:	Azimuth	Plunge	
	:	270	02	
	:	168	78	
P Axis	:	100	45	
T Axis	:	260	45	
		Azimuth	Plunge	Uncertainty
B Axis	:	001	12	33 x 1

One nodal plane is well defined as vertical and striking north. The control on the dip of the second nodal plane is poor, as illustrated by the uncertainty of the B axis in the solution.

In terms of movement on a fault plane, the solution could represent either horizontal sliding (top side east) or vertical motion (east side up).

Interpretation in terms of Benioff seismicity in which the tensional stress axis is parallel to the dip of a southward-dipping Benioff zone is difficult, because the tensional stress axis plunges west.

Plotted in Plate 3.

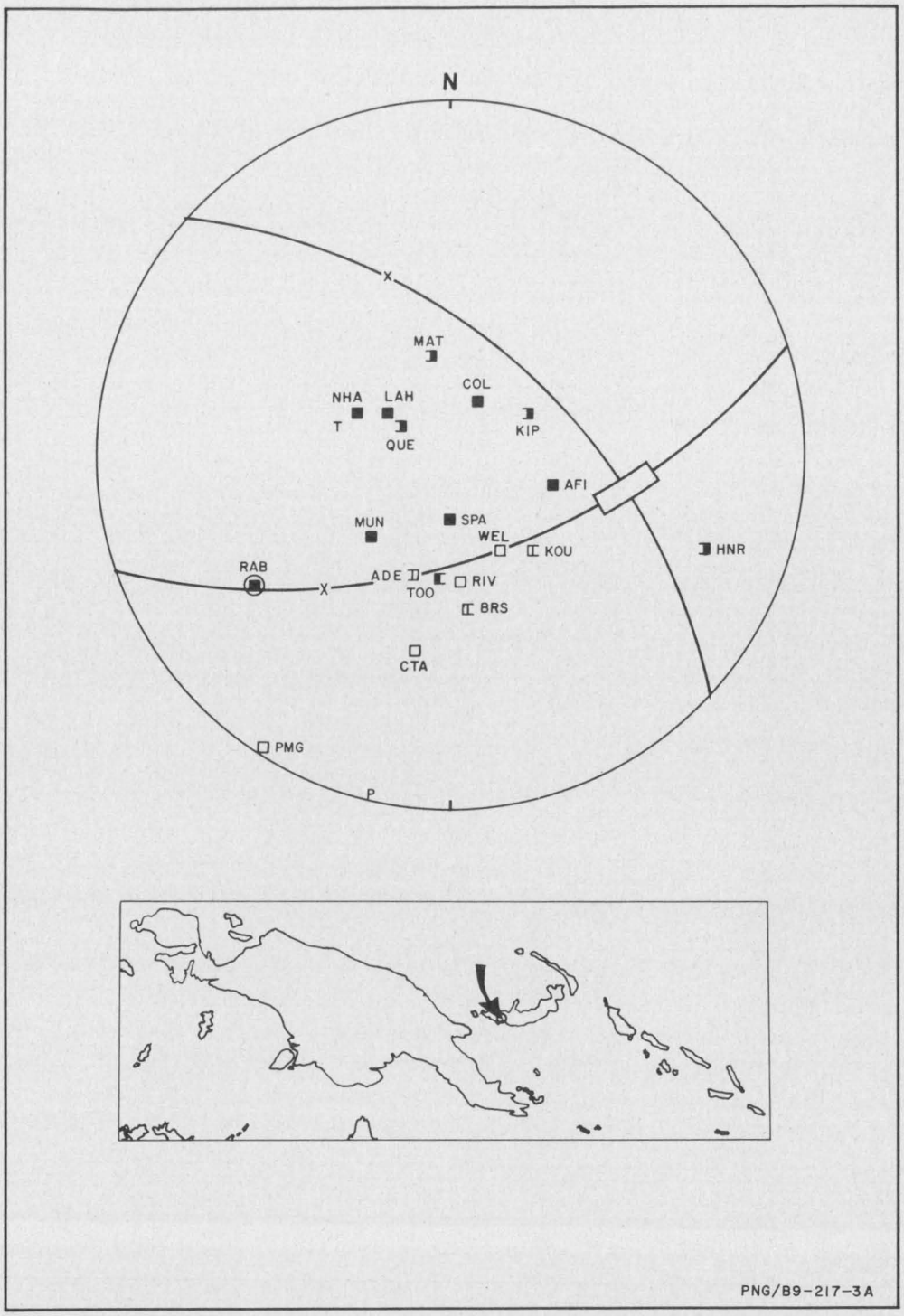
N
X
MAT
COL
NHA
LAH
T
QUE
KIP
AFI
MUN
SPA
WEL
KOU
HNR
RAB
X
ADE
TOO
RIV
BRS
CTA
PMG
P
PNG/89-217-3A

FIGURE 4

Number	: 3			
Location	: 6.0°S, 149.4°E; southwest New Britain			
Origin Time	: 27 February 1963 at 04 30 00.8 UT			
Depth	: 52 km			
Magnitude (M)	: 5.4			
Type	: Dip-slip overthrust			
Nodal Planes	:	Azimuth of Dip	Dip	
	:	162	58	
	:	043	54	
Nodal-Plane Poles	:	Azimuth	Plunge	
	:	342	32	
	:	223	36	
P Axis	:	193	03	
T Axis	:	285	53	
		Azimuth	Plunge	Uncertainty
B Axis	:	101	37	17 x 1

The solution is poor: the orientation of the overthrust depends on the weak HNR P-wave compression, and there are no station readings in the northeast dilatational quadrant.

If the nodal plane dipping northeast is the fault plane, the motion is north-northwest, and consistent with the concept of the Solomon Sea lithosphere underthrusting New Britain. The compressional stress axis is horizontal and oriented south, orthogonal to the New Britain coast.

Plotted in Plate 3.

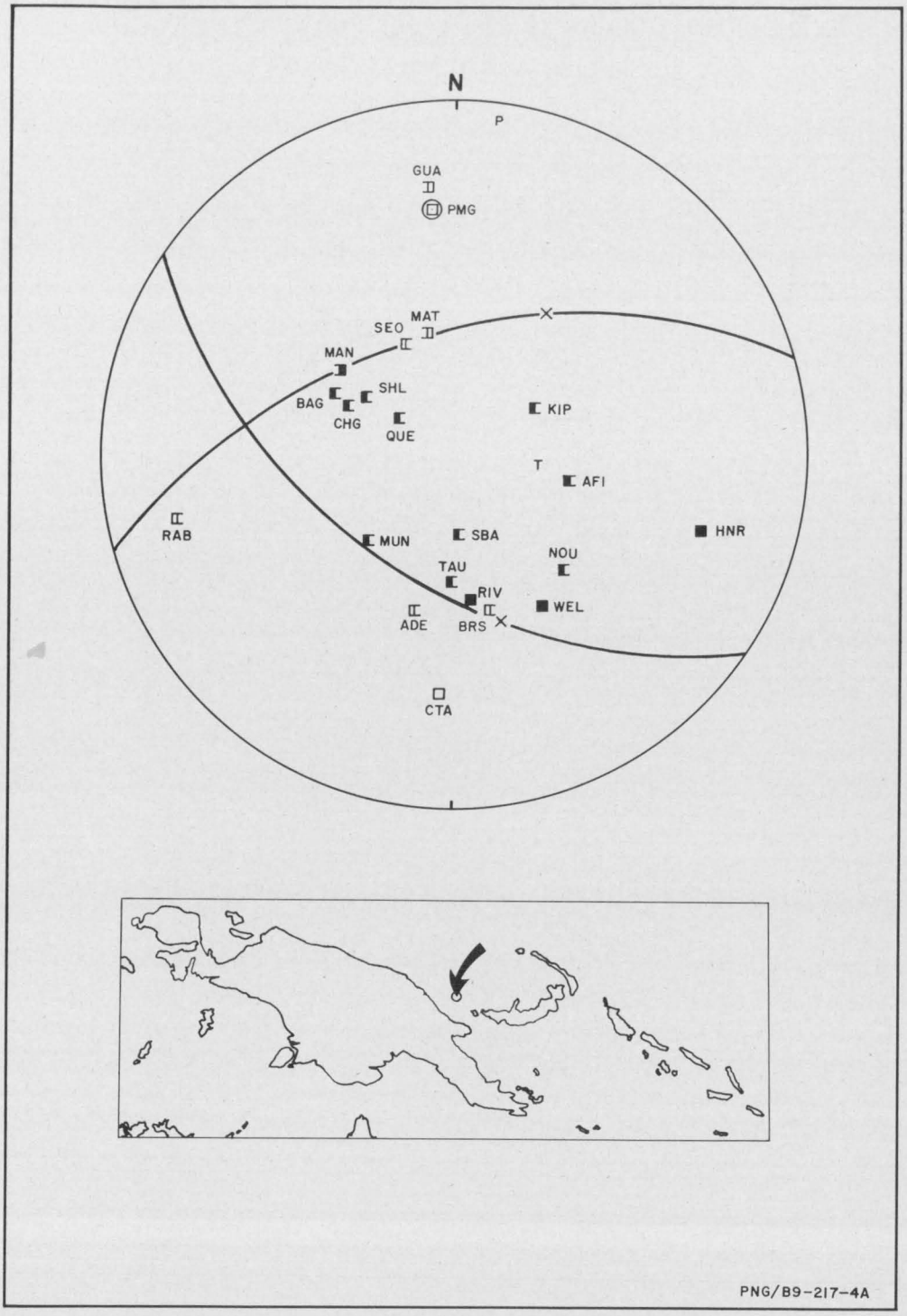
N
P
GUA
PMG
MAT
SEO
MAN
SHL
BAG
CHG
QUE
KIP
T
AFI
RAB
MUN
SBA
HNR
NOU
TAU
RIV
WEL
ADE
BRS
CTA
PNG/89-217-4A

FIGURE 5

Number	: 4			
Location	: 5.4°S, 146.8°E; beneath the Long Island volcano of the South Bismarck Volcanic Arc			
Origin Time	: 12 January 1964 at 11 13 19.4 UT			
Depth	: 227 km			
Magnitude (M)	: 5.7			
Type	: Dip-slip overthrust			
Nodal Planes	:	Azimuth of Dip	Dip	
	:	343	52	
	:	214	51	
Nodal-Plane Poles	:	Azimuth	Plunge	
	:	163	38	
	:	034	39	
P Axis	:	008	01	
T Axis	:	099	62	
		Azimuth	Plunge	Uncertainty
B Axis	:	277	28	1 x 1

Despite the weakness of the P-wave arrivals and the low number of readings used, the solution is tight. It could be interpreted as indicating either a falling lithospheric block (near-vertical tensional stress axis) or compressional contact between the South Bismarck Plate and New Guinea (horizontal compressional stress axis oriented north).

Plotted in Plate 3.

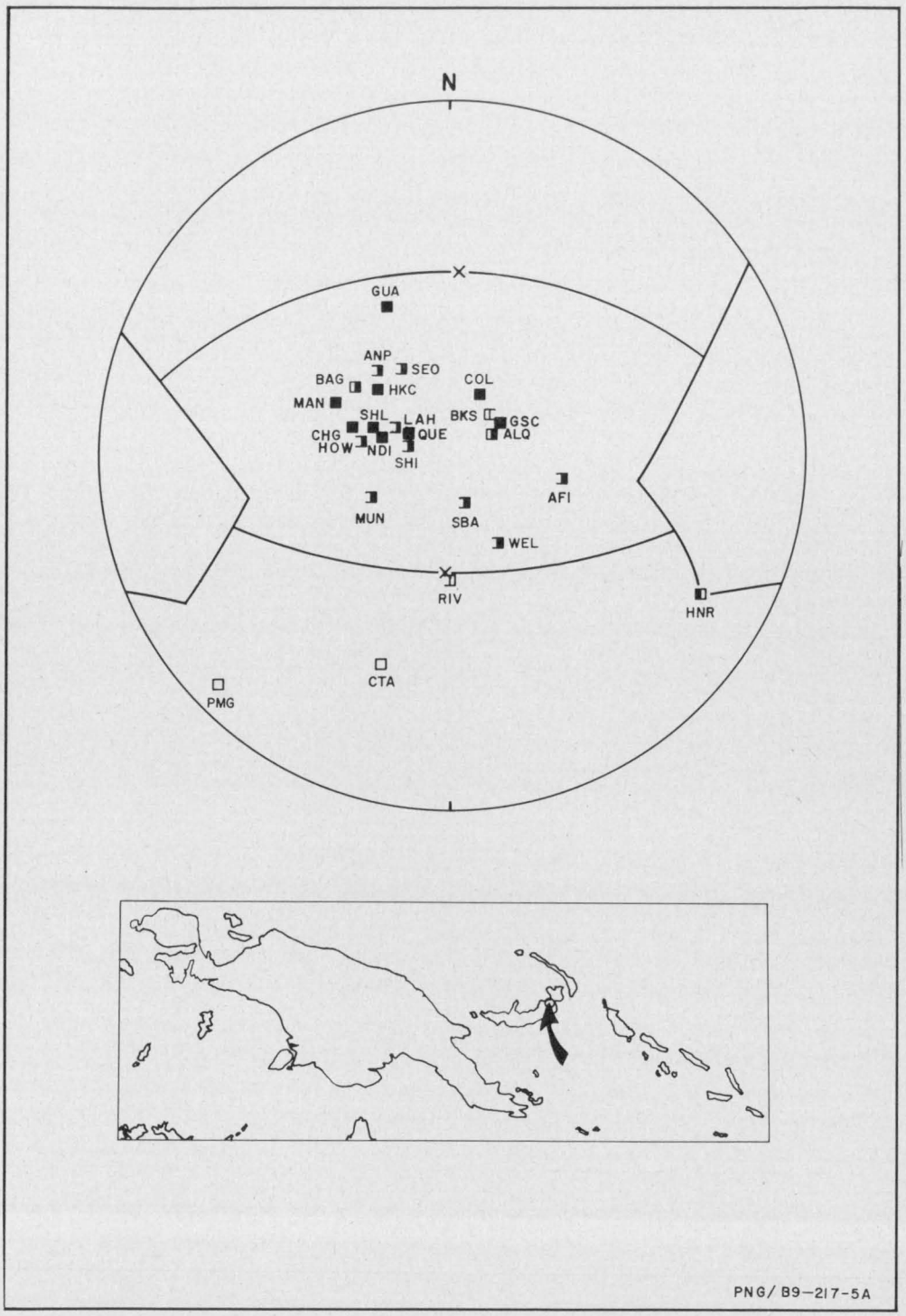
N
GUA
ANP
SEO
BAG
HKC
COL
MAN
SHL
LAH
BKS
GSC
CHG
QUE
ALQ
HOW
NDI
SHI
AFI
MUN
SBA
WEL
RIV
HNR
CTA
PMG
PNG/ 89-217-5A

FIGURE 6

Number	: 5			
Location	: 5.1°S, 151.8°E; Wide Bay, southeast New Britain			
Origin Time	: 14 February 1964 at 16 29 45.3 UT			
Depth	: 58 km			
Magnitude	: 6.1			
Type	: Dip-slip overthrust			
Nodal Planes	:	Azimuth of Dip	Dip	
	:	Too uncertain		
	:			
Nodal-Plane Poles	:	Azimuth	Plunge	
	:			
	:			
P Axis	:			
T Axis	:			
		Azimuth	Plunge	Uncertainty
B Axis	:			

The P-wave arrivals were generally weak, and, although the solution represents an overthrust, the station coverage is insufficient to obtain the orientation, as indicated by the B-axis uncertainty in Figure 6,

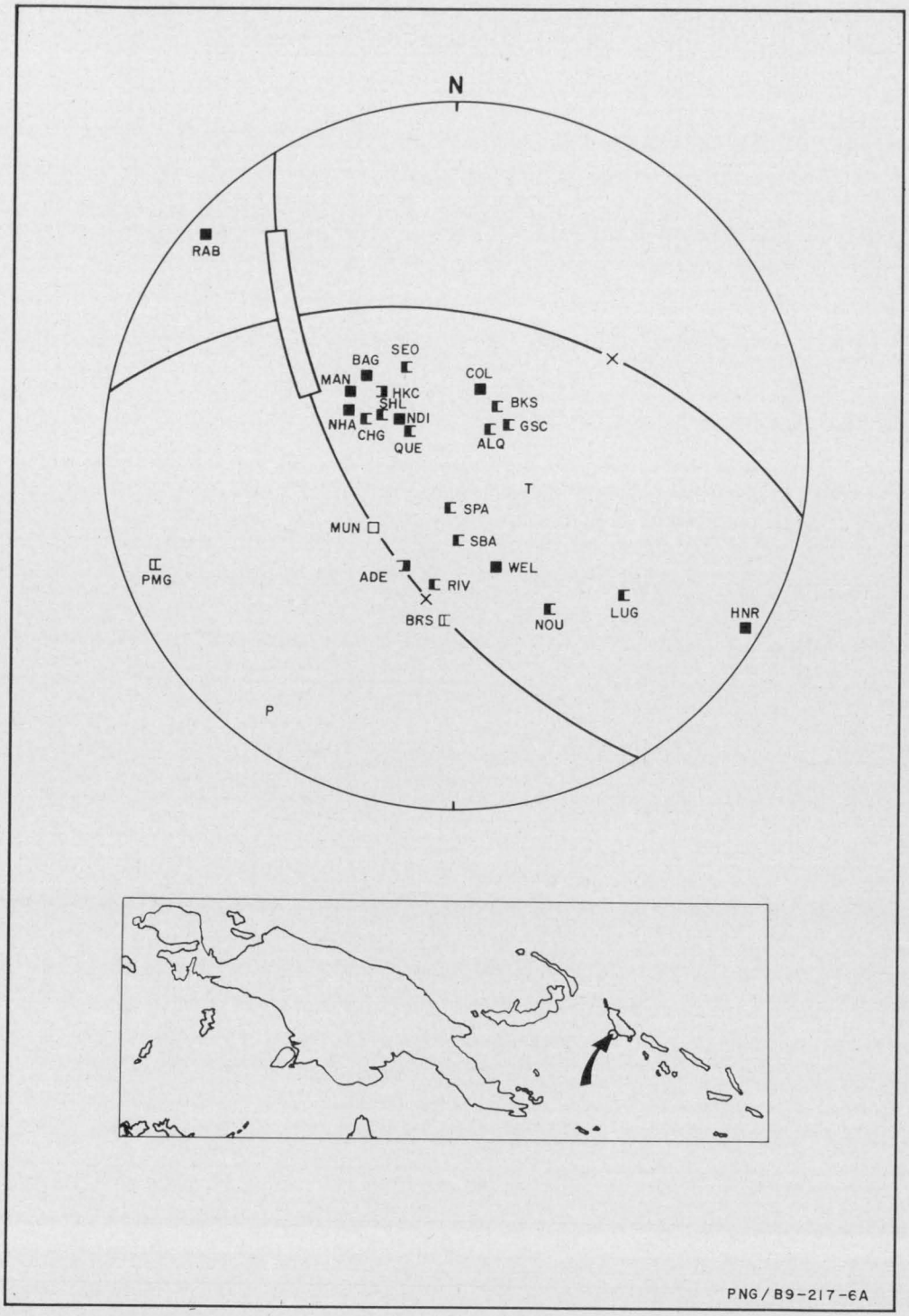
N
RAB
SEO
BAG
MAN
HKC
SHL
NDI
NHA
CHG
QUE
COL
BKS
GSC
ALQ
T
SPA
MUN
SBA
PMG
ADE
WEL
RIV
BRS
NOU
LUG
HNR
P
PNG/B9-217-6A

FIGURE 7

Number	: 6			
Location	: 6.6°S, 155.0°E; Solomon Sea between the Bougainville Trench and southwest Bougainville			
Origin Time	: 17 April 1964 at 05 59 58.9 UT			
Depth	: 74 km			
Magnitude (M)	: 6.0			
Type	: Dip-slip overthrust			
Nodal Planes	:	Azimuth of Dip	Dip	
	:	010	46	
	:	239	56	
Nodal-Plane Poles	:	Azimuth	Plunge	
	:	190	44	
	:	059	34	
P Axis	:	216	07	
T Axis	:	113	64	
		Azimuth	Plunge	Uncertainty
B Axis	:	309	26	39 x 1

One nodal plane of the solution is well defined, but there is no station control over the other, which is restricted by only the orthogonality criterion.

One interpretation of the solution is that the Solomon Sea lithosphere is underthrusting Bougainville. The compressional stress axis is horizontal and oriented southwest, roughly orthogonal to the island.

Plotted in Plate 3.

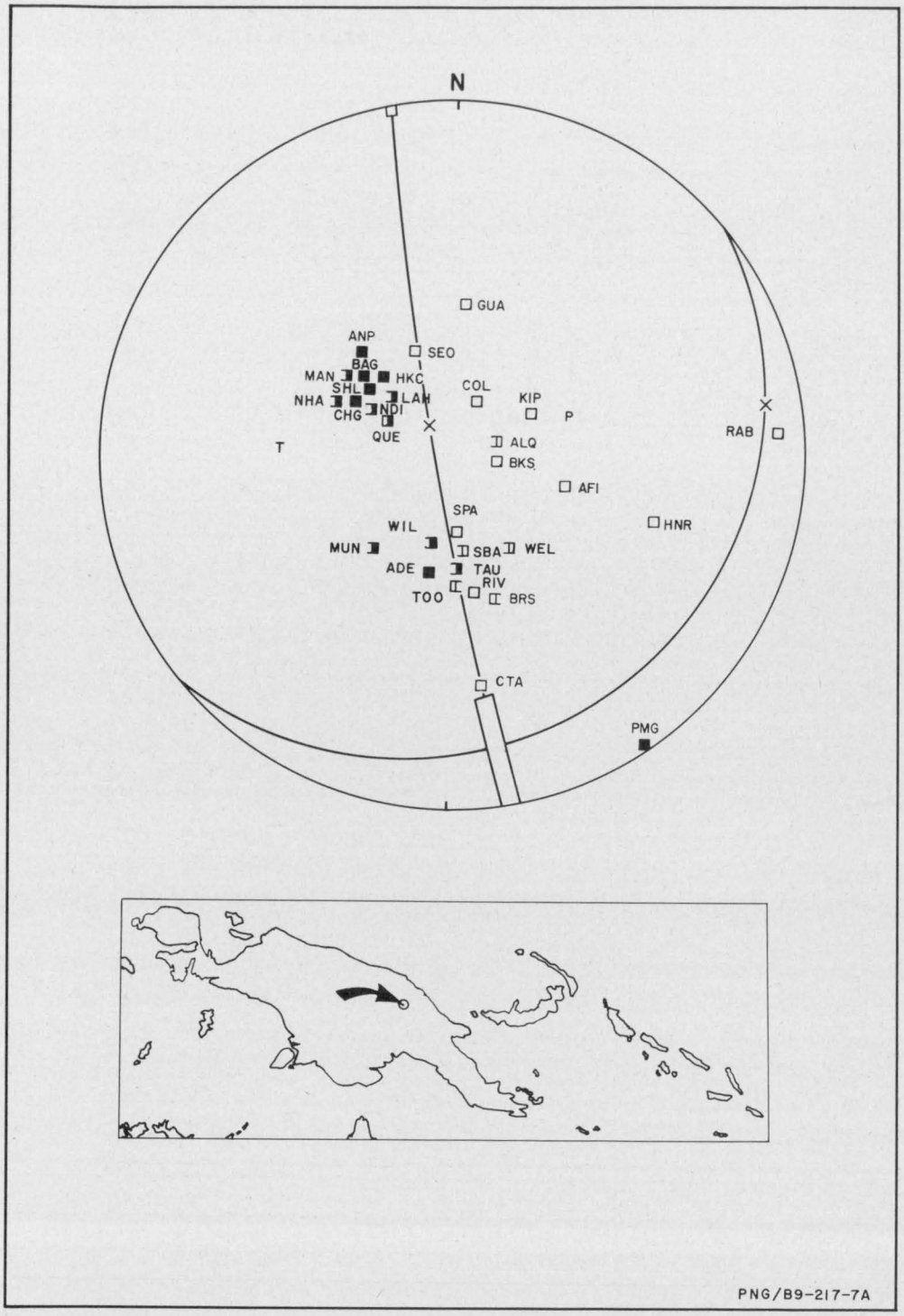
N
GUA
ANP
SEO
BAG
MAN
HKC
SHL
COL
KIP
NHA
LAH
P
CHG
NDI
QUE
RAB
T
ALQ
BKS
AFI
SPA
WIL
HNR
MUN
SBA
WEL
ADE
TAU
RIV
TOO
BRS
CTA
PMG
PNG/B9-217-7A

FIGURE 8

Number	:	7		
Location	:	5.1°S, 144.2°E; northern margin of the New Guinea highlands 170 km west of Madang		
Origin Time	:	24 April 1964 at 05 56 09.8 UT		
Depth	:	99 km		
Magnitude (M)	:	6.8		
Type	:	Dip-slip (non-orthogonal)		
Nodal Planes	:	Azimuth of Dip	Dip	
	:	259	84	
	:	139	13	
Nodal-Plane Poles	:	Azimuth	Plunge	
	:	079	06	
	:	319	77	
P Axis	:	067	50	
T Axis	:	271	38	
		Azimuth	Plunge	Uncertainty
B Axis	:	171	11	—

One nodal plane of the solution is well defined, but there is considerable uncertainty in the orientation of the other.

The station RAB P-wave polarity — a dilatation — cannot be positioned in a dilatational quadrant of an orthogonal solution, and renders the solution non-orthogonal, but the uncertainty in the position of RAB with respect to a nodal plane is sufficient to explain the ambiguity.

Plotted in Plate 3.

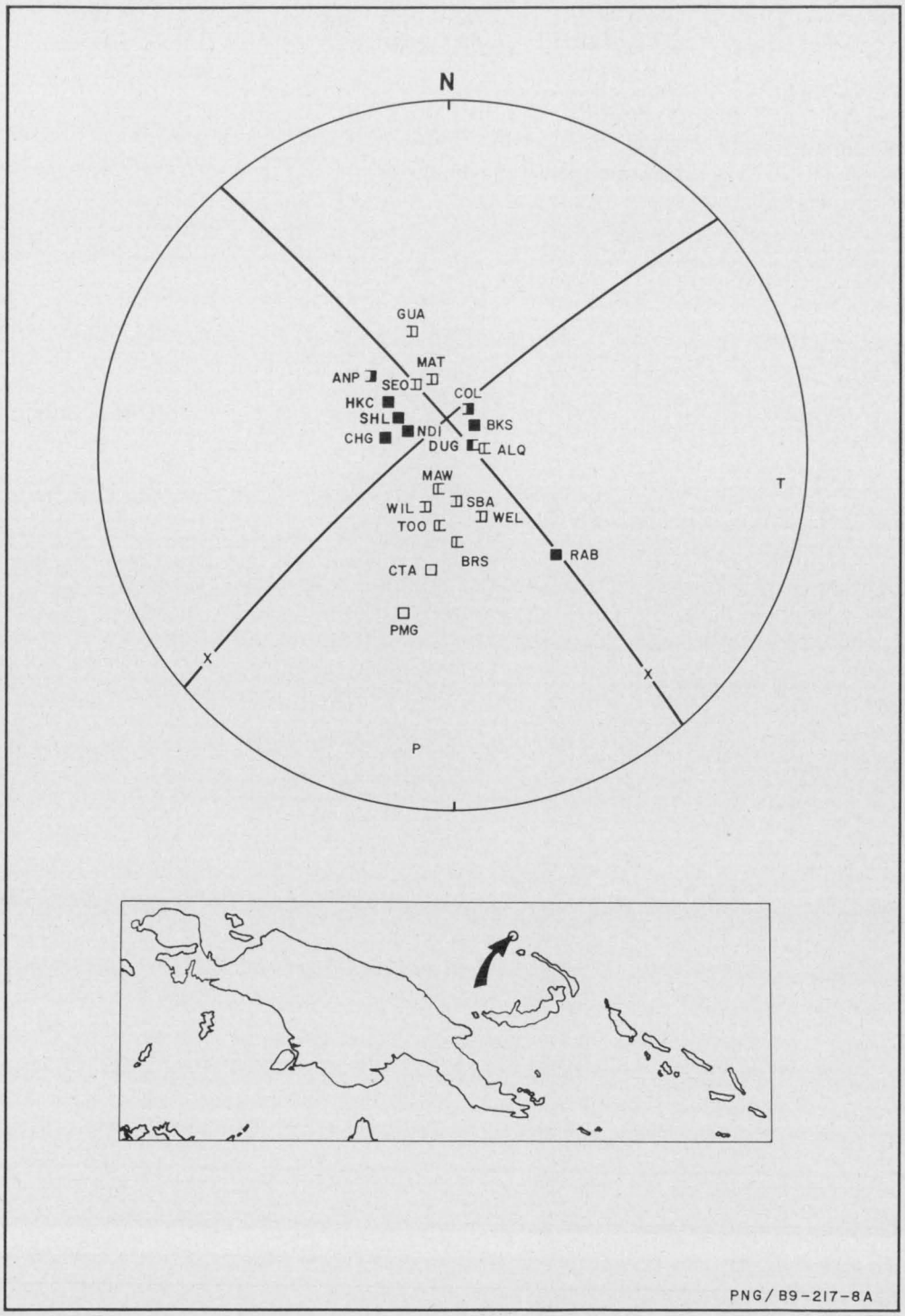
N
GUA
MAT
ANP
SEO
COL
HKC
SHL
BKS
NDI
CHG
DUG
ALQ
MAW
T
WIL
SBA
WEL
TOO
BRS
RAB
CTA
PMG
P
PNG/B9-217-8A

FIGURE 9

Number	: 8			
Location	: 1.8°S, 149.7°E; Mussau Island, 170 km northwest of New Ireland			
Origin Time	: 28 June 1964 at 12 51 35.0 UT			
Depth	: 7 km			
Magnitude (M)	: 6.2			
Type	: Strike-slip (non-orthogonal)			
Nodal Planes	:	Azimuth of Dip	Dip	
	:	319	80	
	:	050	85	
Nodal-Plane Poles	:	Azimuth	Plunge	
	:	139	10	
	:	230	05	
P Axis	:	185	11	
T Axis	:	094	03	
		Azimuth	Plunge	Uncertainty
B Axis	:	349	78	—

Despite the emergent nature of the P-wave arrivals and the small number of stations used in the analysis, the solution is clearly strike-slip.

If the nodal plane which trends northwest is the fault plane, the movement is dextral.

Plotted in Plate 2.

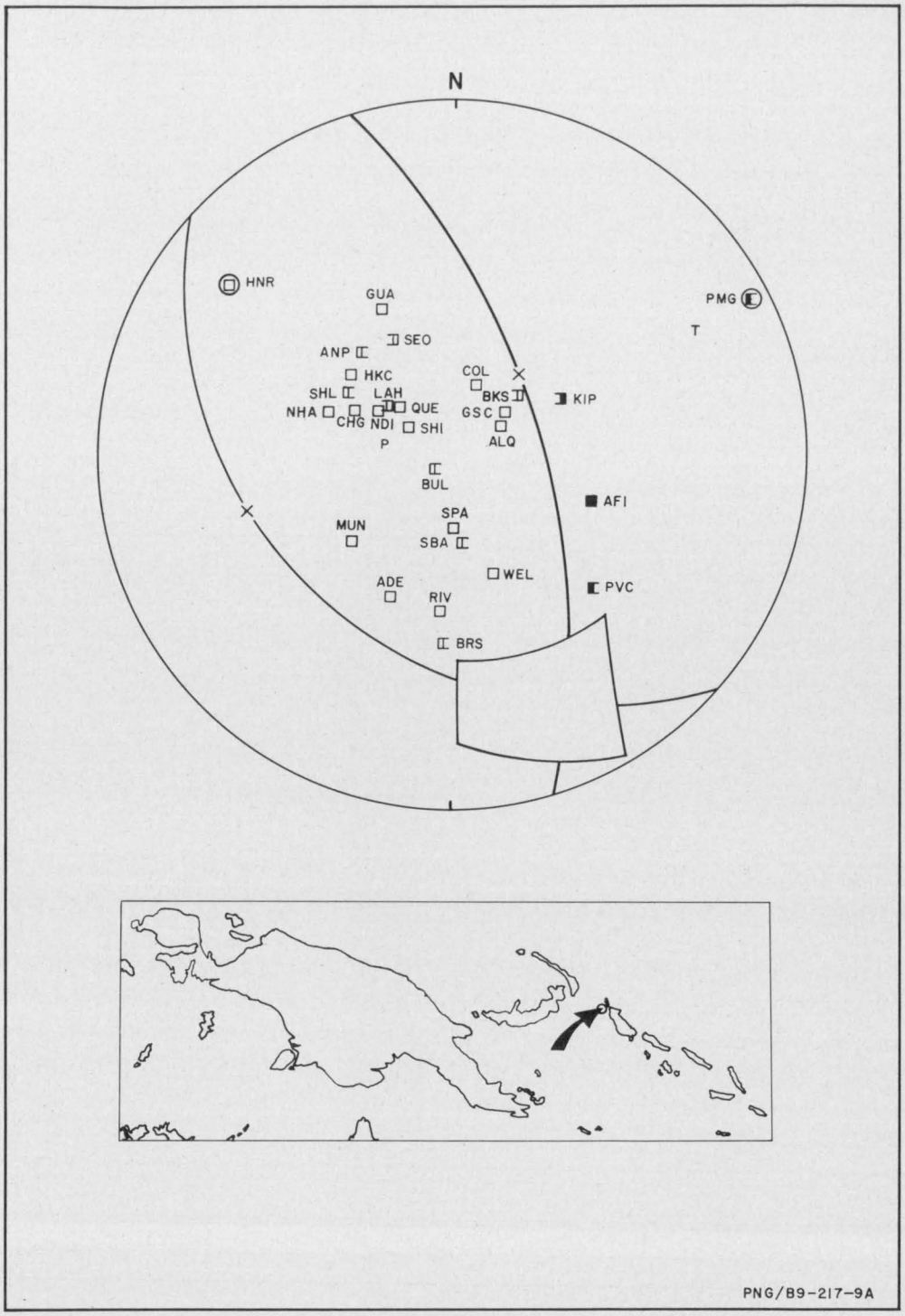
N
HNR
GUA
PMG
T
SEO
ANP
HKC
COL
SHL
LAH
BKS
KIP
NHA
QUE
GSC
CHG
NDI
SHI
ALQ
P
BUL
AFI
SPA
MUN
SBA
WEL
ADE
PVC
RIV
BRS
PNG/B9-217-9A

FIGURE 10

Number	: 9			
Location	: 5.5°S, 154.3°E; Solomon Sea between the northern tip of Bougainville and the Bougainville Trench			
Origin Time	: 13 August 1964 at 00 31 15.0 UT			
Depth	: 392 km			
Magnitude (M)	: 6.5			
Type	: Dip-slip normal			
Nodal Planes	:	Azimuth of Dip	Dip	
	:	075	62	
	:	221	32	
Nodal-Plane Poles	:	Azimuth	Plunge	
	:	255	28	
	:	041	58	
P Axis	:	288	70	
T Axis	:	061	15	
		Azimuth	Plunge	Uncertainty
B Axis	:	156	14	32 x 33

The solution is poor because there are no station readings in the southwest compressional quadrant, and the B-axis uncertainty is large (Fig. 10). However, the compressional stress axis is nearly vertical and the solution is consistent with those of deep earthquakes in which the compressional stress axis parallels the Benioff zone (Isacks & Molnar, 1971).

Plotted in Plate 4.

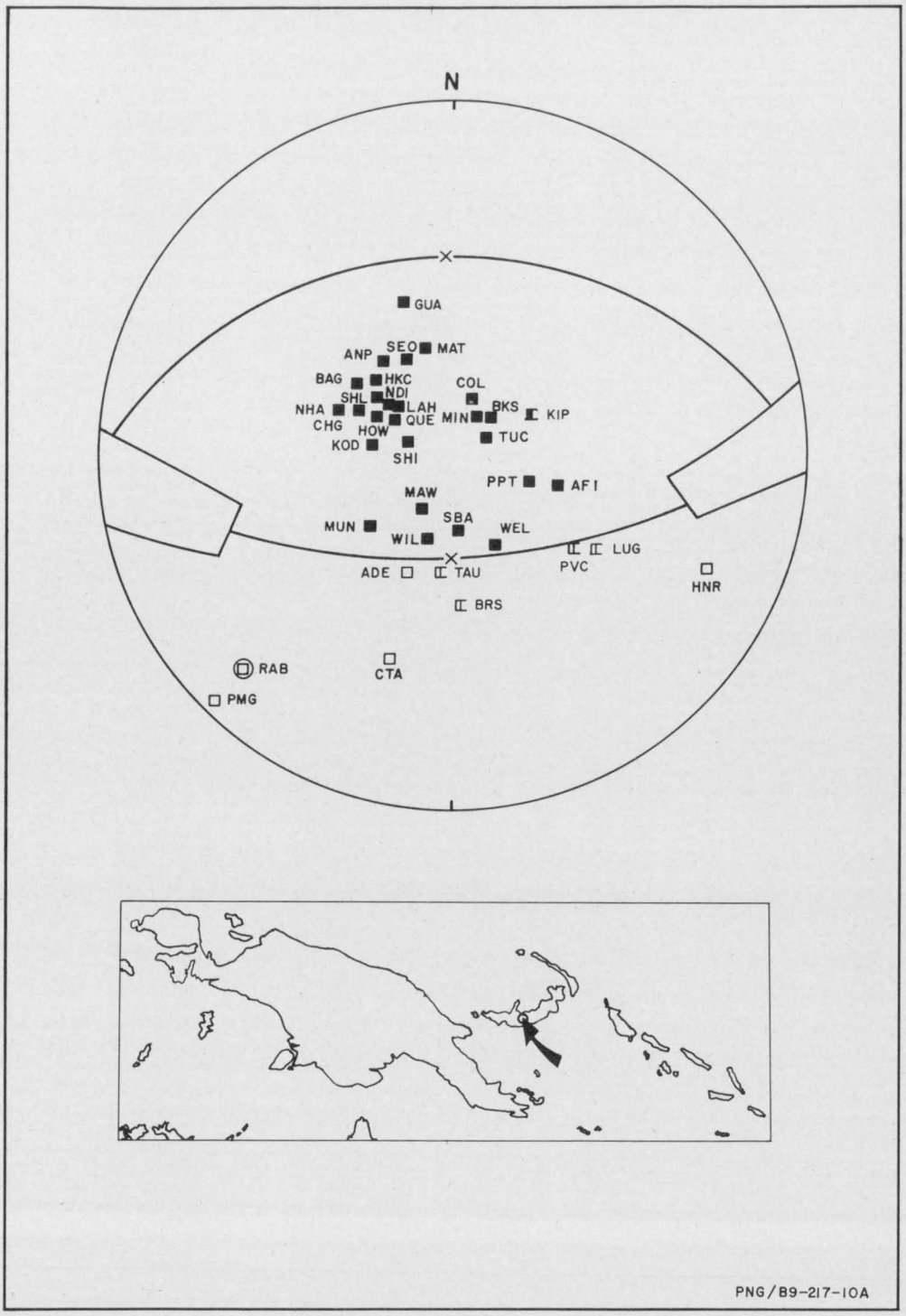
N
GUA
ANP
SEO
MAT
BAG
HKC
COL
SHL
NDI
NHA
LAH
BKS
KIP
CHG
HOW
QUE
MIN
KOD
TUC
SHI
PPT
AFI
MAW
SBA
MUN
WEL
WIL
LUG
PVC
ADE
TAU
HNR
BRS
RAB
CTA
PMG
PNG/89-217-10A

FIGURE 11

Number	: 10			
Location	: 5.7°S, 150.7°E; central New Britain			
Origin Time	: 17 November 1964 at 08 15 41.1 UT			
Depth	: 60 km			
Magnitude (M)	: 7.3			
Type	: Dip-slip overthrust			
Nodal Planes	:	Azimuth of Dip	Dip	
	:	Too uncertain		
	:			
Nodal-Plane Poles	:	Azimuth	Plunge	
	:			
	:			
P Axis	:			
T Axis	:			
		Azimuth	Plunge	Uncertainty
B Axis	:			

One nodal plane of the solution is well defined, but there is little station control over the other. Although the solution is clearly overthrust, the orientation is uncertain.

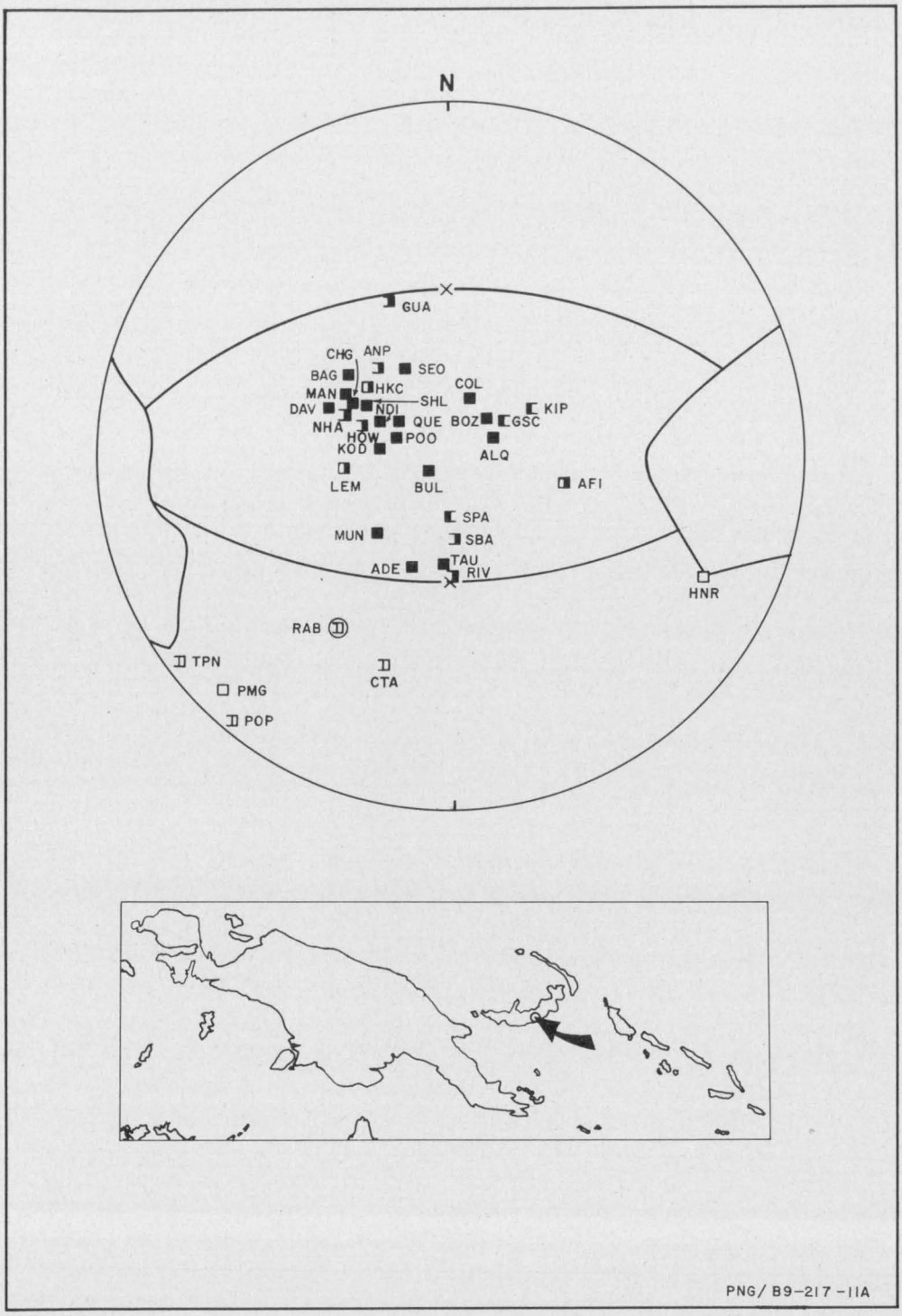
N
GUA
CHG
ANP
BAG
SEO
HKC
COL
MAN
SHL
DAV
NDI
KIP
NHA
QUE
BOZ
GSC
HOW
POO
KOD
ALQ
LEM
BUL
AFI
SPA
MUN
SBA
TAU
ADE
RIV
HNR
RAB
TPN
CTA
PMG
POP
PNG/ B9-217 -11A

FIGURE 12

Number	: 11			
Location	: 5.4°S, 151.2°E; central New Britain			
Origin Time	: 7 December 1964 at 08 58 45.0 UT			
Depth	: 70 km			
Magnitude (M)	: 5.9			
Type	: Dip-slip overthrust			
Nodal Planes	:	Azimuth of Dip	Dip	
	:	Too uncertain		
	:			
Nodal-Plane Poles	:	Azimuth	Plunge	
	:			
	:			
P Axis	:			
T Axis	:			
		Azimuth	Plunge	Uncertainty
B Axis	:			

Although clearly an overthrust solution, the station control over the orientation is poor.

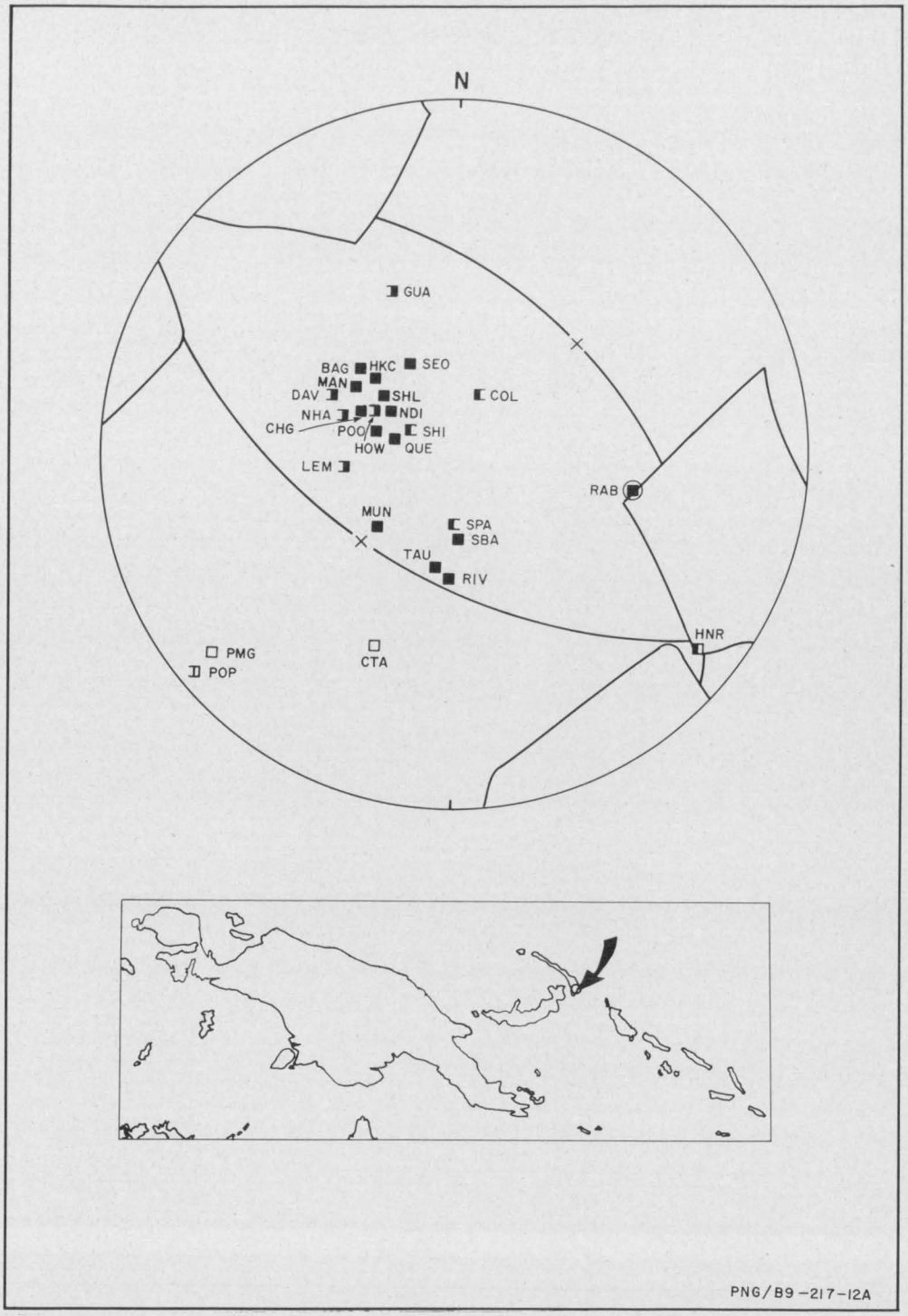
N
GUA
BAG
HKC
SEO
MAN
DAV
SHL
COL
NHA
NDI
CHG
POO
SHI
HOW
QUE
LEM
RAB
MUN
SPA
SBA
TAU
RIV
HNR
PMG
POP
CTA
PNG/B9-217-12A

FIGURE 13

Number	: 12			
Location	: 4.4°S, 153.1°E; southeast New Ireland			
Origin Time	: 24 December 1964 at 18 45 44.0 UT			
Depth	: 78 km			
Magnitude (M)	: 6.1			
Type	: Dip-slip overthrust			
Nodal Planes	:	Azimuth of Dip	Dip	
	:	Too uncertain		
	:			
Nodal-Plane Poles	:	Azimuth	Plunge	
	:			
	:			
P Axis	:			
T Axis	:			
		Azimuth	Plunge	Uncertainty
B Axis	:			

The earthquake occurred at the apex of the New Britain and Bougainville seismic trends. The station distribution is poor and two solutions are possible, both dip-slip overthrust. The preferred trend is northwest, parallel to the Solomon Islands chain.

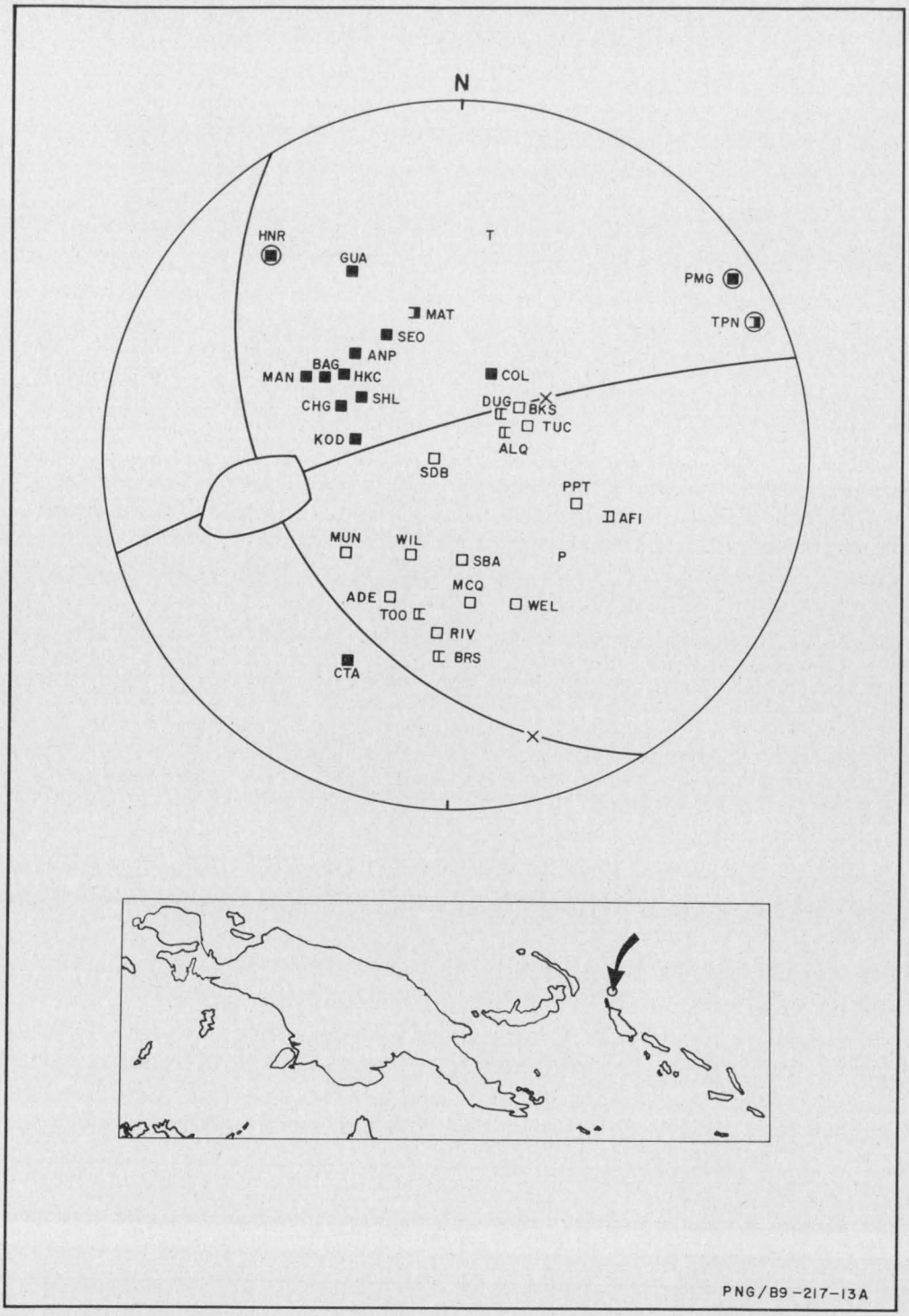
N
HNR
GUA
T
PMG
TPN
MAT
SEO
ANP
BAG
MAN
HKC
COL
CHG
SHL
DUG
BKS
TUC
ALQ
KOD
SDB
PPT
AFI
MUN
WIL
SBA
P
MCQ
ADE
TOO
WEL
RIV
BRS
CTA
PNG/89-217-13A

FIGURE 14

Number	: 13			
Location	: 4.5°S, 155.1°E; 100 km east of Nissan Islands			
Origin Time	: 6 July 1965 at 18 36 47.3 UT			
Depth	: 509 km			
Magnitude (M)	: 6.2			
Type	: Dip-slip normal			
Nodal Planes	:	Azimuth of Dip	Dip	
	:	238	34	
	:	343	80	
Nodal-Plane Poles	:	Azimuth	Plunge	
	:	058	56	
	:	163	10	
P Axis	:	130	44	
T Axis	:	008	27	
		Azimuth	Plunge	Uncertainty
B Axis	:	260	32	26 x 17

The earthquake hypocentre is at an isolated pocket of deep-focus seismicity. The solution is good, except that only one station reading occurs in the southwest quadrant, and none in the northwest quadrant.

Plotted in Plate 4.

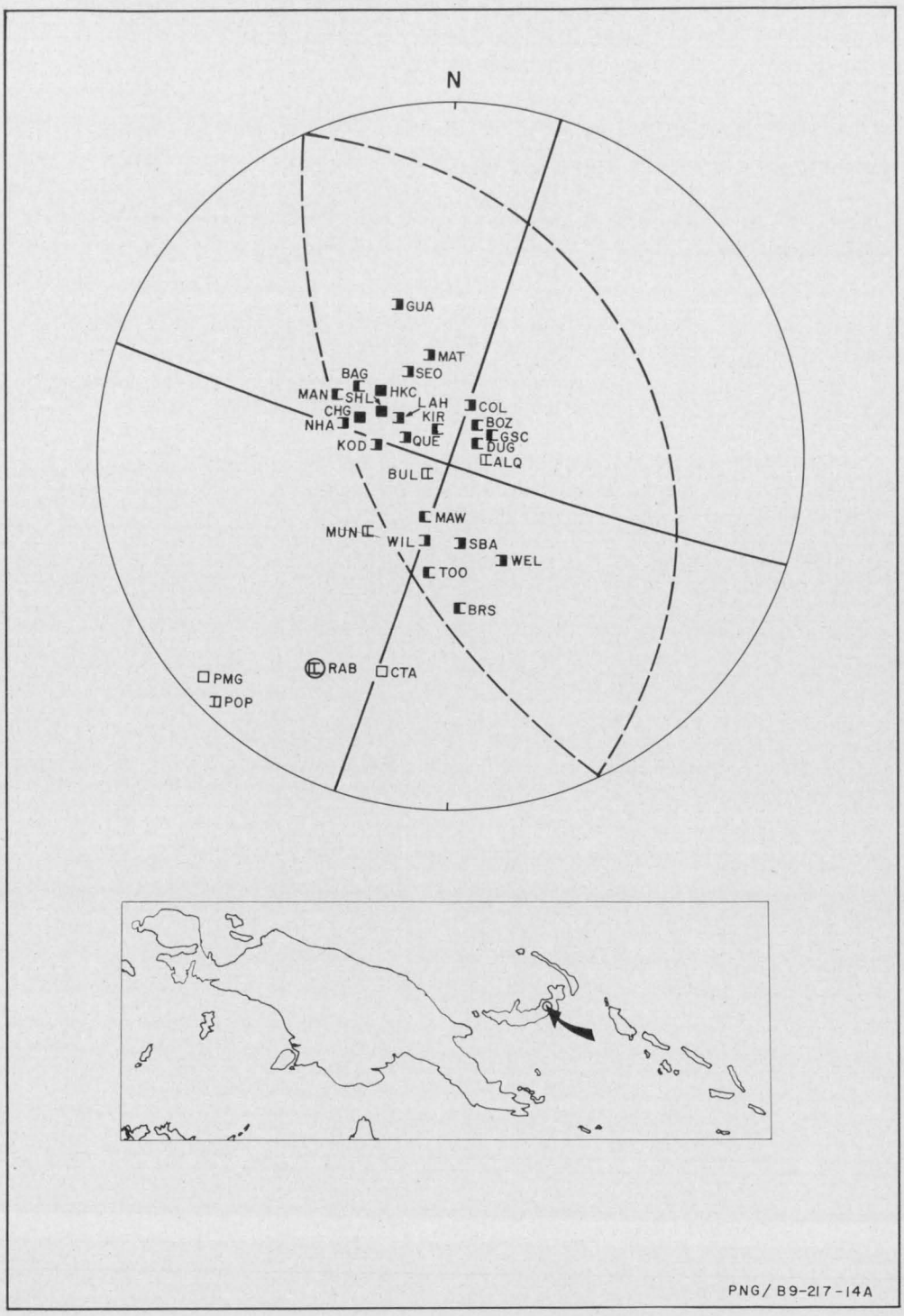
N
GUA
MAT
BAG
SEO
MAN
SHL
HKC
LAH
COL
CHG
KIR
BOZ
NHA
GSC
KOD
QUE
DUG
ALQ
BUL
MAW
MUN
WIL
SBA
WEL
TOO
BRS
RAB
CTA
PMG
POP
PNG/B9-217-14A

FIGURE 15

Number	: 14			
Location	: 5.4°S, 151.5°E; Pomio, southeast New Britain			
Origin Time	: 22 September 1965 at 20 01 50.0 UT			
Depth	: 62 km			
Magnitude (M)	: 5.9			
Type	: Strike-slip or dip-slip overthrust, non-orthogonal			
Nodal Planes	:	Azimuth of Dip	Dip	
	:	Too uncertain		
	:			
Nodal-Plane Poles	:	Azimuth	Plunge	
	:			
	:			
P Axis	:			
T Axis	:			
		Azimuth	Plunge	Uncertainty
B Axis	:			

The solution is poor. Two solutions are possible, both with anomalous readings. In the strike-slip solution, shown by solid lines in Figure 15, stations BOZ, DUG, and GSC recorded anomalous compressions in the northeast dilatational quadrant. In the dip-slip overthrust solution, shown by dashed lines in Figure 15, stations BUL and ALQ recorded anomalous dilatations.

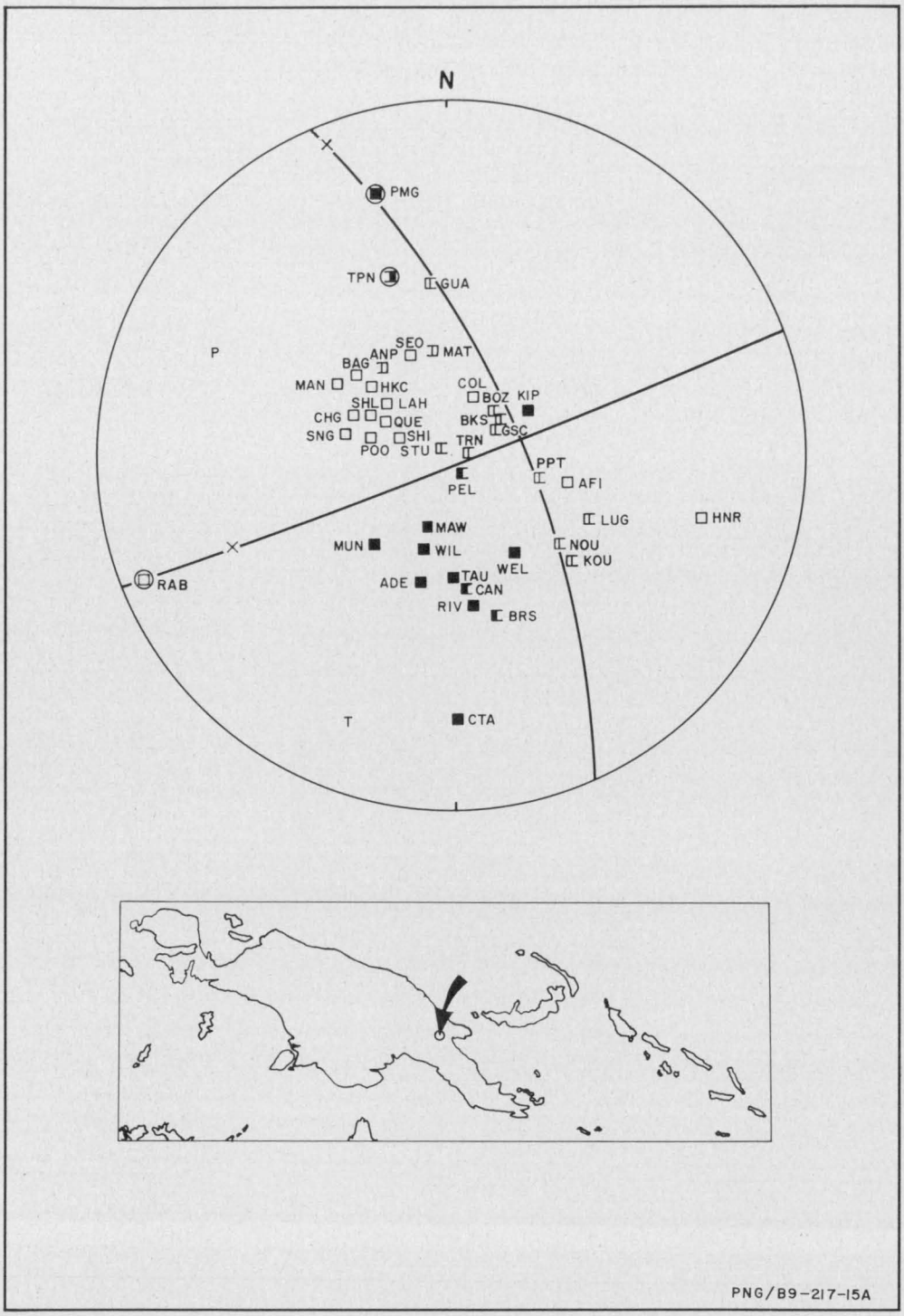
N
PMG
TPN
GUA
P
SEO
ANP
MAT
BAG
MAN
HKC
COL
BOZ
KIP
SHL
LAH
CHG
QUE
BKS
GSC
SNG
SHI
TRN
POO
STU
PPT
PEL
AFI
LUG
HNR
MAW
MUN
WIL
NOU
KOU
WEL
RAB
ADE
TAU
CAN
RIV
BRS
T
CTA
PNG/B9-217-15A

FIGURE 16

Number	: 15			
Location	: 6.4°S, 146.3°E; Markham Valley			
Origin Time	: 7 December 1965 at 22 19 16.0 UT			
Depth	: 118 km			
Magnitude (M)	: 6.4			
Type	: Strike-slip (non-orthogonal)			
Nodal Planes	:	Azimuth of Dip	Dip	
	:	068	67	
	:	159	87	
Nodal-Plane Poles	:	Azimuth	Plunge	
	:	248	23	
	:	339	03	
P Axis	:	297	17	
T Axis	:	202	14	
		Azimuth	Plunge	Uncertainty
B Axis	:	077	68	—

Although there are only two stations in the northeast quadrant, the solution is tight. One station, TPN, is anomalous, but its position on the focal sphere is uncertain.

The strike of one nodal plane is 158° and the trend of the Ramu-Markham lineament is about 130°. If this nodal plane is the fault plane, then the motion is sinistral, which suggests that the lineament (a) involves sinistral motion and (b) extends down to 118 km.

Plotted in Plate 2.

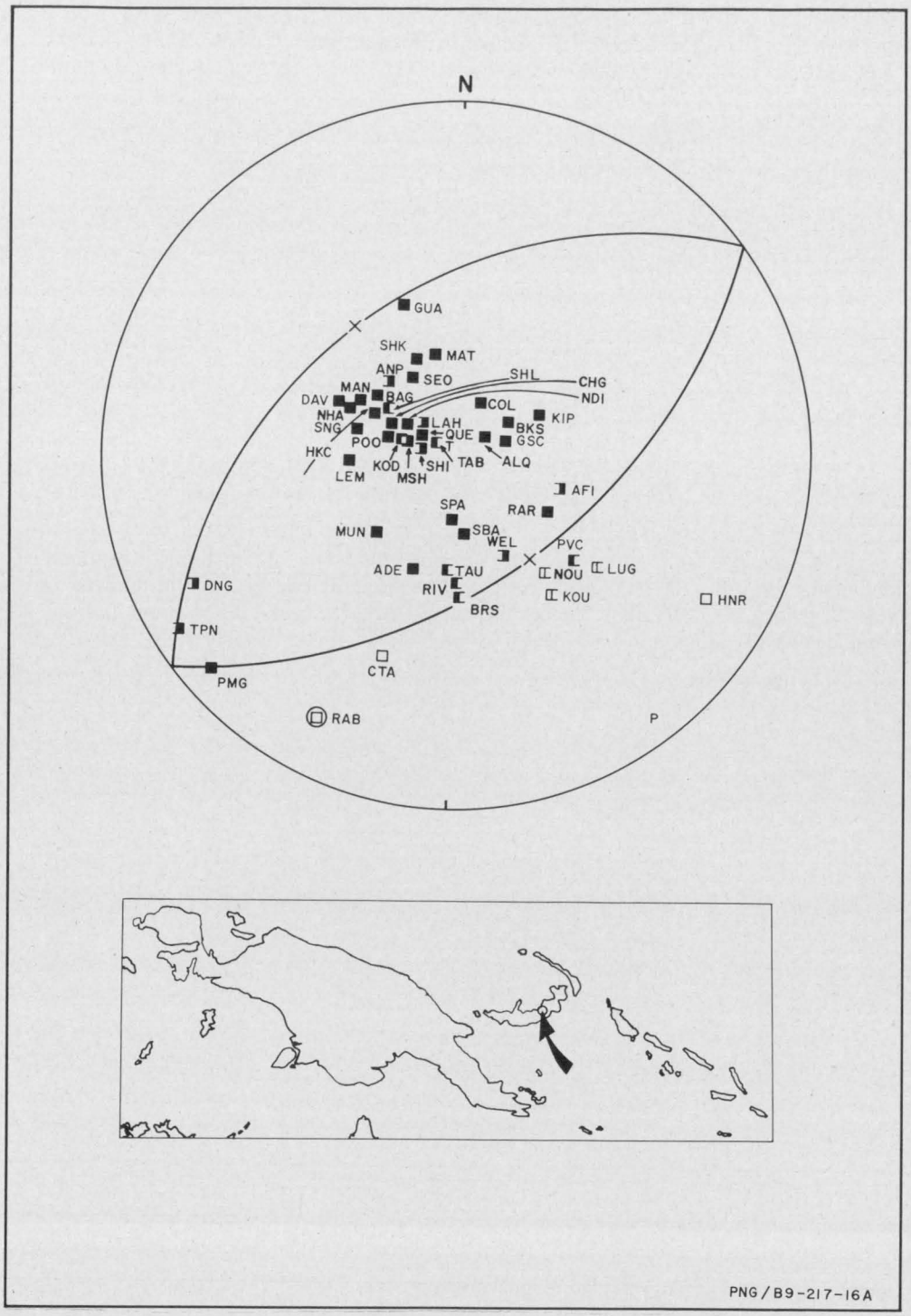
N
GUA
SHK
MAT
ANP
SEO
SHL
CHG
NDI
MAN
BAG
DAV
COL
KIP
NHA
SNG
LAH
QUE
BKS
GSC
POO
HKC
KOD
SHI
TAB
ALQ
LEM
MSH
AFI
SPA
RAR
MUN
SBA
WEL
PVC
ADE
TAU
NOU
LUG
DNG
RIV
KOU
HNR
BRS
TPN
CTA
PMG
RAB
P
PNG/B9-217-16A

FIGURE 17

Number	: 16			
Location	: 5.4°S, 151.6°E; Pomio, southeast New Britain			
Origin Time	: 22 February 1966 at 05 02 40.7 UT			
Depth	: 59 km			
Magnitude (M)	: 6.7			
Type	: Dip-slip overthrust (non-orthogonal)			
Nodal Planes	:	Azimuth of Dip	Dip	
	:	322	41	
	:	142	49	
Nodal-Plane Poles	:	Azimuth	Plunge	
	:	142	49	
	:	322	41	
P Axis	:	142	04	
T Axis	:	322	86	
		Azimuth	Plunge	Uncertainty
B Axis	:	053	00	—

The solution is poor: there are no station readings in the northwest dilatational quadrant. However, the solution is tight with one station, PVC, close to but on the wrong side of a nodal plane.

Plotted in Plate 3.

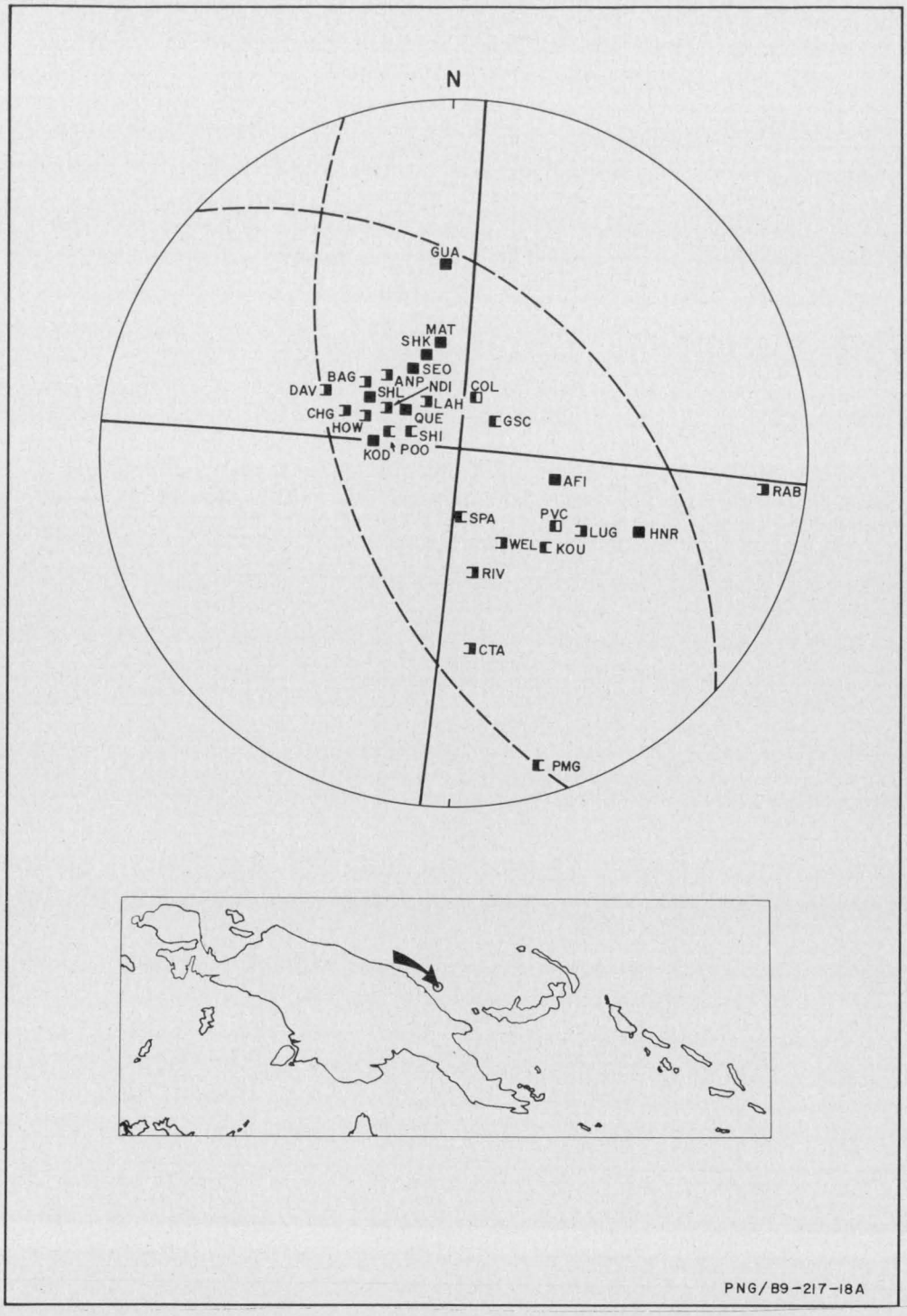
N
GUA
MAT
SHK
SEO
BAG
ANP
NDI
COL
DAV
SHL
LAH
CHG
QUE
GSC
HOW
SHI
KOD
POO
AFI
RAB
SPA
PVC
LUG
HNR
WEL
KOU
RIV
CTA
PMG
PNG/89-217-18A

FIGURE 18

Number	: 17			
Location	: 3.6°S, 145.4°E; Bismarck Sea seismic lineation north of Madang			
Origin Time	: 10 December 1966 at 18 08 14.4 UT			
Depth	: 33 km			
Magnitude (M)	: 6.2			
Type	: Strike-slip or overthrust			
Nodal Planes	:	Azimuth of Dip	Dip	
	:	Too uncertain		
	:			
Nodal-Plane Poles	:	Azimuth	Plunge	
	:			
	:			
P Axis	:			
T Axis	:			
		Azimuth	Plunge	Uncertainty
B Axis	:			

The solution is poor. Two solutions both with anomalous station polarities are possible. The more likely solution is strike-slip, with nodal planes striking east-west and north-south (solid lines in Fig. 17). However, there are no stations in the southwest quadrant, and the short-period polarities of the two stations (COL and GSC) in the northeast quadrant are anomalous compressions. Had the long-period dilatation from COL been strong and clear, the strike-slip solution would be probable, but it was weak and two seconds later than the short-period compression.

The other possible solution is an overthrust oriented roughly northwest (dotted lines in Fig. 17) with the RAB arrival and the COL and PVC long-period arrivals anomalous. If this solution were correct, it would imply that the Bismarck Sea seismic lineation involved motion other than sinistral shear — namely overthrusting — but, as with the shear solution, the overthrust solution cannot be adopted with any certainty.

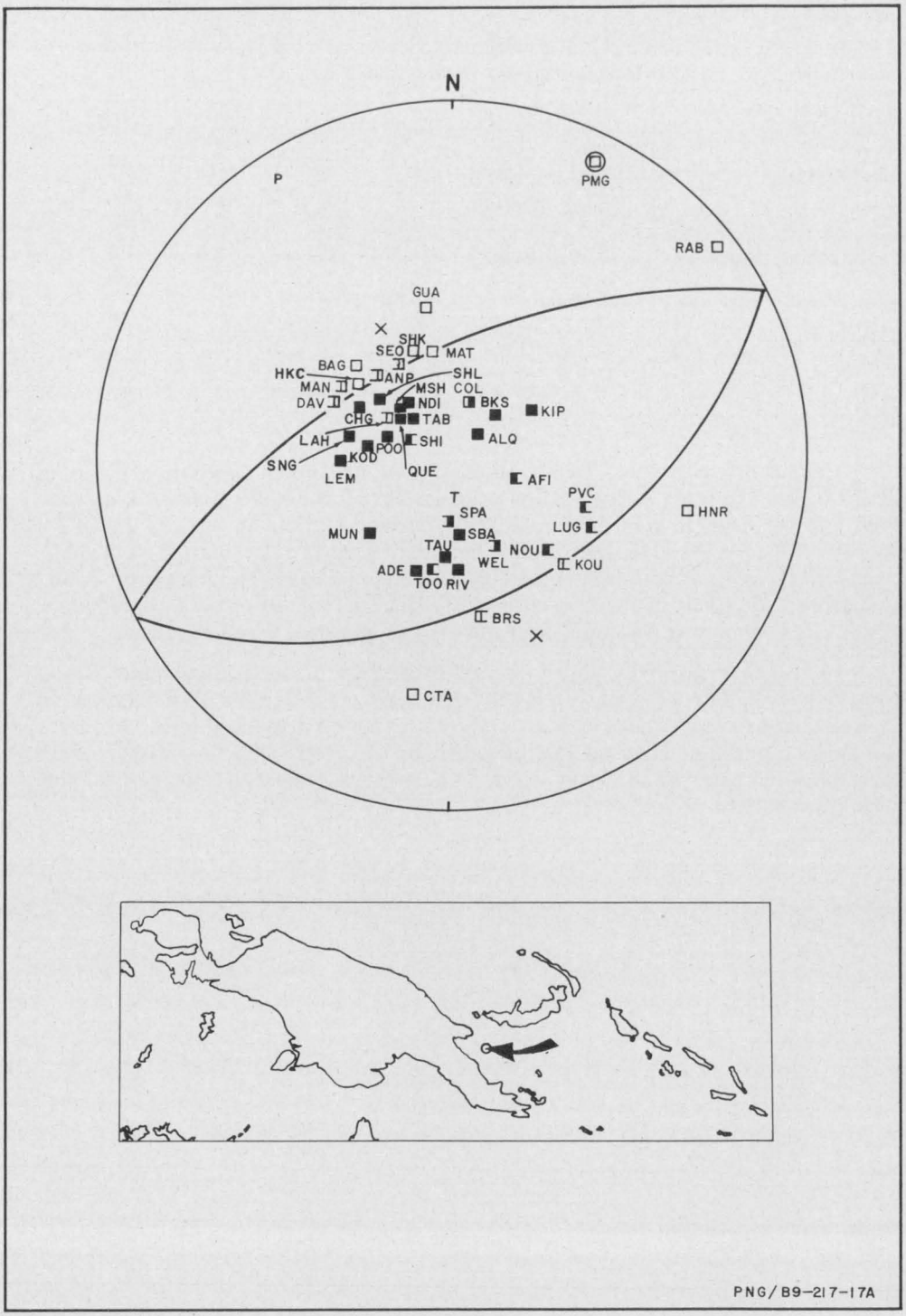
N
P
PMG
RAB
GUA
SHK
SEO
MAT
HKC
BAG
SHL
MAN
MSH
COL
DAV
NDI
BKS
KIP
CHG
TAB
LAH
SHI
ALQ
POO
SNG
KOD
QUE
LEM
AFI
PVC
T
SPA
HNR
MUN
SBA
LUG
TAU
NOU
WEL
KOU
ADE
TOO
RIV
BRS
CTA
PNG/89-217-17A

FIGURE 19

Number	: 18			
Location	: 7.1°S, 148.3°E; Huon Gulf			
Origin Time	: 23 December 1966 at 15 50 21.3 UT			
Depth	: 46 km			
Magnitude (M)	: 7.2			
Type	: Dip-slip overthrusting (non-orthogonal)			
Nodal Planes	:	Azimuth of Dip	Dip	
	:	333	59	
	:	153	44	
Nodal-Plane Poles	:	Azimuth	Plunge	
	:	153	31	
	:	333	46	
P Axis	:	333	04	
T Axis	:	153	80	
		Azimuth	Plunge	Uncertainty
B Axis	:	063	00	—

The solution contains some anomalous features: station LAH recorded a dilatation in a region of P-wave compression, and station COL recorded a small short-period dilatation and a long-period compression.

The solution is non-orthogonal. Both nodal planes are reasonably well defined, but are inclined at 77° relative to each other. For the solution to be orthogonal, the earthquake would have to have occurred in a layer with an anomalously high P-wave velocity.

Plotted in Plate 3.

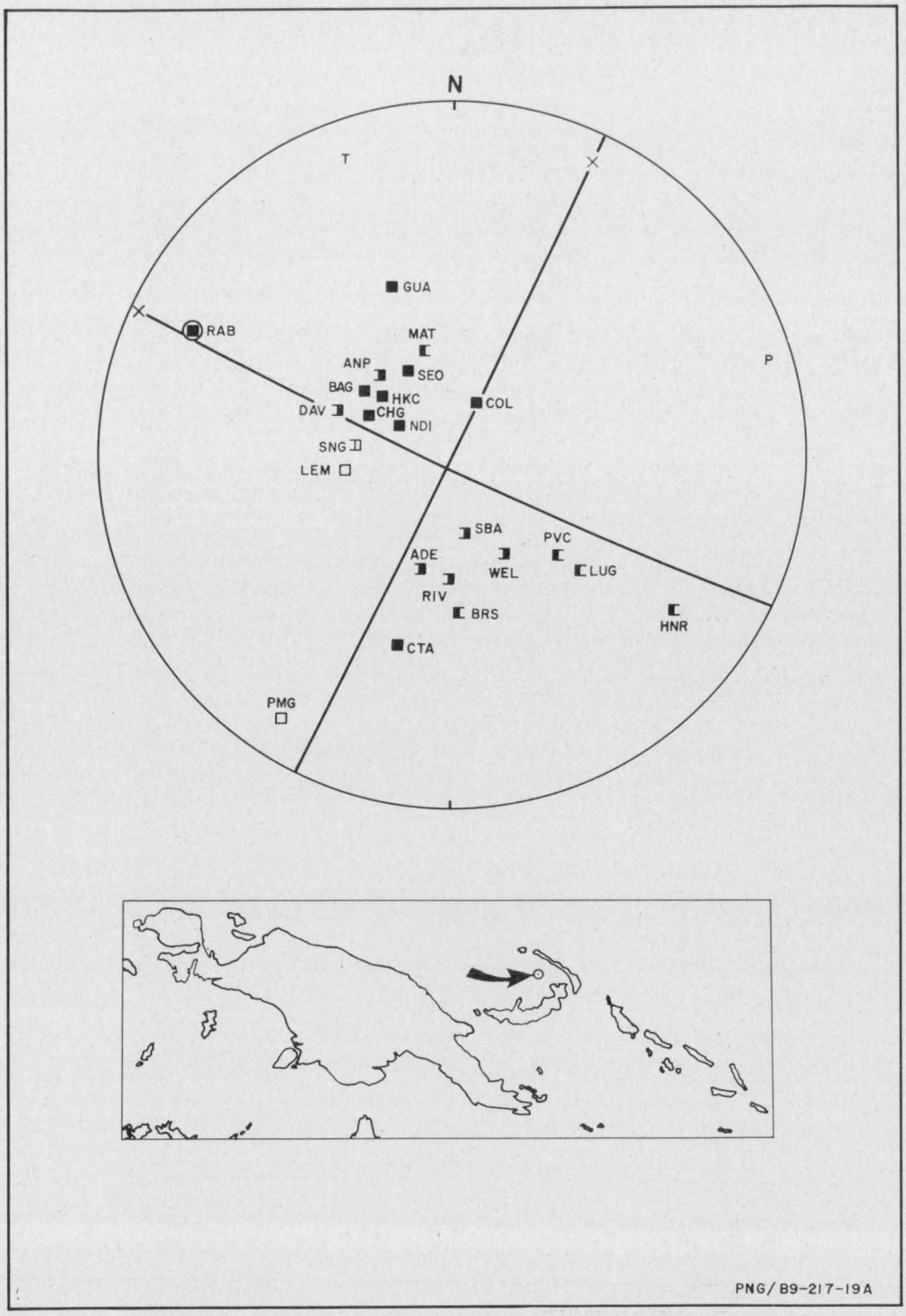
N
T
P
GUA
RAB
MAT
ANP
SEO
BAG
HKC
DAV
CHG
NDI
COL
SNG
LEM
SBA
PVC
ADE
WEL
LUG
RIV
BRS
HNR
CTA
PMG
PNG/B9-217-19A

FIGURE 20

Number	:	19		
Location	:	3.6°S, 150.8°E; on the Bismarck Sea seismic lineation 100 km south of Kavieng		
Origin Time	:	17 March 1967 at 11 24 46.4 UT		
Depth	:	33 km		
Magnitude (M)	:	5.7		
Type	:	Strike-slip		
Nodal Planes	:	Azimuth of Dip	Dip	
	:	115	89	
	:	205	86	
Nodal-Plane Poles	:	Azimuth	Plunge	
	:	295	01	
	:	025	04	
P Axis	:	070	02	
T Axis	:	340	04	
		Azimuth	Plunge	Uncertainty
B Axis	:	189	86	7 x 2

The solution is poor because there are no station readings in the northeast quadrant. However, a dip-slip solution is impossible. If the nodal plane striking west-northwest is the fault plane, the motion is sinistral.

The solution suggests that the Bismarck Sea seismic lineation is a sinistral shear. If the earthquake had occurred on a transform fault in a mid-oceanic ridge, the P-wave polarities would be reversed; hence this possibility is rejected.

Plotted in Plate 2.

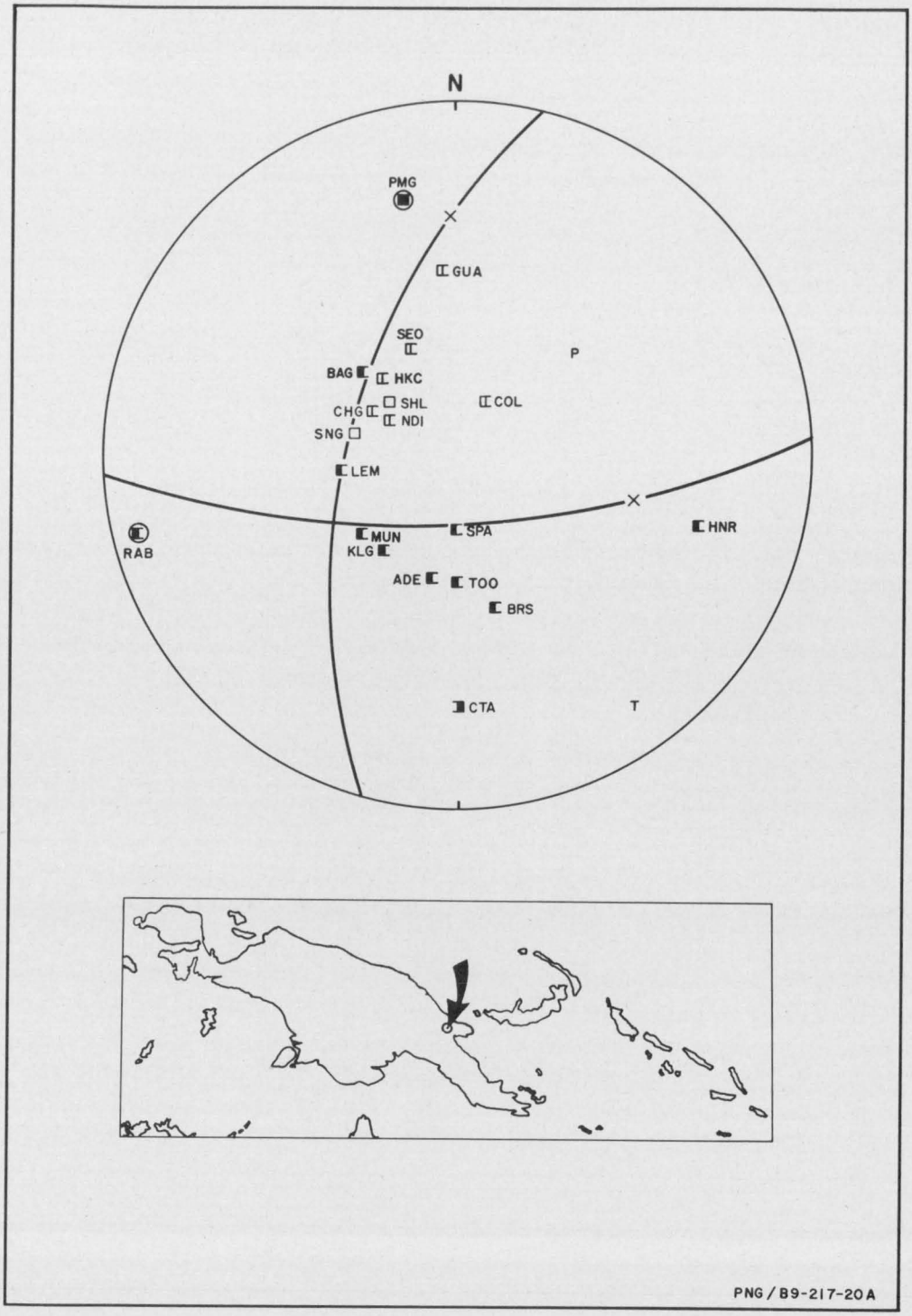
N
PMG
GUA
SEO
P
BAG
HKC
CHG
SHL
NDI
COL
SNG
LEM
RAB
MUN
KLG
SPA
HNR
ADE
TOO
BRS
CTA
T
PNG/89-217-20A

FIGURE 21

Number	: 20			
Location	: 6.0°S, 146.3°E; Finisterre Mountains, northern New Guinea			
Origin Time	: 18 March 1967 at 19 15 35.6 UT			
Depth	: 101 km			
Magnitude (M)	: 5.8			
Type	: Strike-slip (non-orthogonal)			
Nodal Planes	:	Azimuth of Dip	Dip	
	:	283	55	
	:	179	69	
Nodal-Plane Poles	:	Azimuth	Plunge	
	:	103	35	
	:	359	21	
P Axis	:	047	41	
T Axis	:	145	09	
		Azimuth	Plunge	Uncertainty
B Axis	:	244	48	—

The solution is poor because there are no dilatational readings in the southwest dilatational quadrant, and the only station positioned in the quadrant (RAB) recorded a compression. However, the position of RAB on the focal sphere is sufficiently uncertain to account for the discrepancy.

As the B axis plunges at 48°, the solution involves a greater component of strike-slip than dip-slip motion. If the east-trending nodal plane is the fault plane, the motion is sinistral.

Plotted in Plate 2.

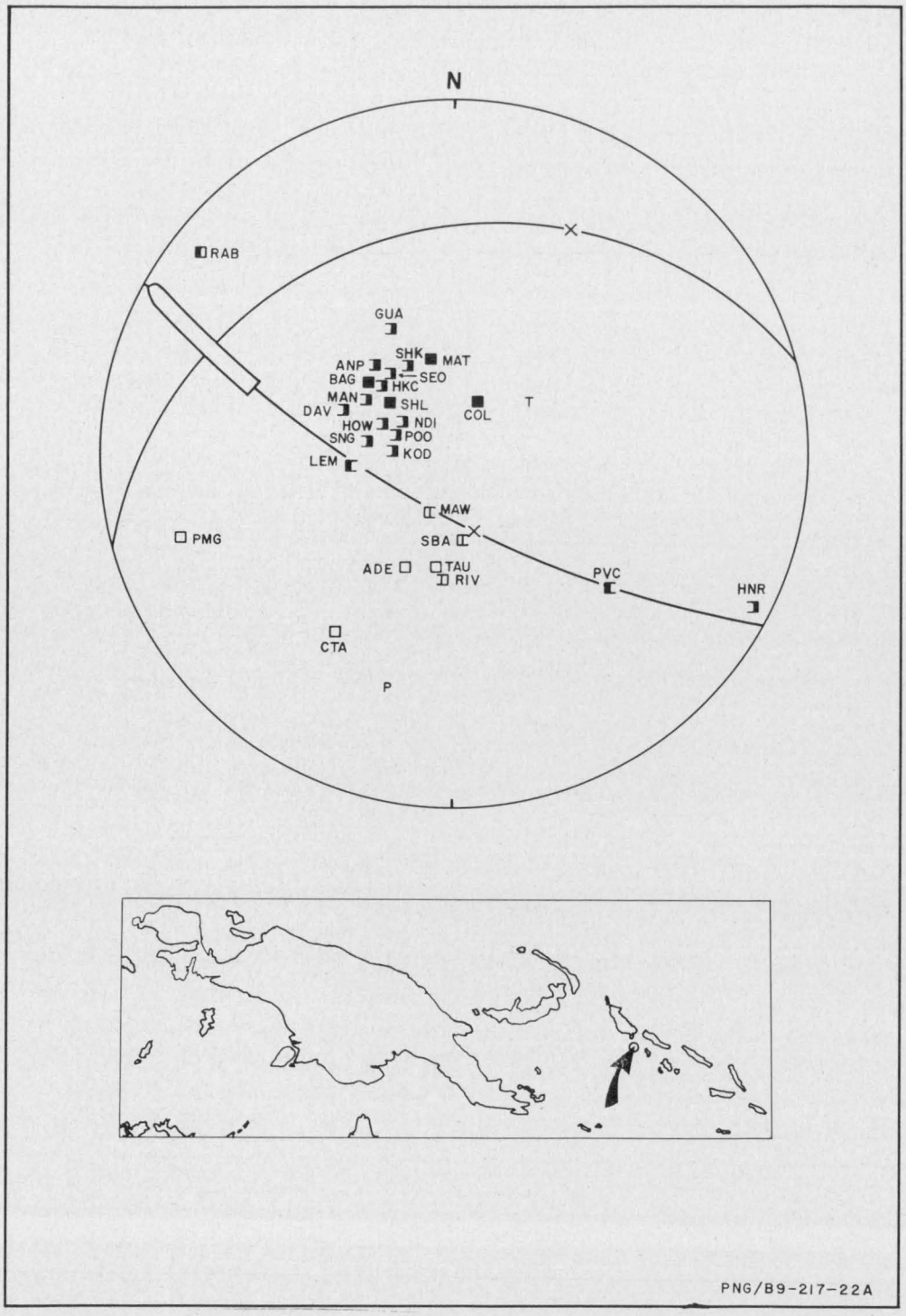
N
RAB
GUA
SHK
MAT
ANP
SEO
BAG
HKC
MAN
SHL
DAV
COL
T
HOW
NDI
SNG
POO
LEM
KOD
MAW
PMG
SBA
ADE
TAU
RIV
PVC
HNR
CTA
P
PNG/B9-217-22A

FIGURE 22

Number	: 21			
Location	: 7.3°S, 155.8°E; 20 km south of Bougainville			
Origin Time	: 10 April 1967 at 15 02 44.5 UT			
Depth	: 47 km			
Magnitude (M)	: 6.1			
Type	: Dip-slip overthrust			
Nodal Planes	:	Azimuth of Dip	Dip	
	:	345	25	
	:	209	71	
Nodal-Plane Poles	:	Azimuth	Plunge	
	:	165	65	
	:	029	19	
P Axis	:	196	24	
T Axis	:	052	60	
		Azimuth	Plunge	Uncertainty
B Axis	:	293	14	30 x 1

The solution is poor because there is almost no station control over one nodal plane whose position is restricted by only the orthogonality criterion.

Plotted in Plate 3.

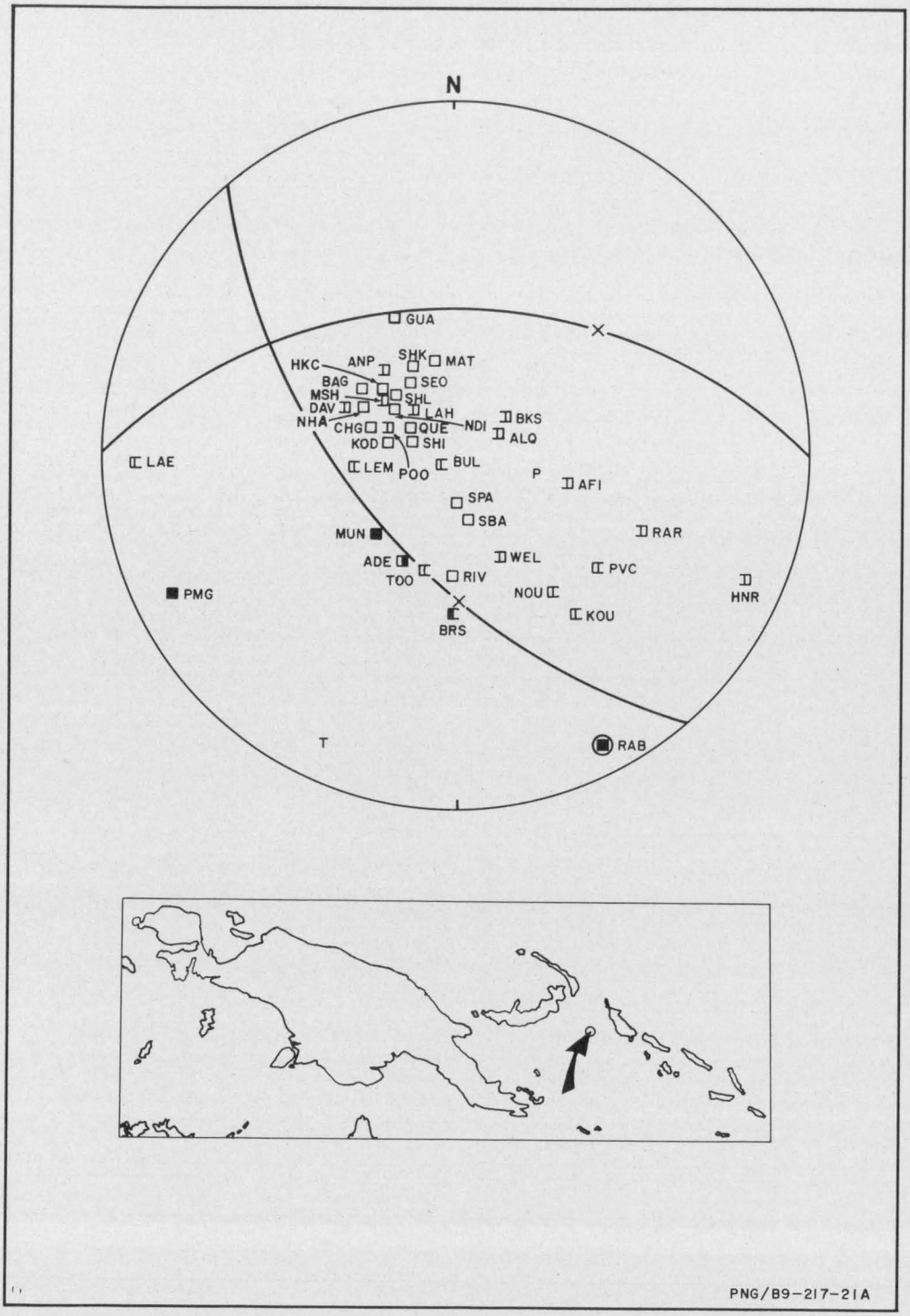
N
GUA
HKC
ANP
SHK
MAT
BAG
SEO
MSH
SHL
DAV
LAH
NHA
CHG
QUE
NDI
BKS
ALQ
KOD
SHI
LAE
LEM
POO
BUL
P
AFI
SPA
SBA
MUN
RAR
ADE
WEL
TOO
RIV
PVC
PMG
NOU
HNR
KOU
BRS
T
RAB
PNG/89-217-21A

FIGURE 23

Number	: 22			
Location	: 6.6°S, 153.4°E; mid-Solomon Sea 150 km west of Bougainville			
Origin Time	: 28 September 1967 at 04 56 56.3 UT			
Depth	: 44 km			
Magnitude (M)	: 6.4			
Type	: Dip-slip normal (non-orthogonal)			
Nodal Planes	:	Azimuth of Dip	Dip	
	:	001	45	
	:	230	57	
Nodal-Plane Poles	:	Azimuth	Plunge	
	:	181	45	
	:	050	33	
P Axis	:	102	63	
T Axis	:	208	07	
		Azimuth	Plunge	Uncertainty
B Axis	:	301	26	—

The solution is poor as there are no station readings in the north quadrants; but it is tight, assuming orthogonality, as station LAE is on the wrong side of a nodal plane.

The solution represents a normal fault, in contrast to the overthrusts associated with earthquakes around the New Britain and Bougainville borders of the Solomon Sea.

Plotted in Plate 3.

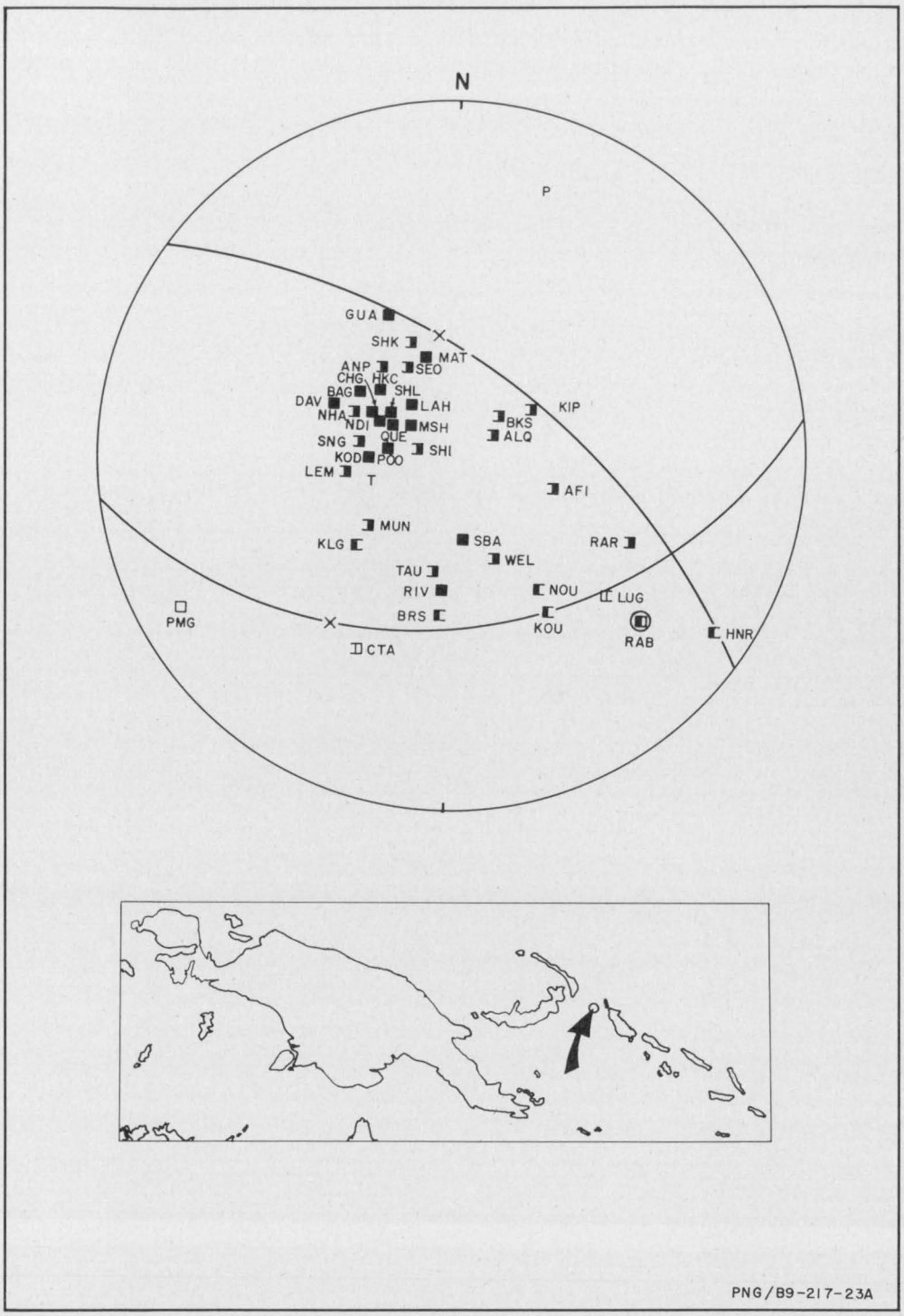
N
P
GUA
SHK
MAT
ANP
SEO
CHG
HKC
BAG
SHL
DAV
LAH
KIP
NHA
NDI
MSH
BKS
QUE
ALQ
SNG
SHI
KOD
POO
LEM
T
AFI
MUN
KLG
SBA
RAR
WEL
TAU
RIV
NOU
LUG
PMG
BRS
KOU
RAB
HNR
CTA
PNG/89-217-23A

FIGURE 24

Number	:	23		
Location	:	5.7°S, 153.9°E; Solomon Sea 50 km west of north Bougainville		
Origin Time	:	4 October 1967 at 17 21 20.7 UT		
Depth	:	52 km		
Magnitude (M)	:	6.7		
Type	:	Dip-slip overthrust		
Nodal Planes	:	Azimuth of Dip	Dip	
	:	035	60	
	:	173	38	
Nodal-Plane Poles	:	Azimuth	Plunge	
	:	215	30	
	:	353	52	
P Axis	:	018	12	
T Axis	:	251	63	
		Azimuth	Plunge	Uncertainty
B Axis	:	113	21	1 x 1

The solution is tight but poor, as there are no station readings in the north dilatational quadrant. The RAB readings, short-period compression and long-period dilatation, are anomalous.

Plotted in Plate 3.

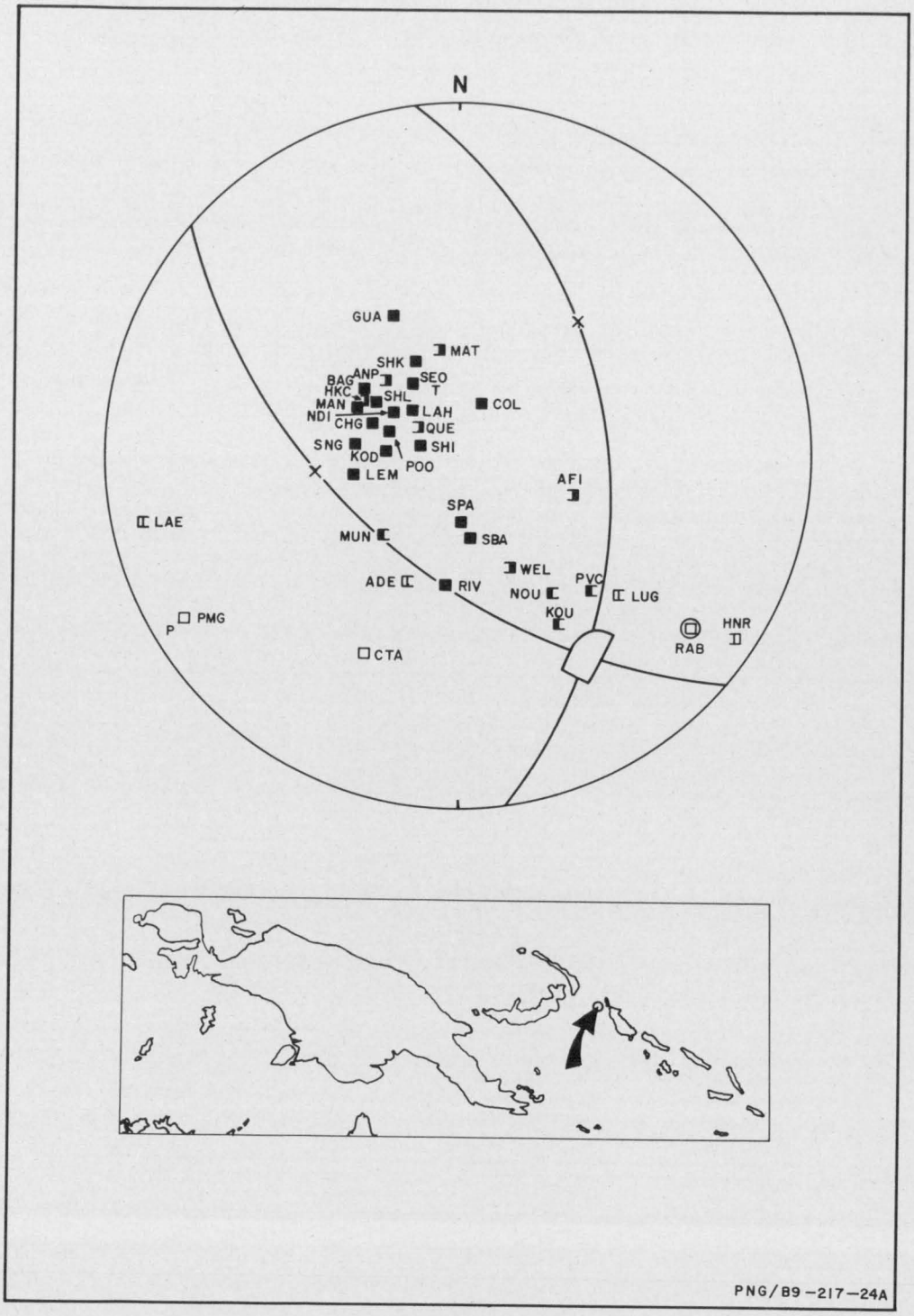
N
GUA
MAT
SHK
ANP
SEO
BAG
HKC
T
SHL
MAN
COL
NDI
LAH
CHG
QUE
SNG
SHI
KOD
POO
LEM
AFI
SPA
LAE
MUN
SBA
WEL
PVC
ADE
RIV
NOU
LUG
KOU
PMG
HNR
RAB
CTA
PNG/89-217-24A

FIGURE 25

Number	:	24		
Location	:	5.6°S, 154.0°E; Solomon Sea 70 km west of north Bougainville		
Origin Time	:	8 October 1967 at 18 08 18.1 UT		
Depth	:	70 km		
Magnitude (M)	:	5.7		
Type	:	Dip-slip overthrust		
Nodal Planes	:	Azimuth of Dip	Dip	
	:	084	44	
	:	220	55	
Nodal-Plane Poles	:	Azimuth	Plunge	
	:	264	46	
	:	040	35	
P Axis	:	240	06	
T Axis	:	343	66	
		Azimuth	Plunge	Uncertainty
B Axis	:	148	23	10 x 6

The solution is good with only a small uncertainty in its orientation and no anomalous station readings, but there are no station readings in the southeast compressional quadrant. The compressional stress axis is horizontal and oriented southwest, orthogonal to Bougainville.

Plotted in Plate 3.

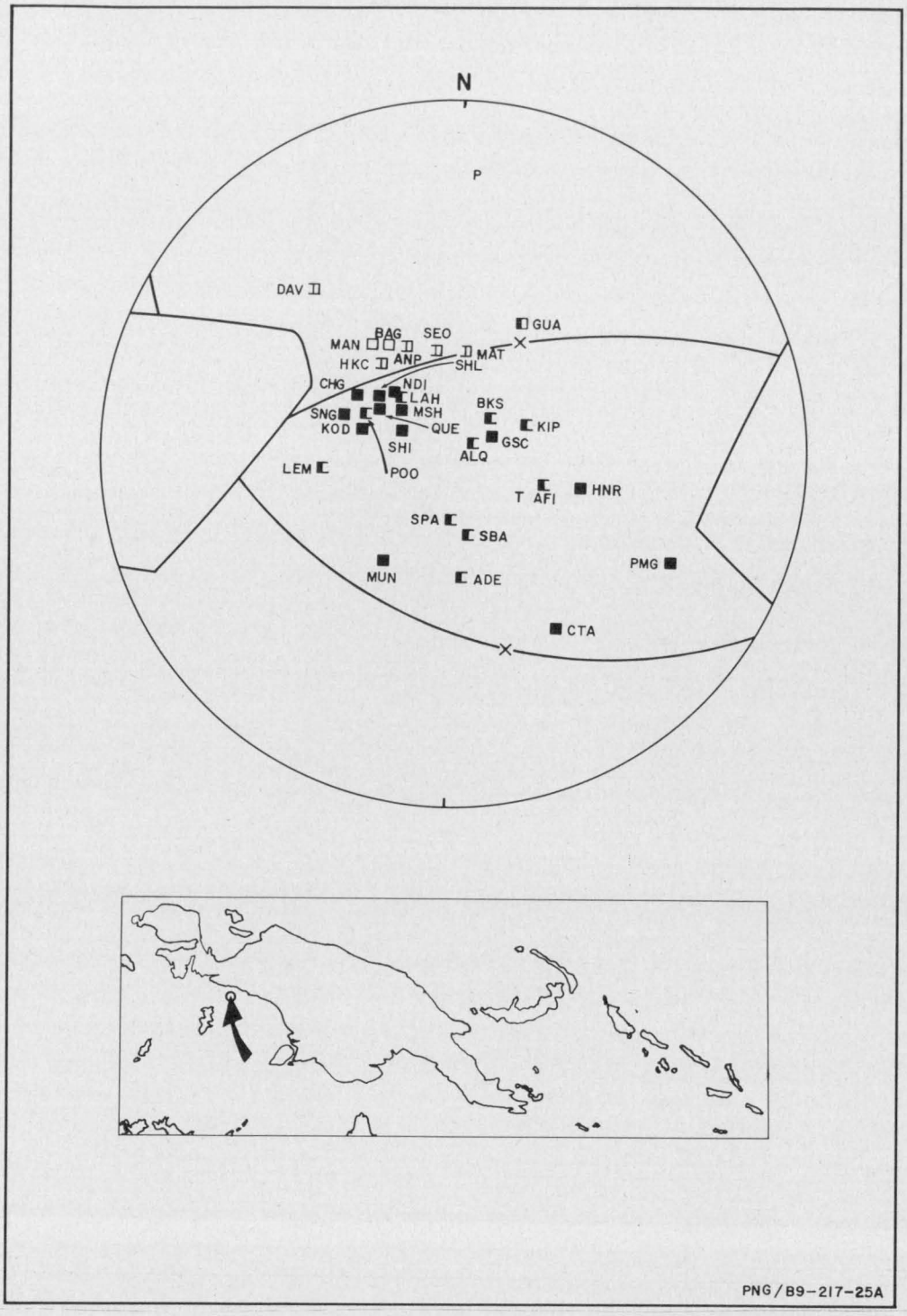
N
P
DAV
BAG
SEO
GUA
MAN
MAT
HKC
ANP
SHL
CHG
NDI
LAH
BKS
SNG
MSH
KOD
QUE
KIP
SHI
ALQ
GSC
LEM
POO
T AFI
HNR
SPA
SBA
PMG
MUN
ADE
CTA
PNG/B9-217-25A

FIGURE 26

Number	: 25			
Location	: 4.8°S, 135.7°E; south coast of Irian Jaya, south of Geelvink Bay			
Origin Time	: 1 November 1967 at 18 56 54.8 UT			
Depth	: 14 km			
Magnitude (M)	: 6.3			
Type	: Dip-slip overthrust			
Nodal Planes	:	Azimuth of Dip	Dip	
	:	Too uncertain		
	:			
Nodal-Plane Poles	:	Azimuth	Plunge	
	:			
	:			
P Axis	:			
T Axis	:			
		Azimuth	Plunge	Uncertainty
B Axis	:			

The solution is poor because there is no station control over one nodal plane, and the orientation of the overthrust can vary considerably. There are no station readings in the south dilatational quadrant.

The approximate orientation of the compressional stress is north, horizontal.

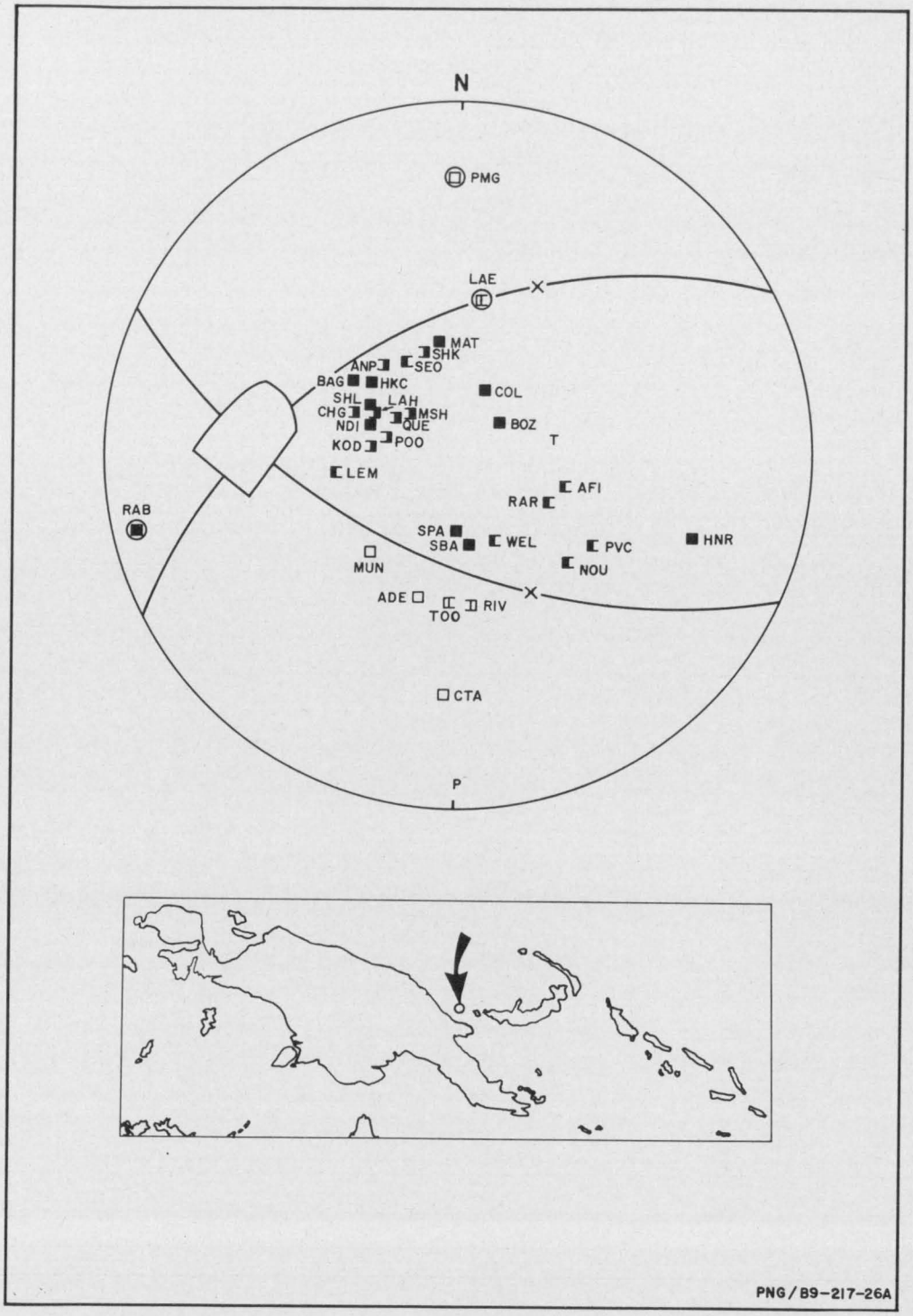
N
PMG
LAE
MAT
SHK
ANP
SEO
BAG
HKC
COL
SHL
LAH
CHG
MSH
NDI
QUE
BOZ
T
KOD
POO
LEM
AFI
RAR
RAB
SPA
SBA
WEL
PVC
HNR
MUN
NOU
ADE
TOO
RIV
CTA
P
PNG/89-217-26A

FIGURE 27

Number	: 26			
Location	: 5.4°S, 147.1°E; Long Island volcano			
Origin Time	: 14 November 1967 at 05 28 36.9 UT			
Depth	: 201 km			
Magnitude (M)	: 6.0			
Type	: Dip-slip overthrust			
Nodal Planes	:	Azimuth of Dip	Dip	
	:	331	48	
	:	204	56	
Nodal-Plane Poles	:	Azimuth	Plunge	
	:	151	42	
	:	024	34	
P Axis	:	178	05	
T Axis	:	080	60	
		Azimuth	Plunge	Uncertainty
B Axis	:	273	28	24 x 16

The earthquake was one of many which occur at about the same hypocentre 200 km beneath the Long Island volcano.

The solution is good with station readings in all quadrants and small uncertainty in the orientation of the B axis.

Plotted in Plate 3.

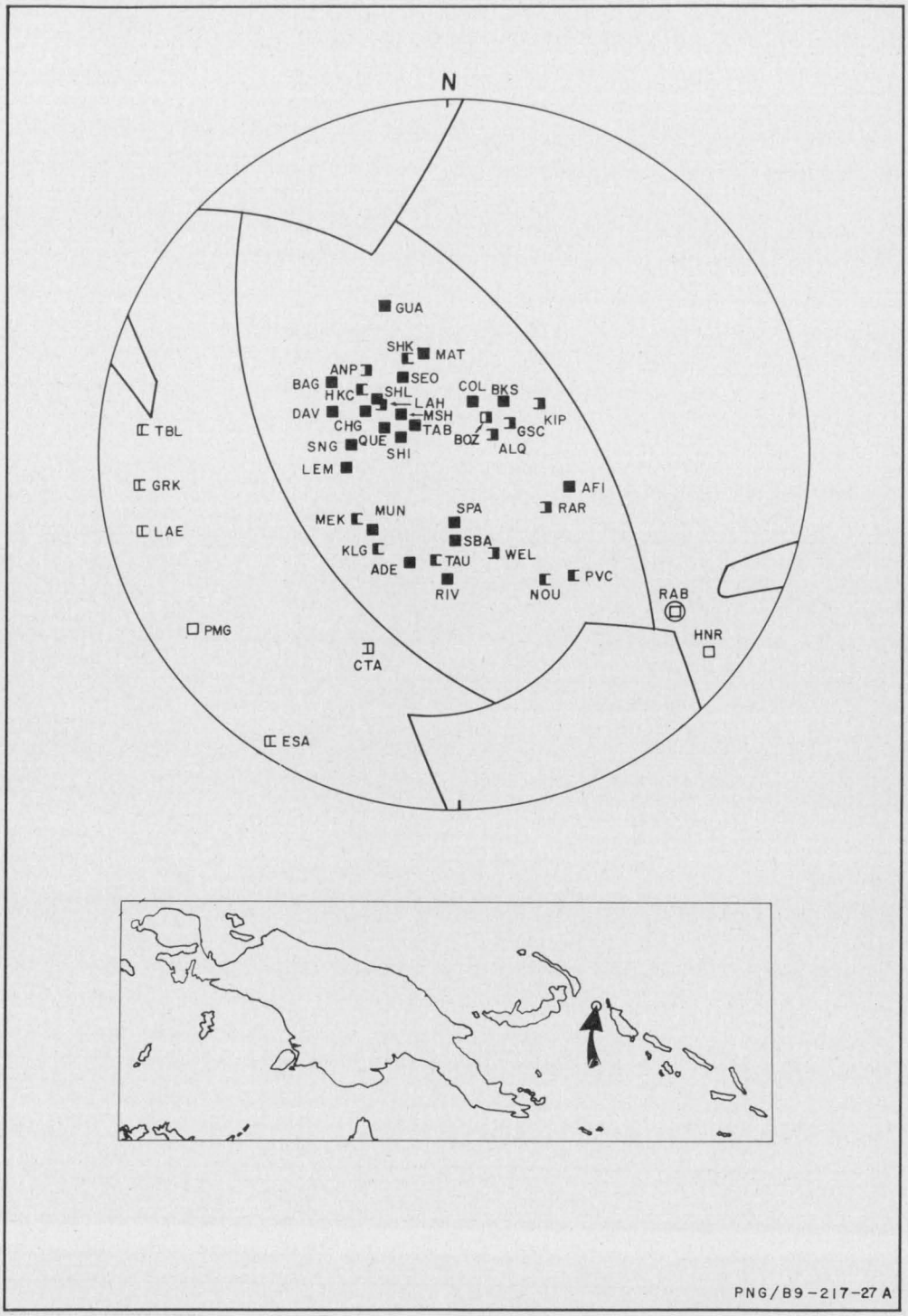
N
GUA
SHK
MAT
ANP
SEO
BAG
HKC
SHL
COL
BKS
LAH
DAV
MSH
KIP
CHG
TAB
GSC
SNG
QUE
BOZ
ALQ
SHI
LEM
TBL
GRK
LAE
AFI
MEK
MUN
SPA
RAR
SBA
KLG
TAU
WEL
ADE
PVC
RIV
NOU
RAB
PMG
HNR
CTA
ESA
PNG/89-217-27 A

FIGURE 28

Number	: 27			
Location	: 5.3°S, 153.7°E; north Solomon Sea 100 km west of Buka Island, on the northeast side of Bougainville Trench			
Origin Time	: 25 December 1967 at 01 23 33.6 UT			
Depth	: 64 km			
Magnitude (M)	: 7.0			
Type	: Dip-slip overthrust			
Nodal Planes	:	Azimuth of Dip	Dip	
	:	Too uncertain		
	:			
Nodal-Plane Poles	:	Azimuth	Plunge	
	:			
	:			
P Axis	:			
T Axis	:			
		Azimuth	Plunge	Uncertainty
B Axis	:			

The solution is poor, and has two possibilities, both of which are overthrusts. There is considerable uncertainty in the orientation of the B axis.

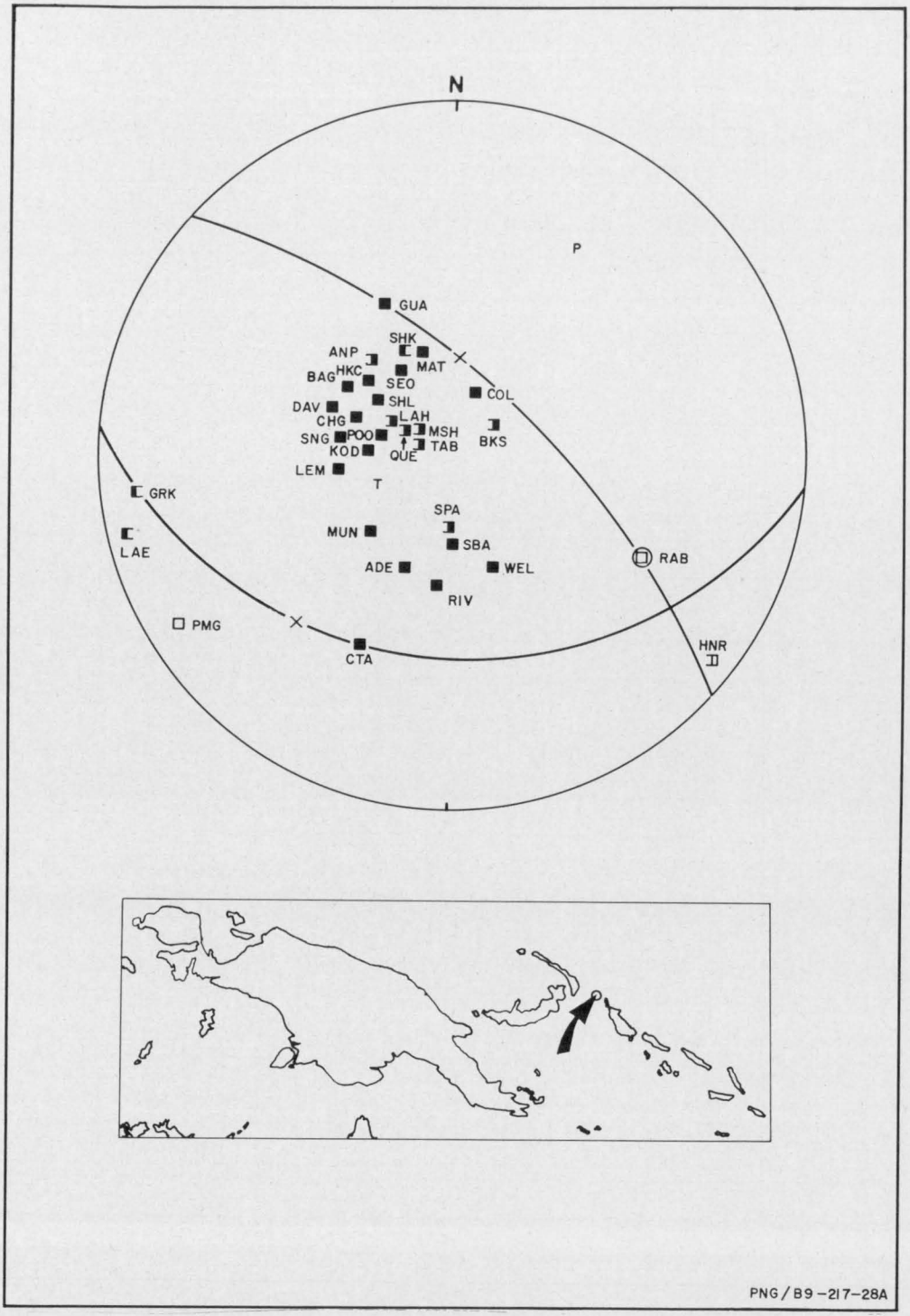
N
P
GUA
SHK
ANP
MAT
BAG
HKC
SEO
COL
SHL
DAV
LAH
CHG
MSH
SNG
POO
TAB
BKS
KOD
QUE
LEM
T
GRK
SPA
MUN
SBA
LAE
ADE
WEL
RAB
RIV
PMG
HNR
CTA
PNG/B9-217-28A

FIGURE 29

Number	:	28		
Location	:	5.1°S, 153.9°E; north Solomon Sea 70 km west of Buka Island, on the northeast side of Bougainville Trench		
Origin Time	:	7 January 1968 at 09 56 40.3 UT		
Depth	:	118 km		
Magnitude (M)	:	6.1		
Type	:	Dip-slip overthrust (non-orthogonal)		
Nodal Planes	:	Azimuth of Dip	Dip	
	:	042	65	
	:	185	31	
Nodal-Plane Poles	:	Azimuth	Plunge	
	:	222	25	
	:	005	59	
P Axis	:	029	18	
T Axis	:	253	66	
		Azimuth	Plunge	Uncertainty
B Axis	:	124	15	—

The orientation of the solution is constrained by the stations LAE and GRK, both of which recorded weak compressions. However, the solution so obtained is non-orthogonal, as LAE and HNR are in the wrong quadrants, but uncertainties in the positions of these stations on the focal sphere could account for the discrepancy.

If LAE and GRK are ignored, the orientation of the solution can swing from its northwest strike through north to northeast.

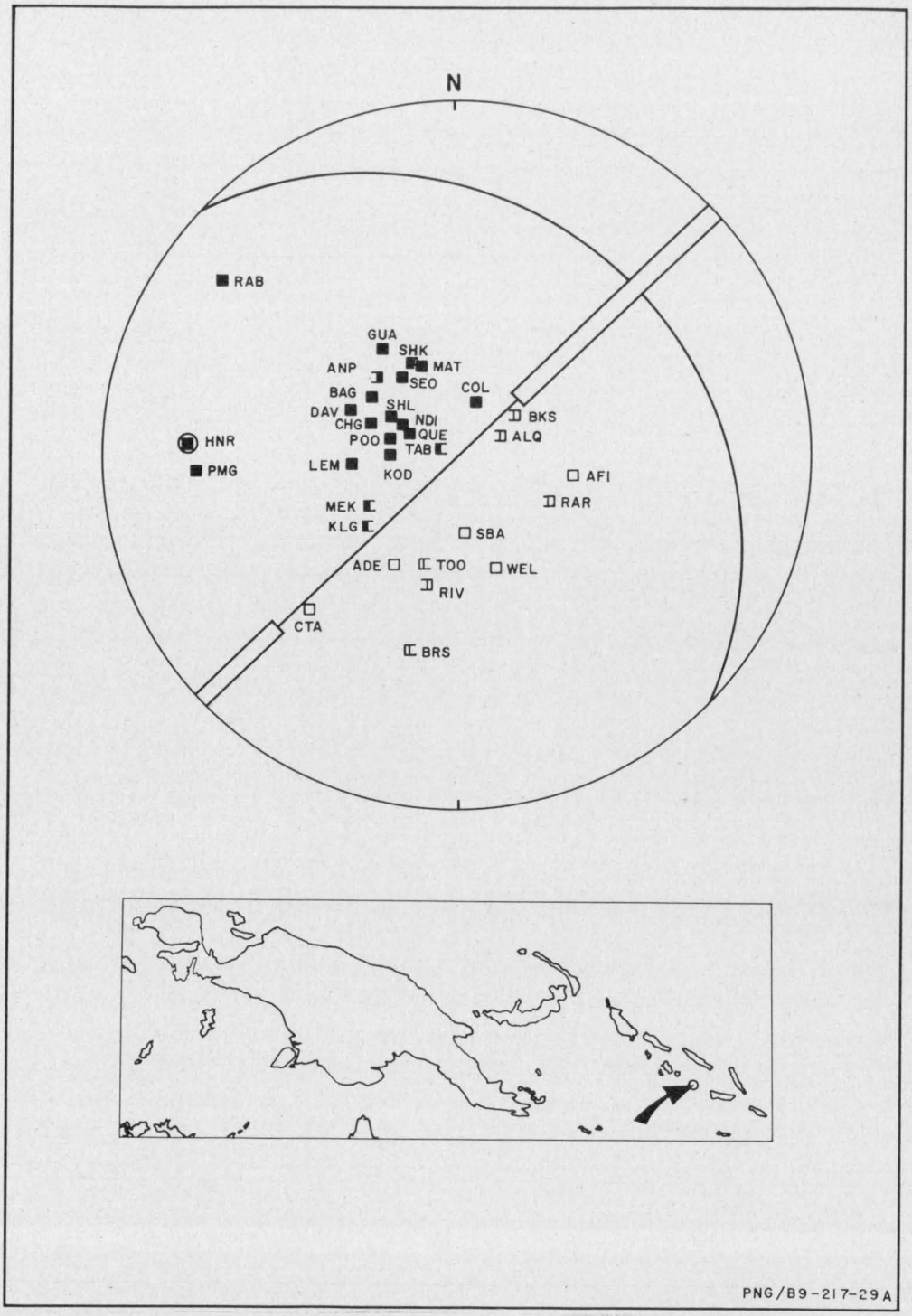
N
RAB
GUA
SHK
MAT
ANP
SEO
COL
BAG
SHL
BKS
DAV
CHG
NDI
ALQ
HNR
POO
QUE
TAB
PMG
LEM
KOD
AFI
RAR
MEK
KLG
SBA
ADE
TOO
WEL
RIV
CTA
BRS
PNG/B9-217-29A

FIGURE 30

Number	: 29			
Location	: 9.4°S, 158.4°E; east Solomon Sea 120 km west of Guadalcanal			
Origin Time	: 19 January 1968 at 06 04 38.2 UT			
Depth	: 33 km			
Magnitude (M)	: 6.5			
Type	: Dip-slip or strike-slip			
Nodal Planes	:	Azimuth of Dip	Dip	
	:	Too uncertain		
	:			
Nodal-Plane Poles	:	Azimuth	Plunge	
	:			
	:			
P Axis	:			
T Axis	:			
		Azimuth	Plunge	Uncertainty
B Axis	:			

The station distribution is inadequate and the solution poor. There are no station readings in the east and northwest to constrain the northwest-striking nodal plane. Both dip-slip and strike-slip solutions are possible, but Johnson & Molnar (1972) obtained a strike-slip solution for the earthquake.

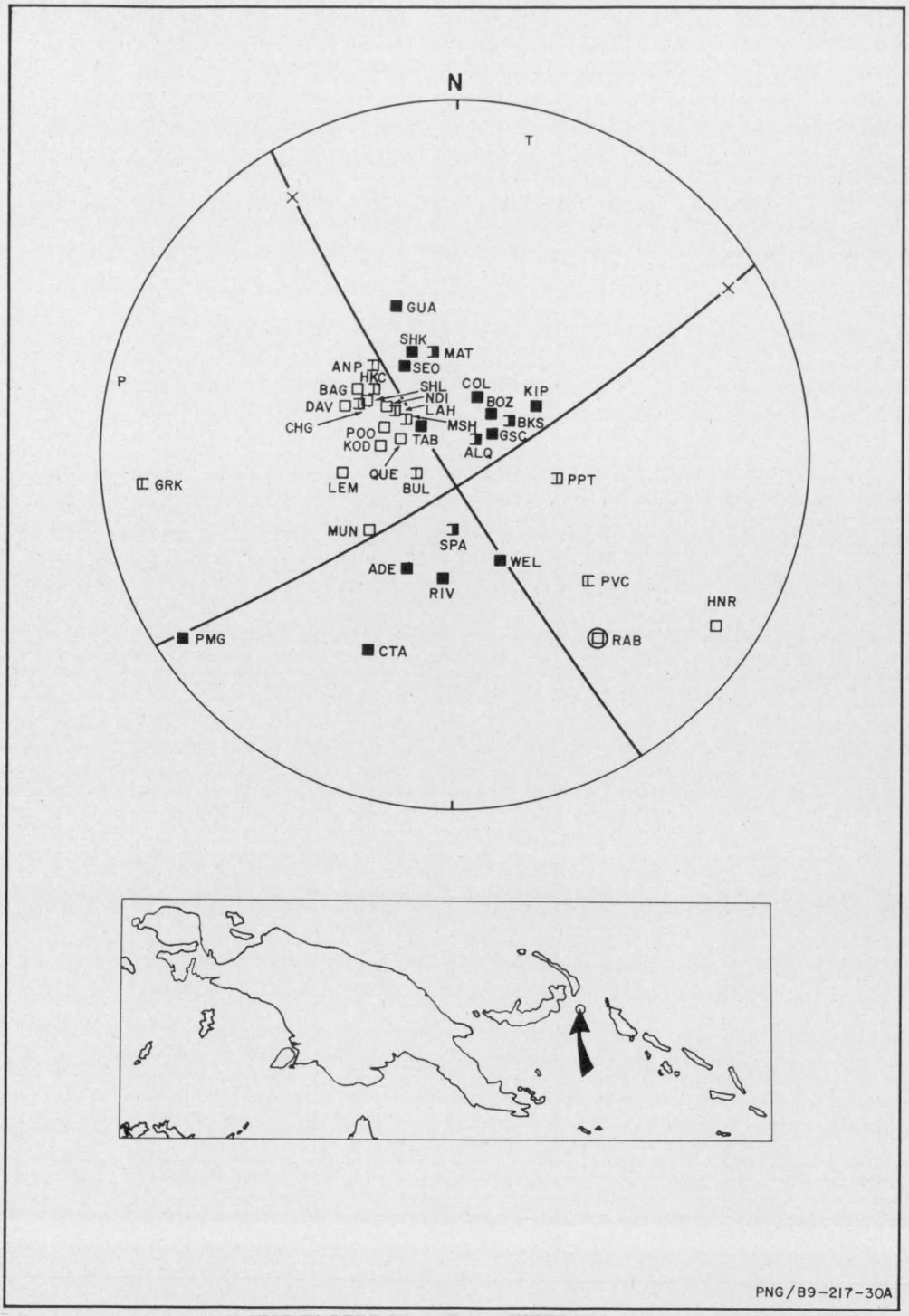
N
T
P
GUA
SHK
MAT
ANP
SEO
HKC
BAG
SHL
COL
KIP
DAV
NDI
BOZ
LAH
CHG
MSH
BKS
POO
GSC
KOD
TAB
ALQ
GRK
LEM
QUE
BUL
PPT
MUN
SPA
ADE
WEL
RIV
PVC
HNR
PMG
CTA
RAB
PNG/B9-217-30A

FIGURE 31

Number	: 30			
Location	: 5.5°S, 153.2°E; north Solomon Sea 60 km south of New Ireland			
Origin Time	: 12 February 1968 at 05 44 47.6 UT			
Depth	: 74 km			
Magnitude (M)	: 7.2			
Type	: Strike-slip			
Nodal Planes	:	Azimuth of Dip	Dip	
	:	239	85	
	:	149	82	
Nodal-Plane Poles	:	Azimuth	Plunge	
	:	059	05	
	:	329	08	
P Axis	:	283	02	
T Axis	:	013	10	
		Azimuth	Plunge	Uncertainty
B Axis	:	180	81	1 x 1

The solution is good: it is tight, with stations in the four quadrants.

If the nodal plane striking northwest is the fault plane, the motion is sinistral.

Plotted in Plate 2.

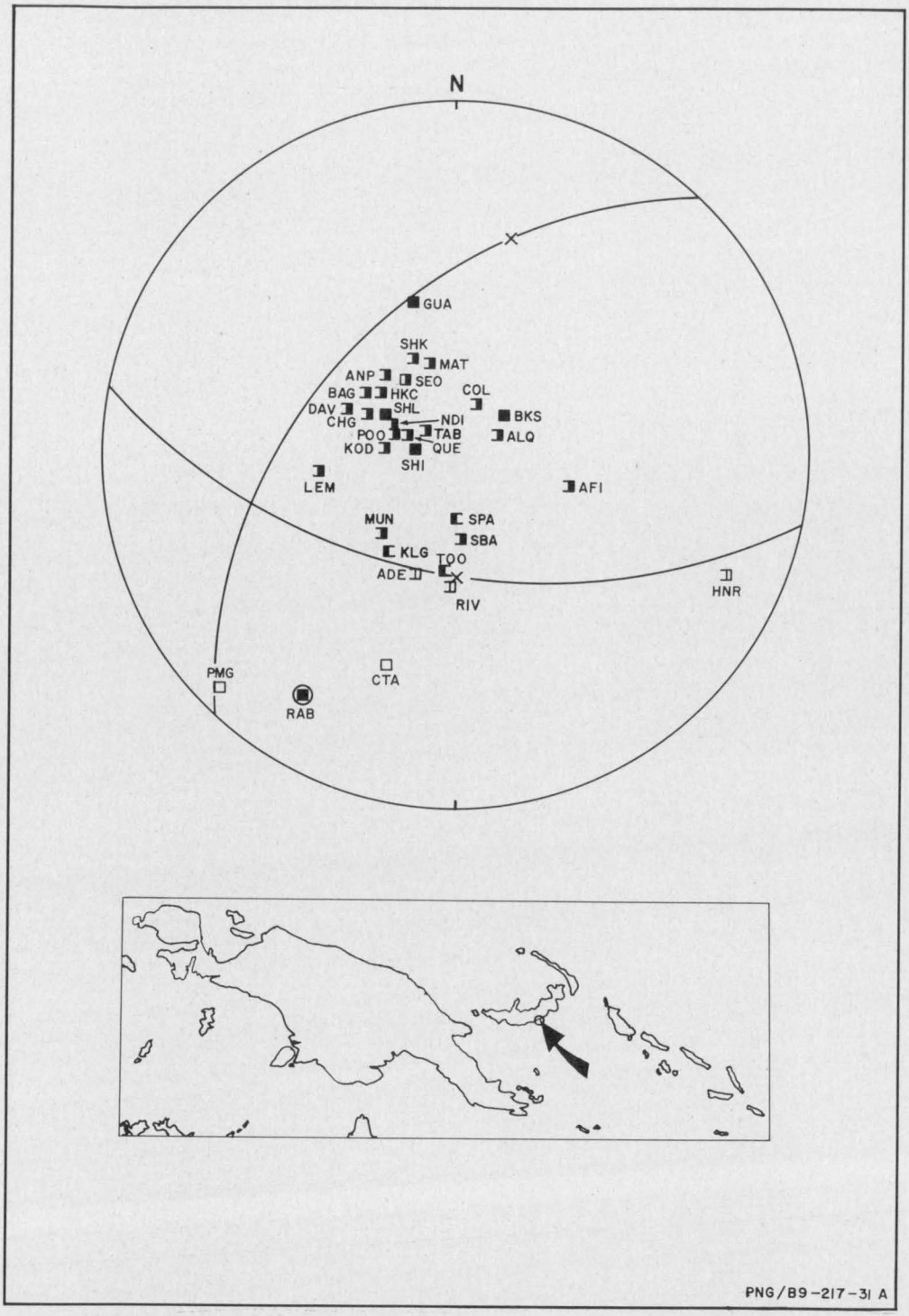
N
GUA
SHK
MAT
ANP
SEO
BAG
HKC
COL
DAV
SHL
CHG
NDI
BKS
POO
TAB
ALQ
KOD
QUE
SHI
LEM
AFI
MUN
SPA
SBA
KLG
TOO
ADE
RIV
HNR
PMG
CTA
RAB
PNG/89-217-31 A

FIGURE 32

Number	: 31			
Location	: 5.9°S, 151.1°E; southeast New Britain coast			
Origin Time	: 7 March 1968 at 13 22 16.6 UT			
Depth	: 39 km			
Magnitude (M)	: 6.0			
Type	: Dip-slip overthrust (non-orthogonal)			
Nodal Planes	:	Azimuth of Dip	Dip	
	:	Too uncertain		
	:			
Nodal-Plane Poles	:	Azimuth	Plunge	
	:			
	:			
P Axis	:			
T Axis	:			
		Azimuth	Plunge	Uncertainty
B Axis	:			

The solution is poor. An orthogonal solution was not obtained because the RAB arrival is a compression well within a dilatational quadrant. Its position on the focal sphere is uncertain. However, if the earthquake occurred at a shallow depth within (but not below) the crust, the RAB recording would fit the solution.

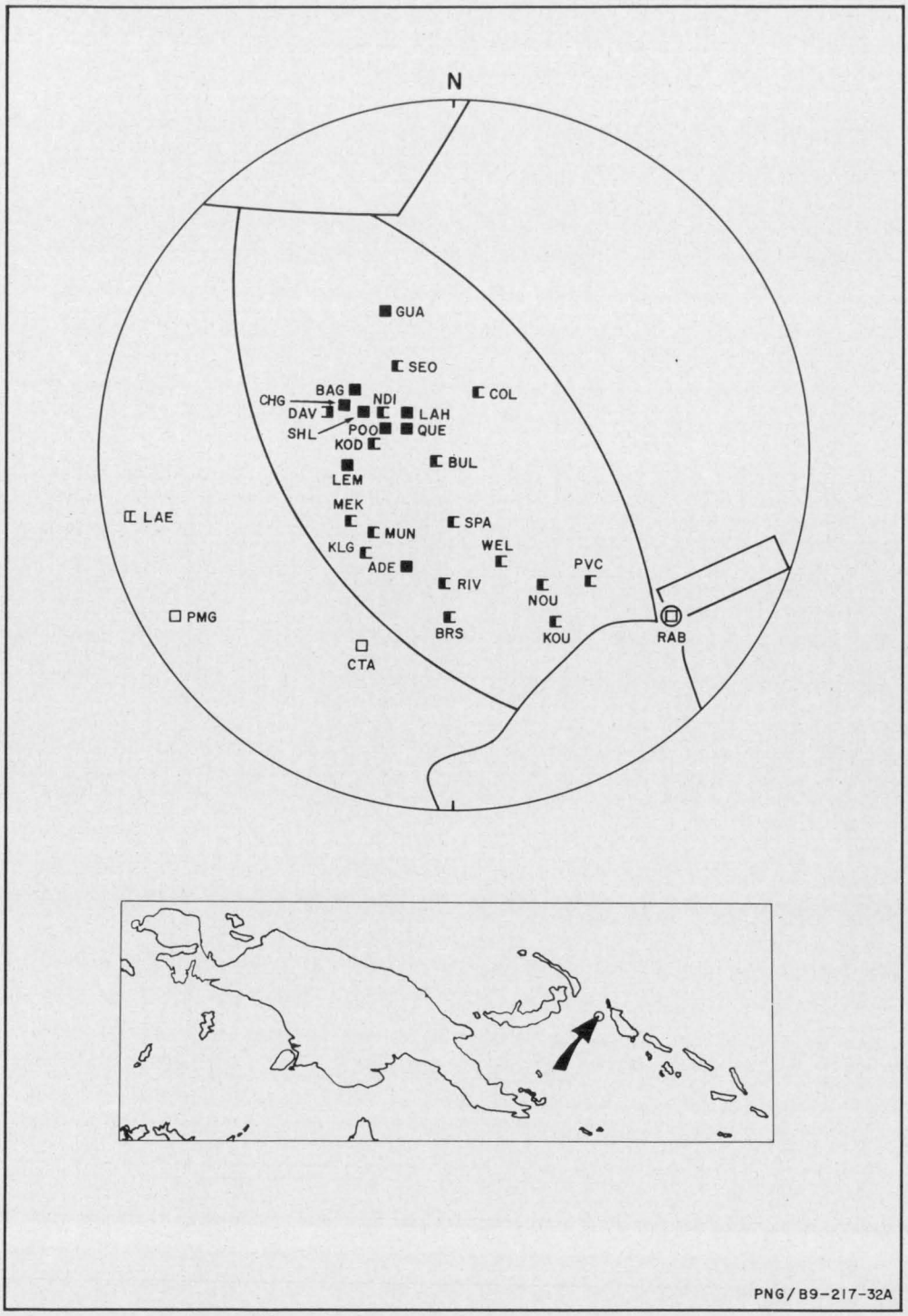
N
GUA
SEO
BAG
CHG
NDI
COL
DAV
LAH
SHL
POO
QUE
KOD
BUL
LEM
MEK
LAE
SPA
MUN
KLG
WEL
ADE
PVC
RIV
NOU
PMG
BRS
KOU
RAB
CTA
PNG/89-217-32A

FIGURE 33

Number	: 32			
Location	: 5.6°S, 154.0°E; 70 km west of the northern tip of Bougainville			
Origin Time	: 9 March 1968 at 03 19 23.7 UT			
Depth	: 86 km			
Magnitude (M)	: 6.0			
Type	: Dip-slip overthrust			
Nodal Planes	:	Azimuth of Dip	Dip	
	:	Too uncertain		
	:			
Nodal-Plane Poles	:	Azimuth	Plunge	
	:			
	:			
P Axis	:			
T Axis	:			
		Azimuth	Plunge	Uncertainty
B Axis	:			

The station distribution is poor and two overthrust solutions are possible. The strike can vary from north to northwest, parallel to Bougainville.

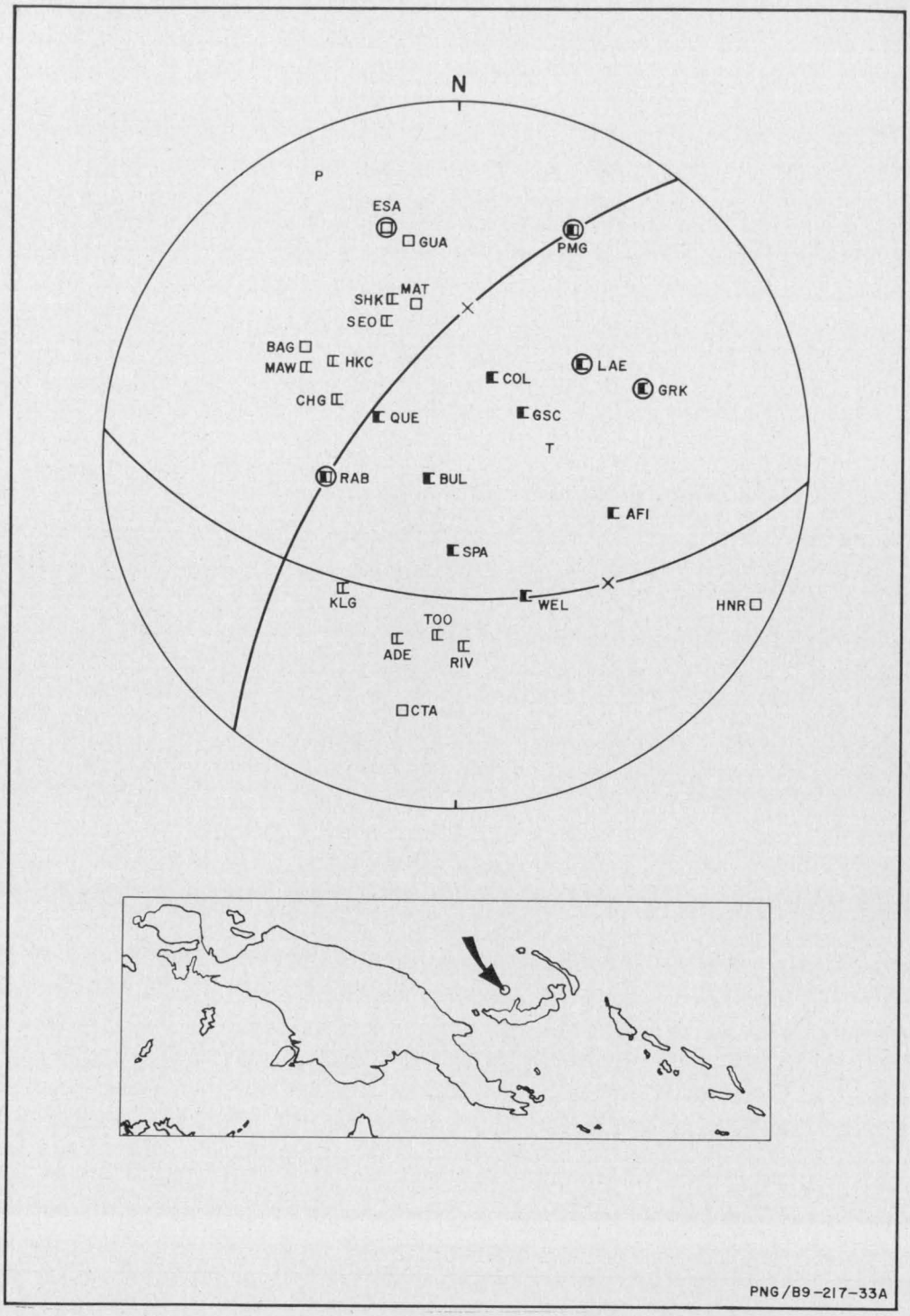
N
P
ESA
GUA
PMG
SHK
MAT
SEO
BAG
MAW
HKC
COL
LAE
GRK
CHG
QUE
GSC
T
RAB
BUL
AFI
SPA
KLG
WEL
HNR
TOO
ADE
RIV
CTA
PNG/B9-217-33A

FIGURE 34

Number	:	33		
Location	:	4.6°S, 149.4°E; Vitu Island, southeast Bismarck Sea		
Origin Time	:	24 April 1968 at 13 59 14.5 UT		
Depth	:	565 km		
Magnitude (M)	:	5.9		
Type	:	Dip-slip overthrust		
Nodal Planes	:	Azimuth of Dip	Dip	
	:	309	60	
	:	184	46	
Nodal-Plane Poles	:	Azimuth	Plunge	
	:	129	30	
	:	004	44	
P Axis	:	334	08	
T Axis	:	077	59	
		Azimuth	Plunge	Uncertainty
B Axis	:	239	31	1 x 1

The solution is based mainly on short-period P-wave arrivals, for at most stations the long-period recordings were too weak. Stations PMG and RAB recorded first-motion compressions on the short period, and first-motion dilatations a fraction of a second later on the long period. The possible explanation for this anomaly is that the stations are on or close to a nodal plane, and the nodal plane orientation differs slightly for the two wave types. The nodal plane was drawn through the two stations.

The most significant aspect of the solution is the northwest horizontal orientation of the compressional stress axis, which contrasts with the observations of Isacks & Molnar (1971) that the compressional stress axes of deep-focus earthquakes tend to parallel the dip of the Benioff zone.

Plotted in Plate 4.

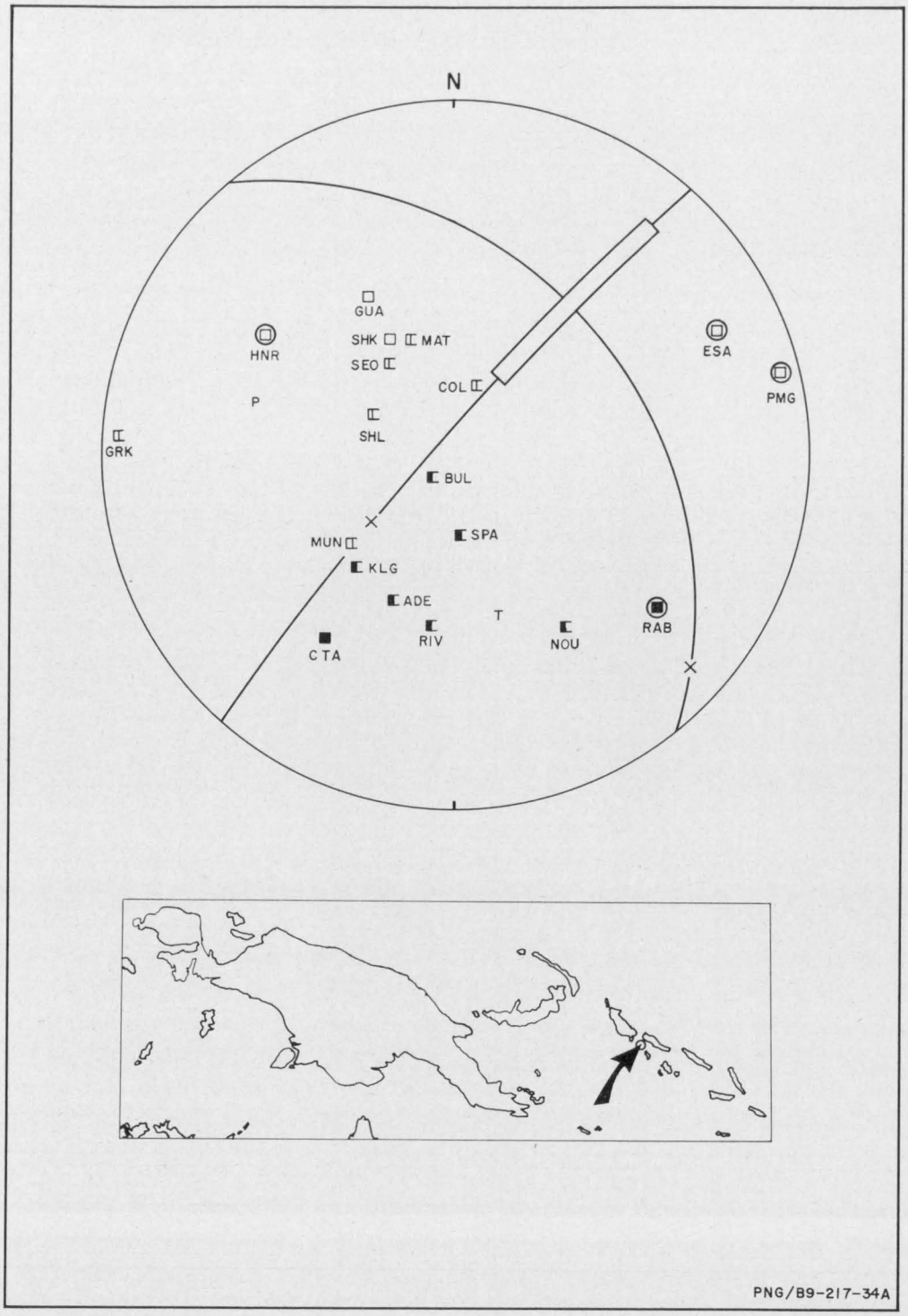
N
GUA
HNR
SHK
MAT
SEO
COL
ESA
PMG
P
SHL
GRK
BUL
MUN
SPA
KLG
ADE
T
RAB
RIV
NOU
CTA
PNG/89-217-34A

FIGURE 35

Number	: 34			
Location	: 7.1°S, 156.2°E; 40 km southeast of Bougainville			
Origin Time	: 25 April 1968 at 17 14 27.7 UT			
Depth	: 419 km			
Magnitude (M)	: 5.3			
Type	: Dip-slip or strike-slip			
Nodal Planes	:	Azimuth of Dip	Dip	
	:	312	84	
	:	052	34	
Nodal-Plane Poles	:	Azimuth	Plunge	
	:	132	06	
	:	232	56	
P Axis	:	285	30	
T Axis	:	163	41	
		Azimuth	Plunge	Uncertainty
B Axis	:	038	34	54 x 1

The solution is poor: most P-wave arrivals were weak and recorded only by short-period seismographs. Although one nodal plane is well constrained, there is little control over the orientation of the other, and the solution can be either strike-slip or dip-slip.

Neither the compressional axis nor the tensional axis tend to parallel the Benioff zone, which is vertical at the earthquake hypocentre.

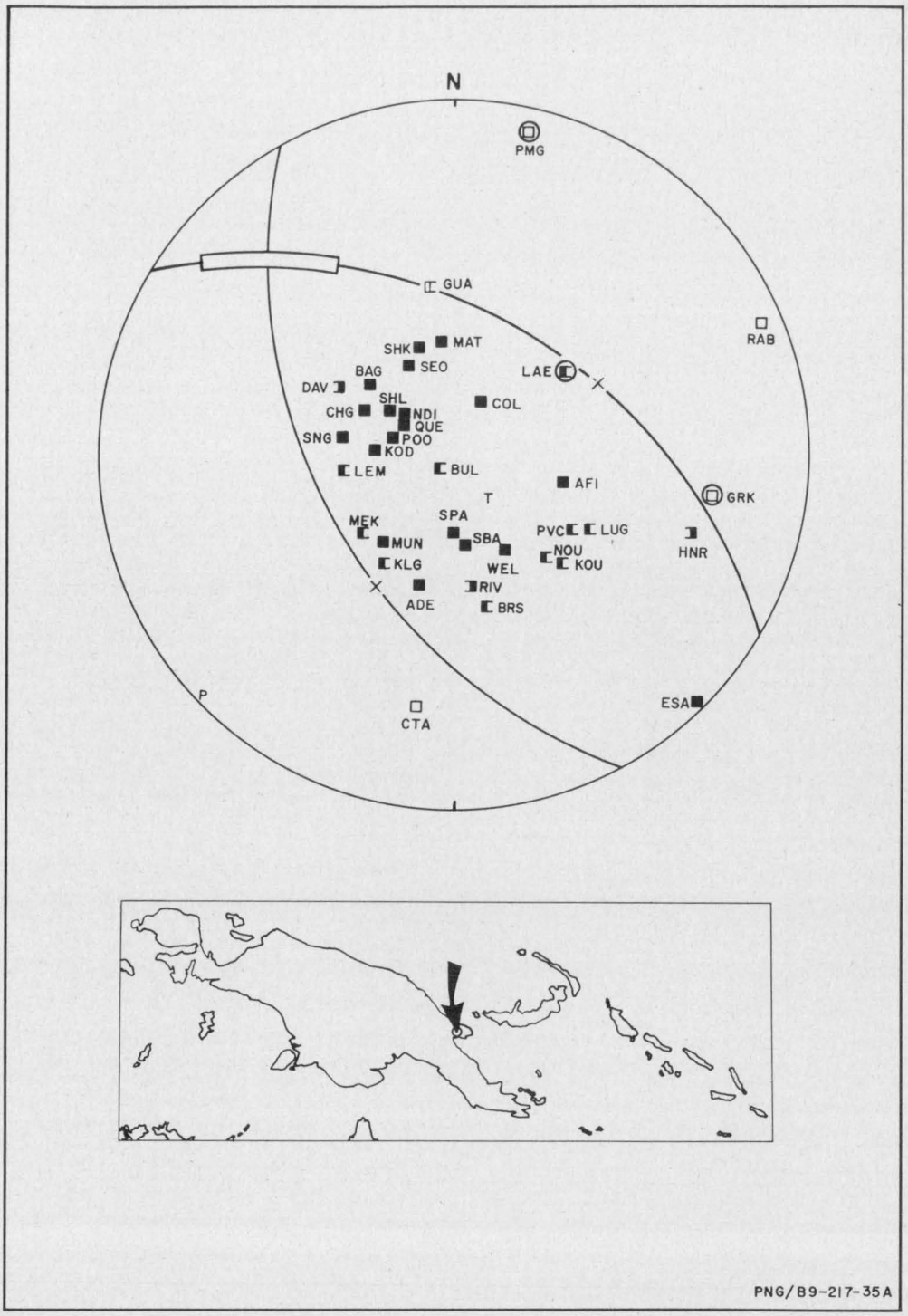
N
PMG
GUA
RAB
SHK
MAT
BAG
SEO
LAE
DAV
SHL
COL
CHG
NDI
QUE
SNG
POO
KOD
LEM
BUL
AFI
GRK
T
MEK
SPA
PVC
LUG
MUN
SBA
NOU
HNR
KLG
WEL
KOU
RIV
ADE
BRS
P
CTA
ESA
PNG/89-217-35A

FIGURE 36

Number	: 35			
Location	: 6.4°S, 147.3°E; Huon Peninsula			
Origin Time	: 11 May 1968 at 15 33 41.2 UT			
Depth	: 76 km			
Magnitude (M)	: 5.8			
Type	: Dip-slip overthrust			
Nodal Planes	:	Azimuth of Dip	Dip	
	:	031	46	
	:	241	48	
Nodal-Plane Poles	:	Azimuth	Plunge	
	:	211	44	
	:	061	42	
P Axis	:	227	01	
T Axis	:	133	75	
		Azimuth	Plunge	Uncertainty
B Axis	:	317	15	28 x 1

Although there is only one station (CTA) in the southwest quadrant, the solution, an overthrust striking northwest, is reasonably good.

The compressional stress axis is horizontal, and about orthogonal to the north coast of the Huon Peninsula. In view of the rapid elevation of the Huon Peninsula in Pleistocene and Recent times (Thompson, 1967) the earthquake may be related to a continuation of this process.

Plotted in Plate 3.

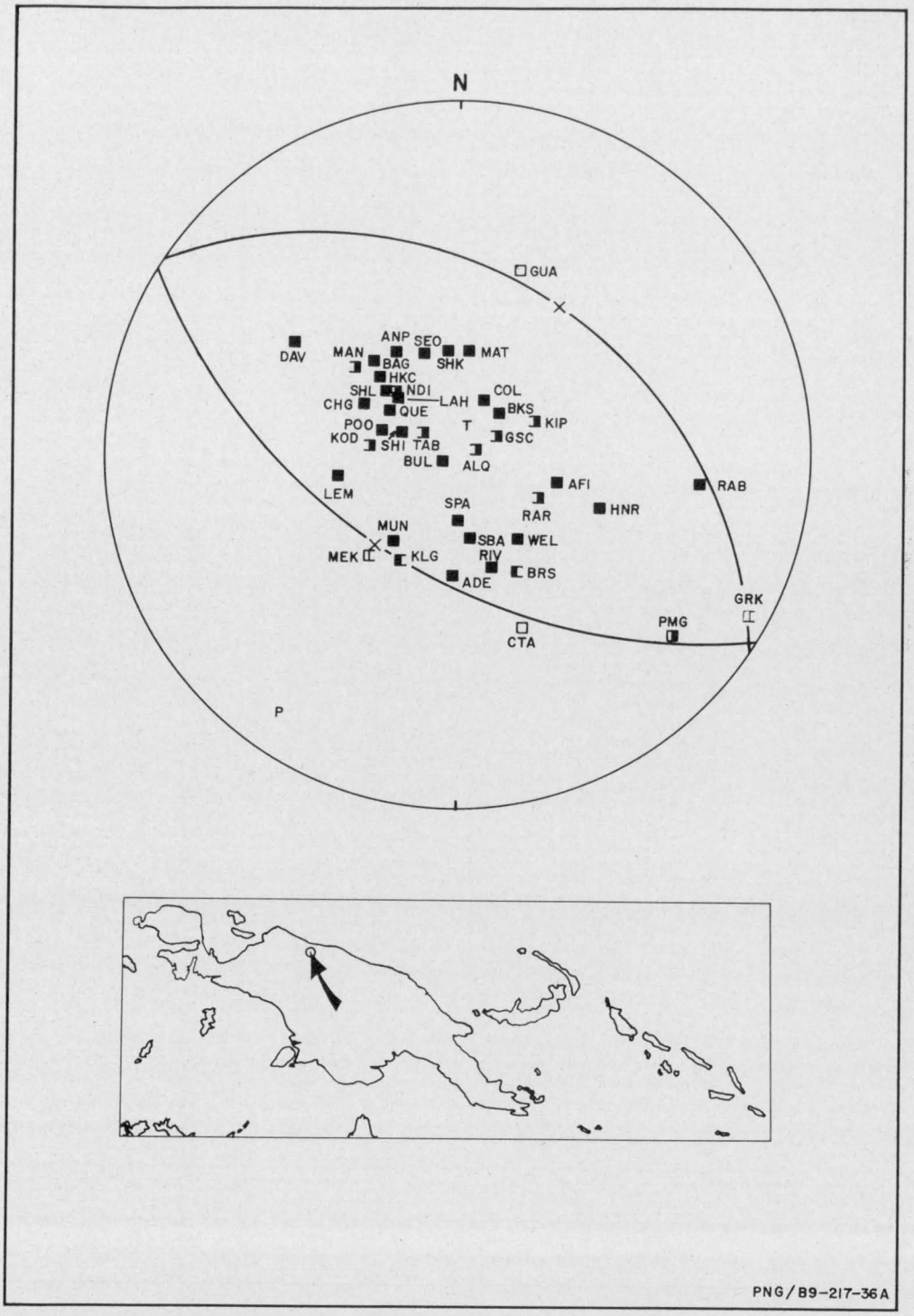
N
GUA
ANP
SEO
DAV
MAN
MAT
BAG
SHK
HKC
SHL
NDI
COL
CHG
LAH
QUE
BKS
POO
T
KIP
KOD
SHI
TAB
GSC
BUL
ALQ
LEM
AFI
RAB
SPA
HNR
RAR
MUN
SBA
WEL
MEK
KLG
RIV
BRS
ADE
GRK
PMG
CTA
P
PNG/89-217-36A

FIGURE 37

Number	: 36			
Location	: 2.9°S, 139.3°E; Irian Jaya 200 km west of Vanimo			
Origin Time	: 28 May 1968 at 13 27 18.7 UT			
Depth	: 65 km			
Magnitude (M)	: 6.7			
Type	: Dip-slip overthrust			
Nodal Planes	:	Azimuth of Dip	Dip	
	:	036	37	
	:	213	53	
Nodal-Plane Poles	:	Azimuth	Plunge	
	:	216	53	
	:	033	37	
P Axis	:	214	08	
T Axis	:	036	81	
		Azimuth	Plunge	Uncertainty
B Axis	:	123	01	1 x 1

The solution is an overthrust with the compressional stress axis horizontal and oriented southwest, orthogonal to the north coast of Irian Jaya. The PMG arrivals are of opposite polarity, but weak, and the station is probably on a nodal plane.

Plotted in Plate 3.

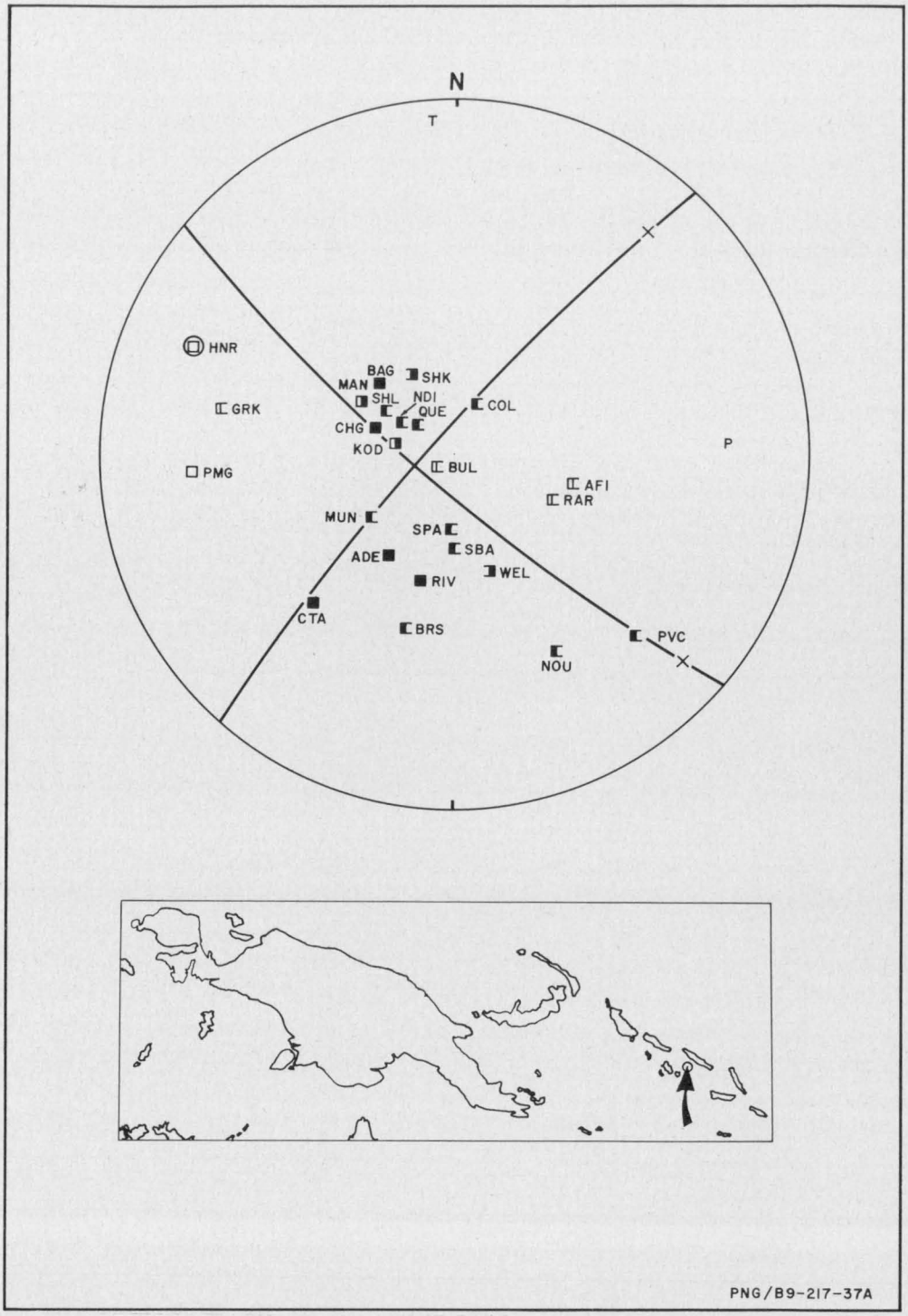
N
T
HNR
BAG
SHK
MAN
SHL
NDI
QUE
COL
GRK
CHG
KOD
P
PMG
BUL
AFI
RAR
MUN
SPA
SBA
ADE
WEL
RIV
CTA
BRS
PVC
NOU
PNG/B9-217-37A

FIGURE 38

Number	: 37			
Location	: 8.1°S, 158.6°E; New Georgia Sound			
Origin Time	: 2 June 1968 at 08 18 36.2 UT			
Depth	: 35 km			
Magnitude (M)	: 5.8			
Type	: Strike-slip			
Nodal Planes	:	Azimuth of Dip	Dip	
	:	312	82	
	:	221	79	
Nodal-Plane Poles	:	Azimuth	Plunge	
	:	132	08	
	:	041	11	
P Axis	:	087	14	
T Axis	:	356	02	
		Azimuth	Plunge	Uncertainty
B Axis	:	257	76	1 x 1

The P-wave arrivals were weak, but a clear strike-slip solution was obtained, mainly from short-period recordings.

If the nodal plane striking northwest, parallel to the Solomon Islands chain, is the fault plane, the solution is sinistral.

Plotted in Plate 2.

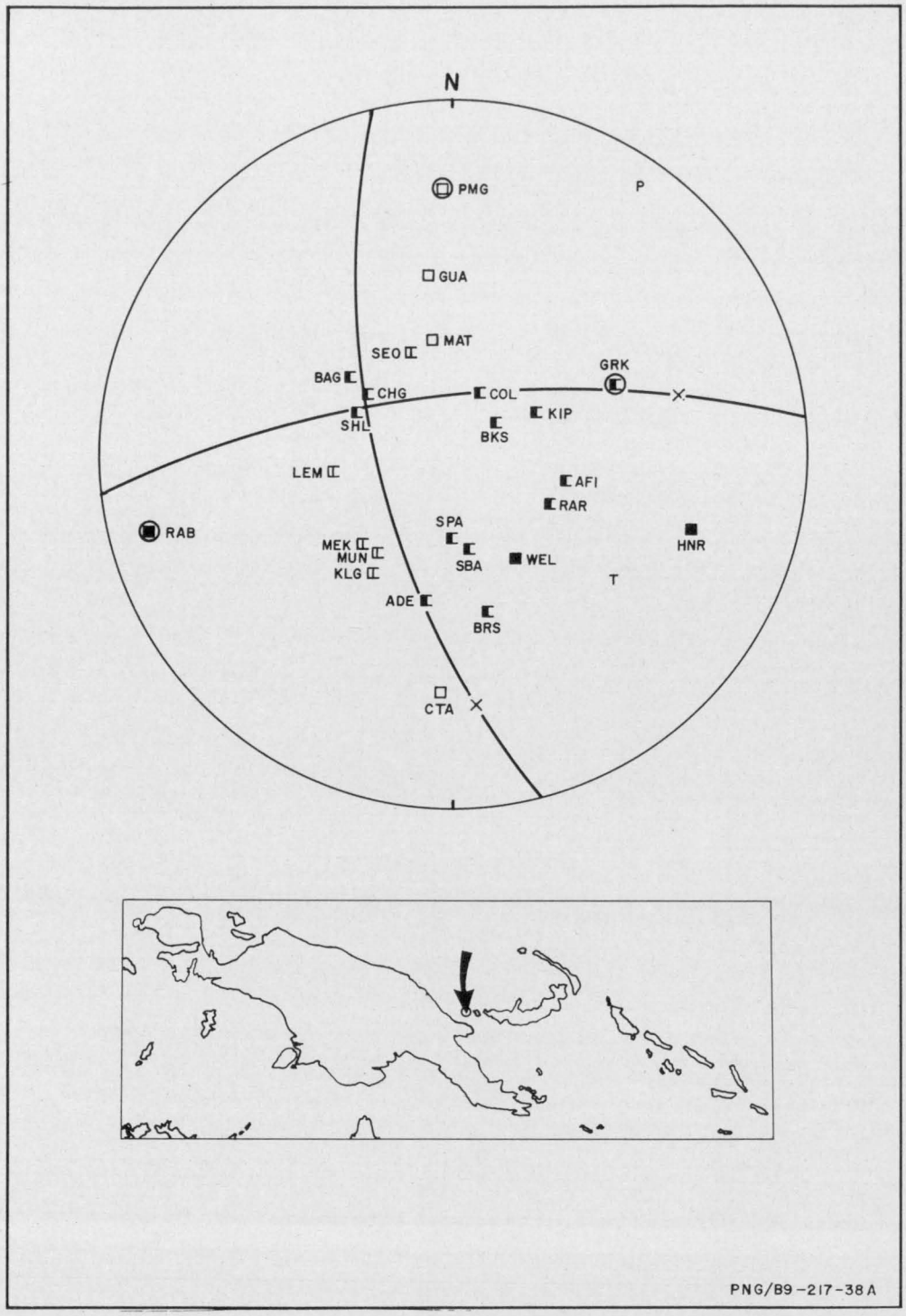
N
PMG
P
GUA
MAT
SEO
BAG
CHG
COL
GRK
SHL
KIP
BKS
LEM
AFI
RAR
SPA
RAB
HNR
MEK
MUN
KLG
SBA
WEL
T
ADE
BRS
CTA
PNG/89-217-38A

FIGURE 39

Number	: 38			
Location	: 5.4°S, 147.0°E; Long Island volcano			
Origin Time	: 3 June 1968 at 09 17 46.2 UT			
Depth	: 190 km			
Magnitude (M)	: 5.9			
Type	: Strike-slip (non-orthogonal)			
Nodal Planes	:	Azimuth of Dip	Dip	
	:	257	67	
	:	354	71	
Nodal-Plane Poles	:	Azimuth	Plunge	
	:	077	23	
	:	174	19	
P Axis	:	035	03	
T Axis	:	126	30	
		Azimuth	Plunge	Uncertainty
B Axis	:	300	60	—

The solution is non-orthogonal because station RAB recorded a compression in a dilatational quadrant. However, horizontal refraction of the seismic ray between the focus and Rabaul may account for the discrepancy.

Two other solutions for earthquakes with the same hypocentre (No. 4, 12 January 1964; and No. 26, 14 November 1967) are dip-slip overthrust.

Plotted in Plate 2.

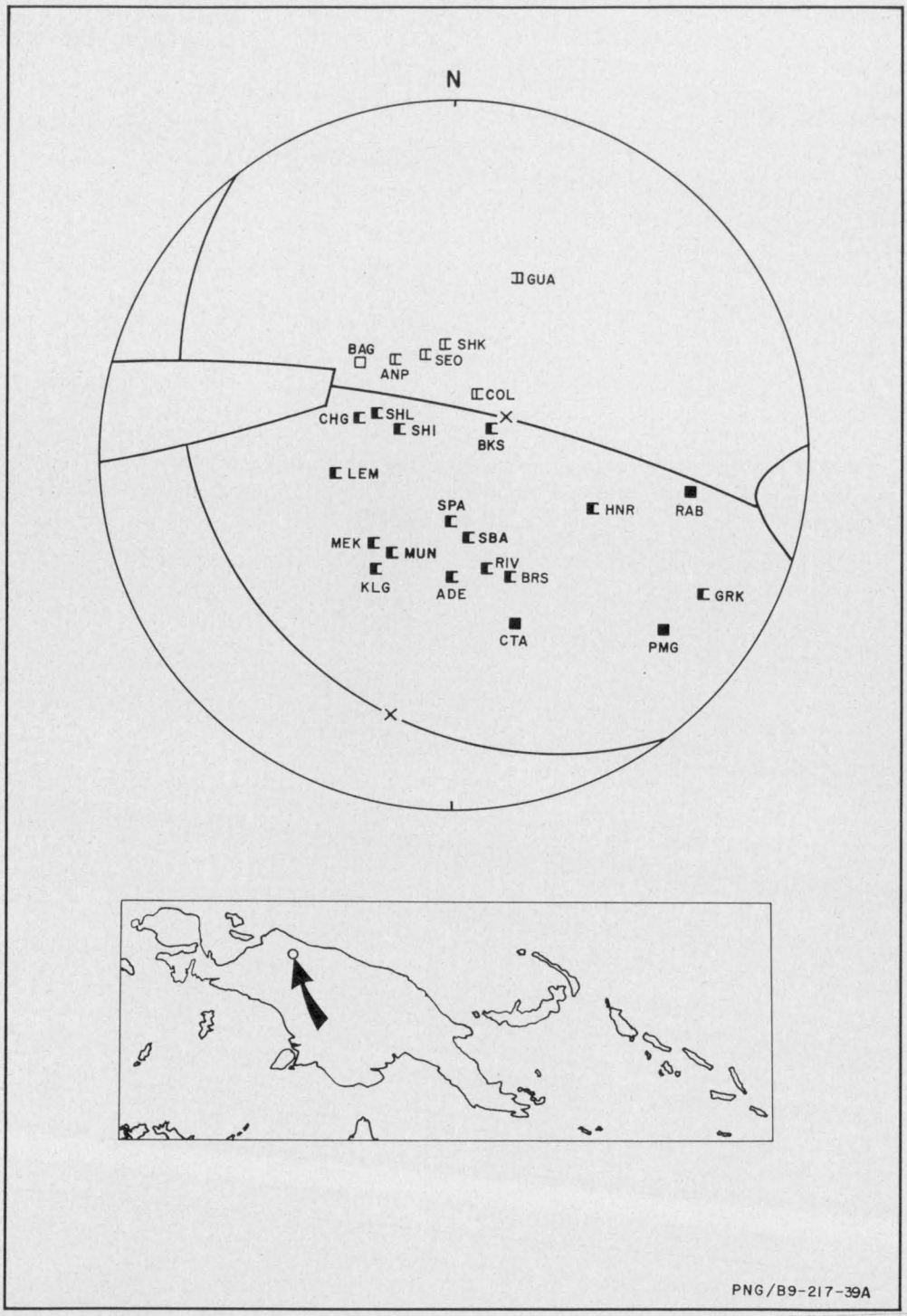
N
GUA
BAG
SHK
SEO
ANP
COL
CHG
SHL
SHI
BKS
LEM
SPA
HNR
RAB
SBA
MEK
MUN
RIV
KLG
ADE
BRS
GRK
CTA
PMG
PNG/B9-217-39A

FIGURE 40

Number	: 39			
Location	: 2.7°S, 138.9°E; Irian Jaya 250 km west of Vanimo			
Origin Time	: 2 July 1968 at 18 40 10.1 UT			
Depth	: 62 km			
Magnitude (M)	: 6.3			
Type	: Dip-slip overthrust or strike slip			
Nodal Planes	:	Azimuth of Dip	Dip	
	:	Too uncertain		
	:			
Nodal-Plane Poles	:	Azimuth	Plunge	
	:			
	:			
P Axis	:			
T Axis	:			
		Azimuth	Plunge	Uncertainty
B Axis	:			

The earthquake was weakly recorded and the solution is based mainly on short-period P-wave recordings. There is no control over one nodal plane, and its dip can vary from horizontal to 50°.

The approximate orientation of the tensional stress axis is south; it plunges 60°.

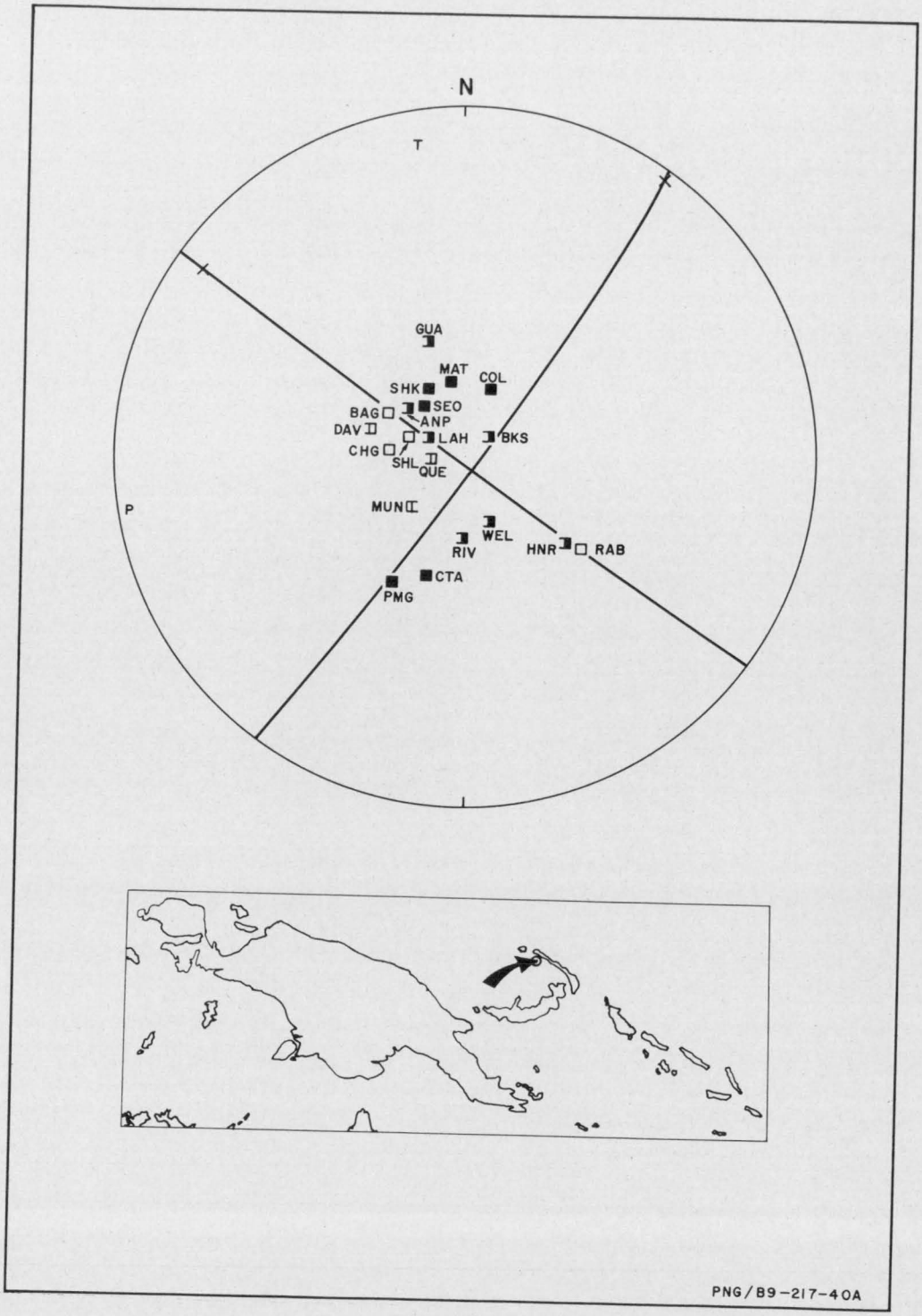
N
T
P
GUA
MAT
COL
SHK
SEO
BAG
ANP
DAV
LAH
BKS
CHG
SHL
QUE
MUN
WEL
RIV
HNR
RAB
CTA
PMG
PNG/89-217-40A

FIGURE 41

Number	:	40		
Location	:	3.2°S, 150.7°E; 30 km south of Kavieng, New Ireland, at the eastern end of the Bismarck Sea seismic lineation.		
Origin Time	:	21 July 1968 at 05 52 10.4 UT		
Depth	:	5 km		
Magnitude (M)	:	6.1		
Type	:	Strike-slip		
Nodal Planes	:	Azimuth of Dip	Dip	
	:	216	89	
	:	126	85	
Nodal-Plane Poles	:	Azimuth	Plunge	
	:	036	01	
	:	306	05	
P Axis	:	262	03	
T Axis	:	352	05	
		Azimuth	Plunge	Uncertainty
B Axis	:	141	84	1 x 1

The strike-slip solution is well defined, although there is only one station in the eastern dilatational quadrant.

If the nodal plane striking northwest, parallel to New Ireland, is the fault plane, the motion is sinistral, with the Pacific side moving northwest past the Bismarck Sea side.

Plotted in Plate 2.

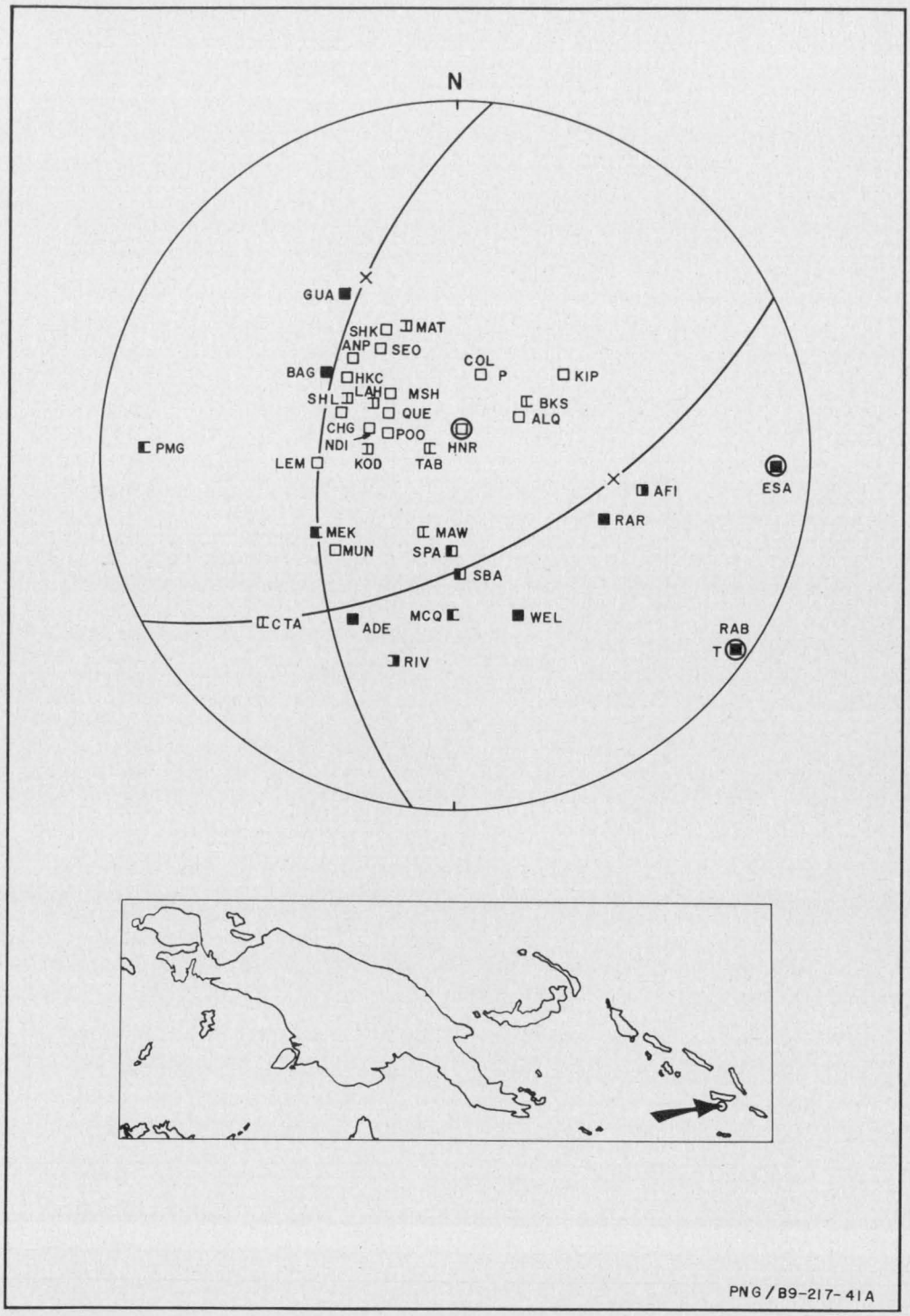
N
GUA
SHK
MAT
ANP
SEO
COL
P
KIP
BAG
HKC
LAH
MSH
SHL
BKS
QUE
ALQ
CHG
POO
PMG
NDI
HNR
LEM
KOD
TAB
AFI
ESA
RAR
MEK
MAW
MUN
SPA
SBA
CTA
ADE
MCQ
WEL
RAB
T
RIV
PNG/89-217-41A

FIGURE 42

Number	: 41			
Location	: 10.1°S, 159.9°E; 15 km south of Guadalcanal			
Origin Time	: 18 August 1968 at 18 38 30.6 UT			
Depth	: 538 km			
Magnitude (M)	: 6.2			
Type	: Dip-slip normal			
Nodal Planes	:	Azimuth of Dip	Dip	
	:	276	49	
	:	154	58	
Nodal-Plane Poles	:	Azimuth	Plunge	
	:	096	41	
	:	334	32	
P Axis	:	028	57	
T Axis	:	127	05	
		Azimuth	Plunge	Uncertainty
B Axis	:	220	52	2 x 2

The solution is tight but three stations recorded opposite-polarity P arrivals on the short-period and long-period seismographs.

Plotted in Plate 4.

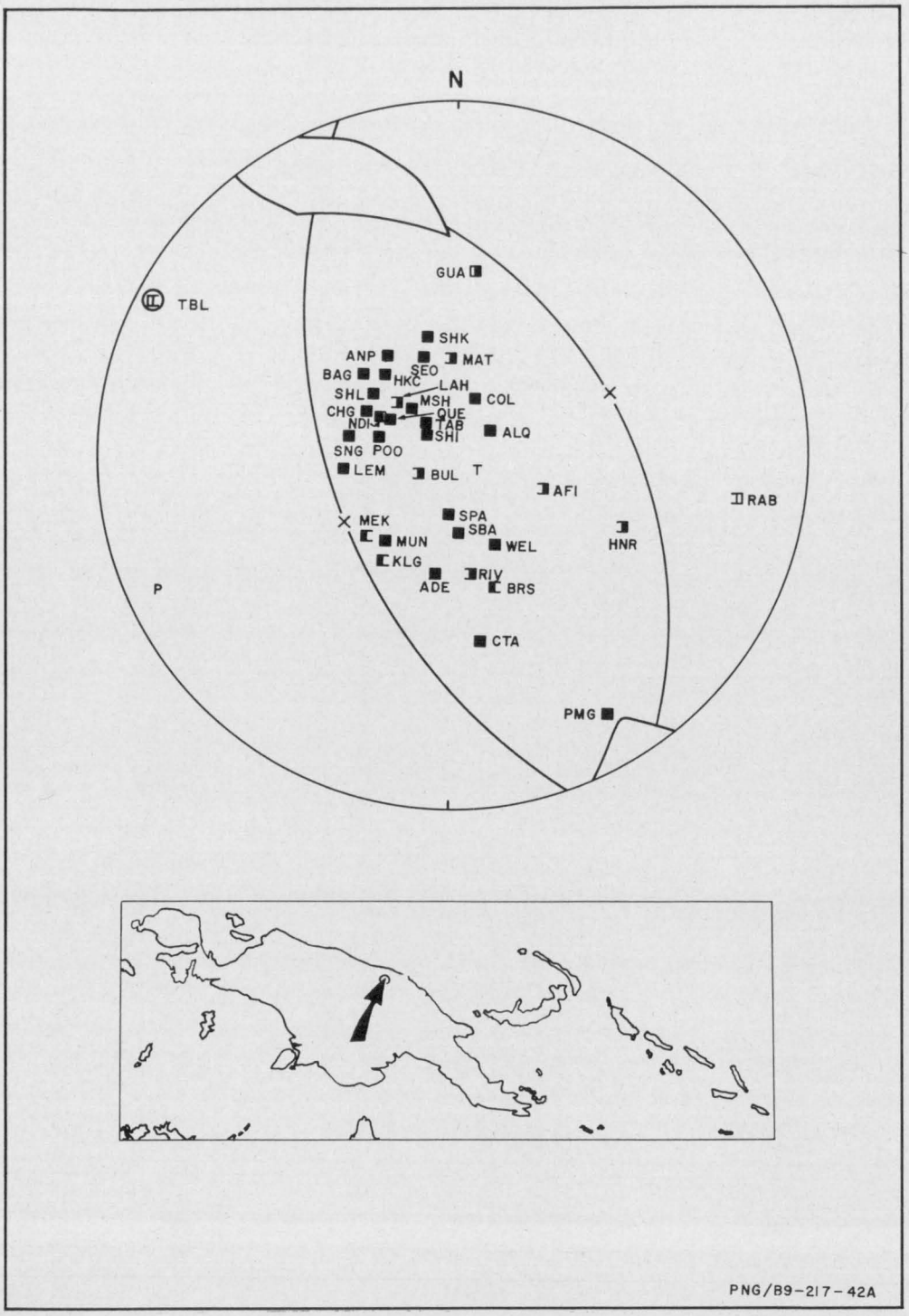
N
GUA
TBL
SHK
ANP
MAT
BAG
SEO
HKC
LAH
SHL
MSH
COL
CHG
QUE
NDI
TAB
ALQ
SHI
SNG
POO
LEM
BUL
T
AFI
RAB
MEK
SPA
SBA
MUN
WEL
HNR
KLG
RIV
ADE
BRS
P
CTA
PMG
PNG/89-217-42A

FIGURE 43

Number	: 42			
Location	: 3.7°S, 143.0°E; 60 km west of Wewak			
Origin Time	: 8 September 1968 at 15 12 23.8 UT			
Depth	: 29 km			
Magnitude (M)	: 6.2			
Type	: Dip-slip overthrust			
Nodal Planes	:	Azimuth of Dip	Dip	
	:	056	40	
	:	250	51	
Nodal-Plane Poles	:	Azimuth	Plunge	
	:	236	50	
	:	070	39	
P Axis	:	245	06	
T Axis	:	112	81	
		Azimuth	Plunge	Uncertainty
B Axis	:	334	05	44 x 12

The solution is poor because there are only two station readings in the dilatational quadrants. Johnson & Molnar (1972) obtained a strike-slip solution for this earthquake.

Plotted in Plate 3.

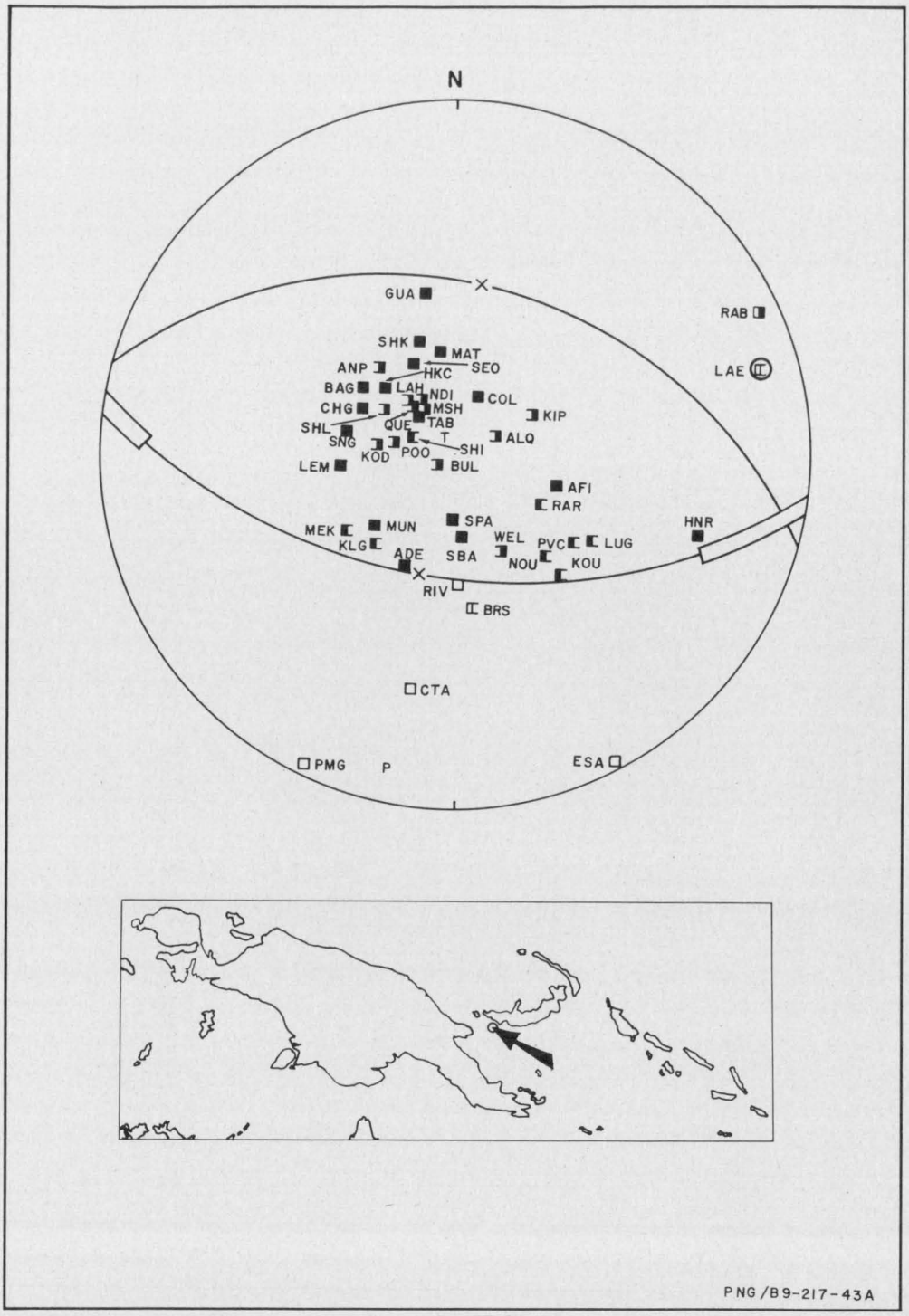
N
GUA
RAB
SHK
MAT
ANP
SEO
HKC
LAE
BAG
LAH
NDI
COL
CHG
MSH
KIP
SHL
QUE
TAB
SNG
T
ALQ
KOD
POO
SHI
LEM
BUL
AFI
RAR
MEK
MUN
SPA
HNR
KLG
WEL
PVC
LUG
ADE
SBA
NOU
KOU
RIV
BRS
CTA
PMG
P
ESA
PNG/B9-217-43A

FIGURE 44

Number	:	43		
Location	:	6.1°S, 148.7°E; southwest New Britain coast		
Origin Time	:	16 September 1968 at 13 55 36.1 UT		
Depth	:	59 km		
Magnitude (M)	:	6.3		
Type	:	Dip-slip overthrust		
Nodal Planes	:	Azimuth of Dip	Dip	
	:	014	38	
	:	188	52	
Nodal-Plane Poles	:	Azimuth	Plunge	
	:	194	52	
	:	008	38	
P Axis	:	190	07	
T Axis	:	346	82	
		Azimuth	Plunge	Uncertainty
B Axis	:	100	02	30 x 7

One nodal plane of the solution is poorly constrained and is restricted only by the orthogonality criterion. The Rabaul station long-period P-wave reading is anomalous, for it is a compressive precursor to a dilatation. However, there is enough uncertainty in the position of RAB on the focal sphere to move it closer to the nodal plane than indicated on the projection.

Plotted in Plate 3.

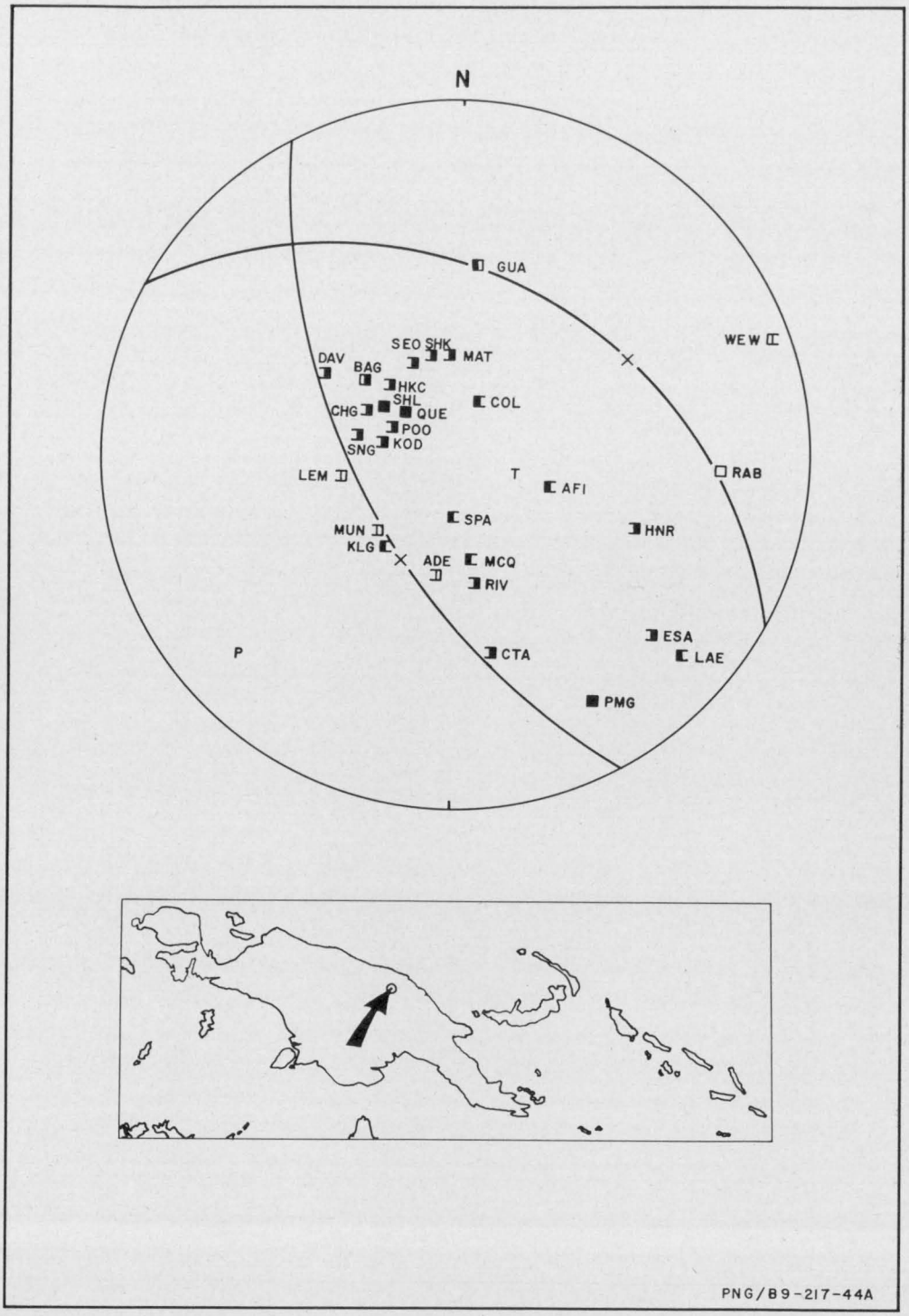
N
GUA
WEW
SEO
SHK
MAT
DAV
BAG
HKC
SHL
COL
CHG
QUE
POO
SNG
KOD
LEM
T
AFI
RAB
SPA
HNR
MUN
KLG
ADE
MCQ
RIV
ESA
P
CTA
LAE
PMG
PNG/B9-217-44A

FIGURE 45

Number	:	44		
Location	:	3.7°S, 143.3°E; 40 km southwest of Wewak		
Origin Time	:	27 September 1968 at 19 06 42.2 UT		
Depth	:	7 km		
Magnitude (M)	:	6.4		
Type	:	Dip-slip overthrust (non-orthogonal)		
Nodal Planes	:	Azimuth of Dip	Dip	
	:	028	37	
	:	242	58	
Nodal-Plane Poles	:	Azimuth	Plunge	
	:	208	53	
	:	062	32	
P Axis	:	228	12	
T Axis	:	102	70	
		Azimuth	Plunge	Uncertainty
B Axis	:	321	16	—

The solution is reasonably good except that ADE and the short-period component of BAG are dilatations in the compressional quadrant. The most likely explanation is that the first P-wave motion was obscured or too small to be detected and a later pulse was taken.

The compressional stress axis is almost horizontal and oriented southwest, orthogonal to the northern New Guinea coastline.

Plotted in Plate 3.

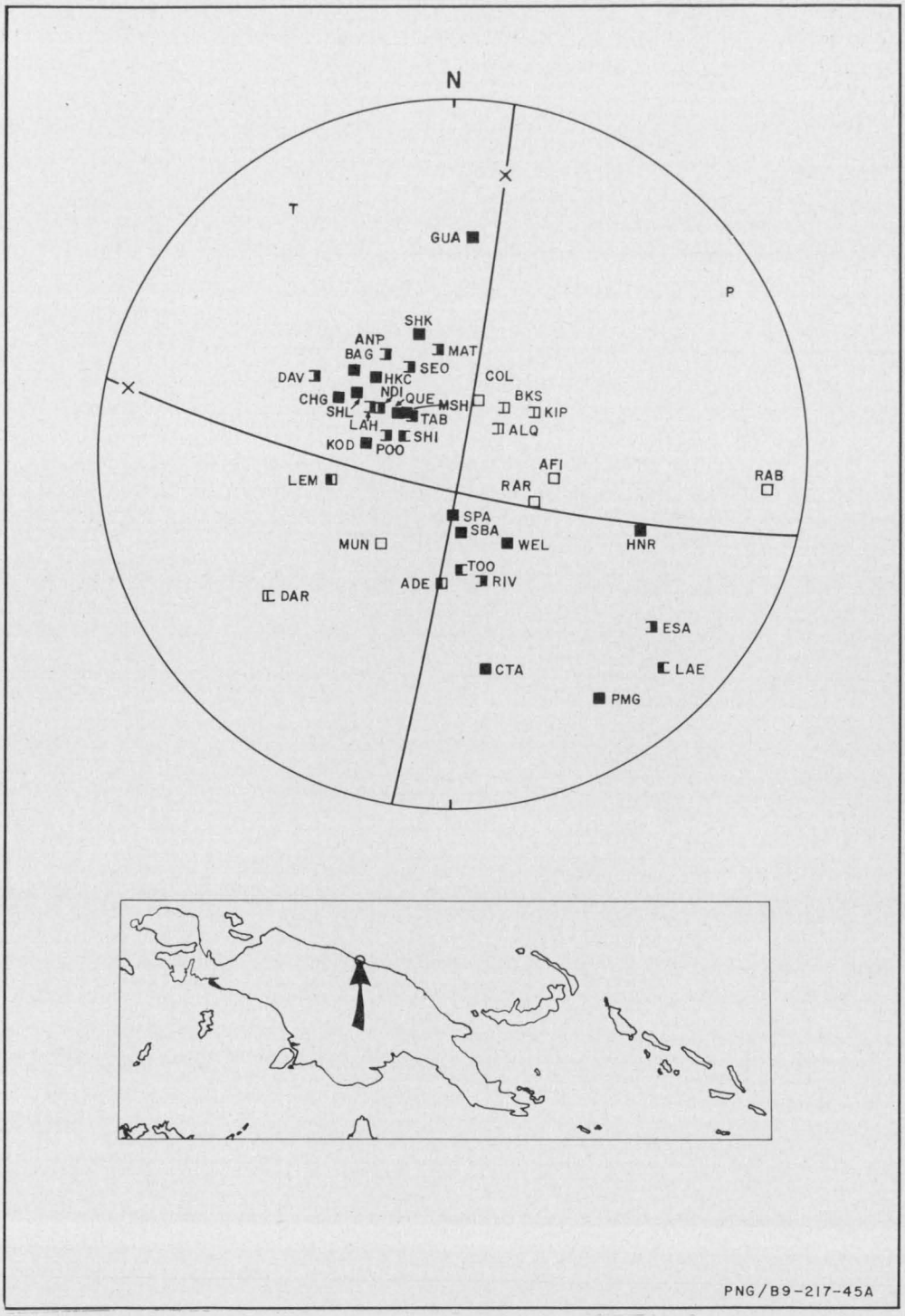
N
T
P
GUA
SHK
ANP
BAG
MAT
SEO
DAV
HKC
COL
CHG
NDI
QUE
MSH
BKS
KIP
SHL
TAB
ALQ
LAH
SHI
KOD
POO
AFI
LEM
RAR
RAB
SPA
SBA
MUN
WEL
HNR
TOO
ADE
RIV
DAR
ESA
CTA
LAE
PMG
PNG/B9-217-45A

FIGURE 46

Number	: 45			
Location	: 3.3°S, 143.3°E; 40 km northwest of Wewak			
Origin Time	: 23 October 1968 at 21 04 41.3 UT			
Depth	: 12 km			
Magnitude (M)	: 6.8			
Type	: Strike-slip			
Nodal Planes	:	Azimuth of Dip	Dip	
	:	102	86	
	:	193	80	
Nodal-Plane Poles	:	Azimuth	Plunge	
	:	282	04	
	:	013	10	
P Axis	:	058	04	
T Axis	:	327	11	
		Azimuth	Plunge	Uncertainty
B Axis	:	171	78	8 x 1

Although the P-wave arrivals were generally weak, the solution is tight. If the nodal plane trending west-northwest (almost parallel to the northern New Guinea coast) is the fault plane, the motion is sinistral.

Plotted in Plate 2.

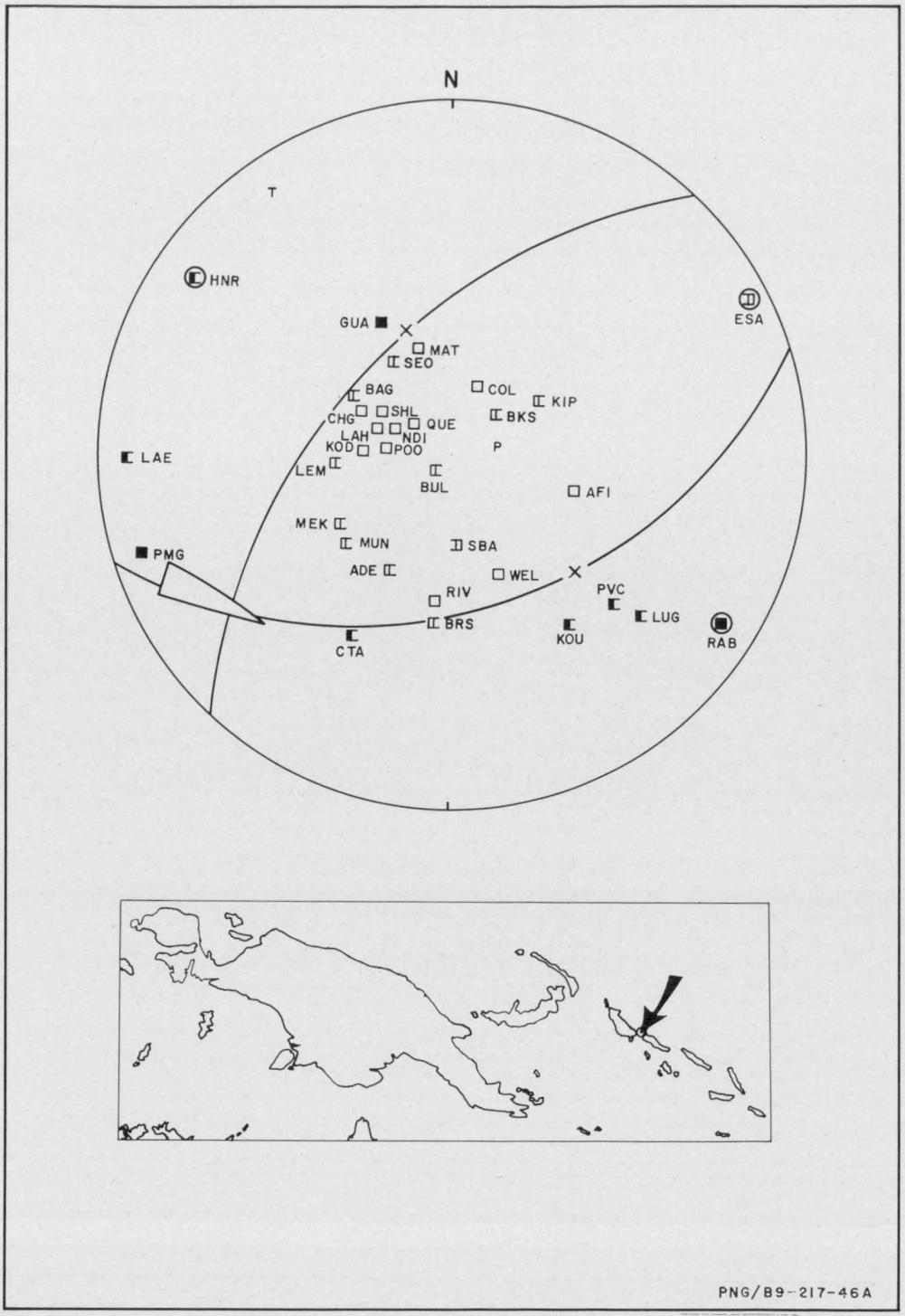
N
T
HNR
ESA
GUA
MAT
SEO
BAG
COL
KIP
CHG
SHL
BKS
QUE
LAH
NDI
KOD
POO
P
LAE
LEM
BUL
AFI
MEK
MUN
SBA
PMG
ADE
WEL
PVC
RIV
LUG
BRS
KOU
RAB
CTA
PNG/89-217-46A

FIGURE 47

Number	: 46			
Location	: 6.8°S, 156.2°E; southeast tip of Bougainville			
Origin Time	: 28 November 1968 at 16 30 32.1 UT			
Depth	: 169 km			
Magnitude (M)	: 5.9			
Type	: Dip-slip normal			
Nodal Planes	:	Azimuth of Dip	Dip	
	:	312	52	
	:	163	42	
Nodal-Plane Poles	:	Azimuth	Plunge	
	:	132	38	
	:	343	48	
P Axis	:	074	75	
T Axis	:	326	05	
		Azimuth	Plunge	Uncertainty
B Axis	:	235	15	20 x 6

The solution, which is good with only a small uncertainty in the orientation of the B axis, might be interpreted either as a pull of Bougainville northwest away from the rest of the Solomon Islands or as vertical pressure with a descending lithospheric slab, but both interpretations are anomalous because the earthquake occurred at intermediate depth.

The tensional stress axis is horizontal, oriented northwest (parallel to the Solomon Islands chain) and the compressional stress axis is near-vertical.

Plotted in Plate 3.

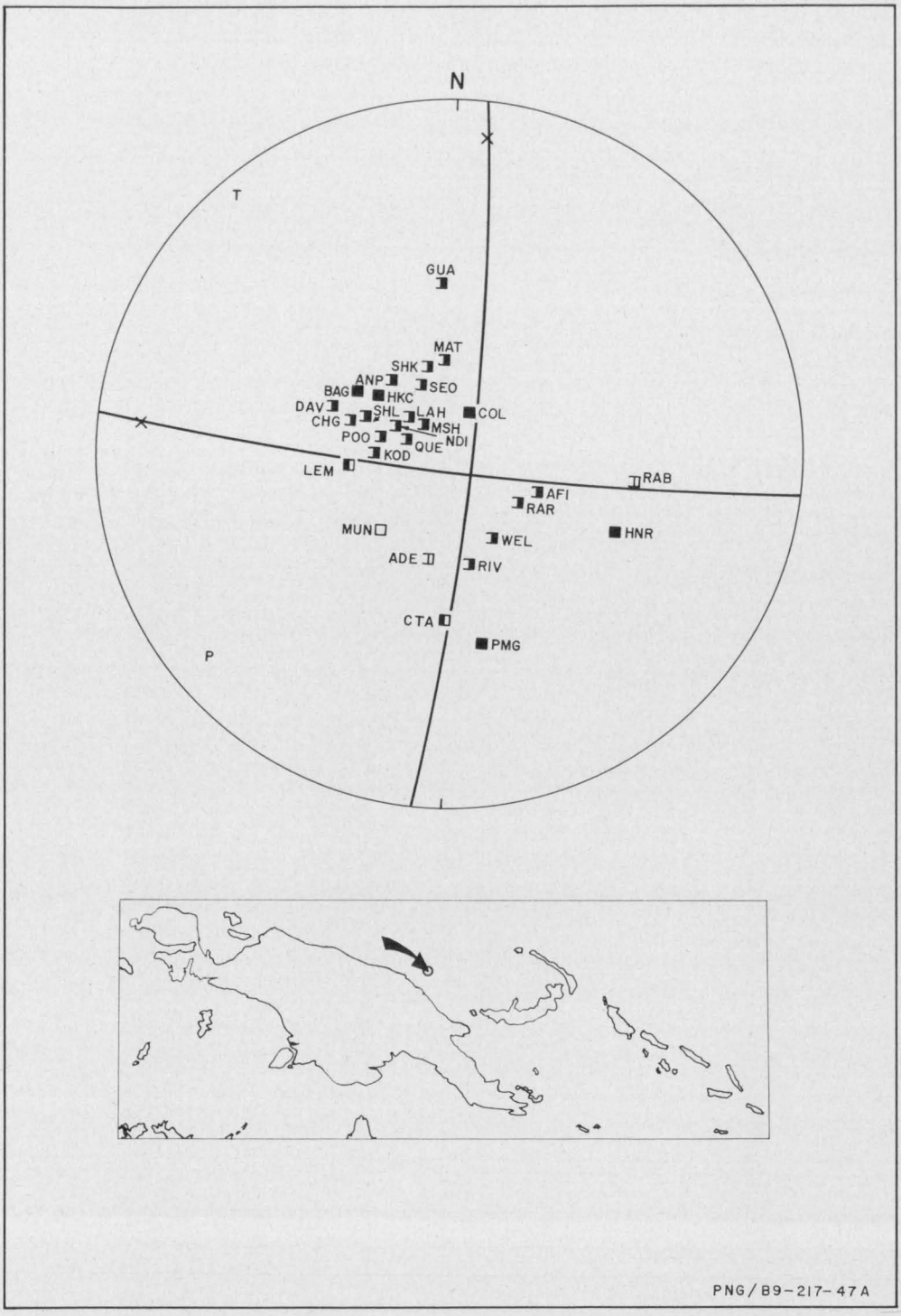
N
T
P
GUA
MAT
SHK
ANP
BAG
SEO
HKC
DAV
SHL
LAH
COL
CHG
MSH
POO
QUE
NDI
KOD
LEM
RAB
AFI
RAR
MUN
HNR
WEL
ADE
RIV
CTA
PMG
PNG/B9-217-47A

FIGURE 48

Number	:	47		
Location	:	3.4°S, 145.9°E; Bismarck Sea seismic lineation north of Madang		
Origin Time	:	7 December 1968 at 04 57 49.0 UT		
Depth	:	15 km		
Magnitude (M)	:	6.3		
Type	:	Strike-slip		
Nodal Planes	:	Azimuth of Dip	Dip	
	:	095	83	
	:	185	84	
Nodal-Plane Poles	:	Azimuth	Plunge	
	:	275	07	
	:	005	06	
P Axis	:	230	08	
T Axis	:	320	02	
		Azimuth	Plunge	Uncertainty
B Axis	:	133	81	1 x 1

The solution is strike-slip. It is well defined despite the small number of stations in the southwest and northeast quadrants. Two stations (LEM and CTA) recorded short-period compressions and long-period dilatations, but each station lies on a nodal plane.

The hypocentre lies on the Bismarck Sea seismic lineation, and, if the east-west-trending nodal plane is the fault plane, the solution is consistent with the hypothesis that the seismic lineation is a sinistral transcurrent fault.

Plotted in Plate 2.

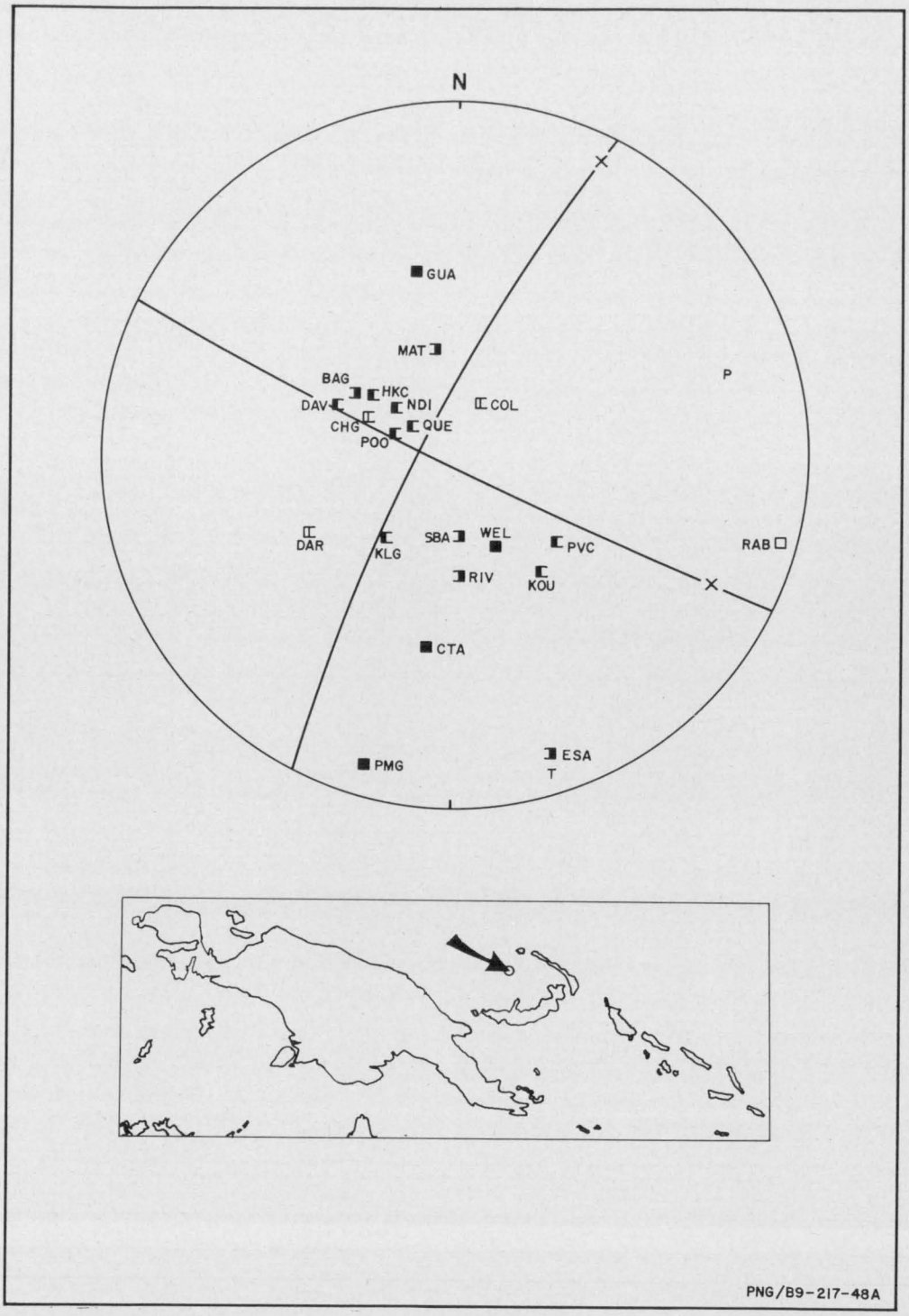
N
GUA
MAT
BAG
HKC
DAV
NDI
COL
CHG
QUE
POO
P
DAR
KLG
SBA
WEL
PVC
RAB
RIV
KOU
CTA
PMG
ESA
T
PNG/89-217-48A

FIGURE 49

Number	:	48		
Location	:	3.4°S, 148.8°E; Bismarck Sea seismic lineation 200 km south-east of Manus Island		
Origin Time	:	22 December 1968 at 15 27 18.9 UT		
Depth	:	33 km		
Magnitude (M)	:	5.4		
Type	:	Strike-slip		
Nodal Planes	:	Azimuth of Dip	Dip	
	:	296	79	
	:	205	86	
Nodal-Plane Poles	:	Azimuth	Plunge	
	:	116	11	
	:	025	04	
P Axis	:	071	79	
T Axis	:	161	85	
		Azimuth	Plunge	Uncertainty
B Axis	:	228	78	10 x 1

The solution is poor, as arrivals were weak and emergent. The strike-slip solution depends on the P-wave dilatations recorded by stations CHG and COL, but these are weak and uncertain. If these two readings are ignored, an overthrust solution is possible.

CONCLUSIONS

Earthquakes associated with both strike-slip and dip-slip faulting occur through New Guinea and the Solomon Islands; the majority of earthquake solutions are dip-slip overthrust.

The most active part of the seismic zone is the New Britain/north Solomon Sea/Bougainville section, in which the seismicity forms Benioff zones dipping northwest beneath New Britain and the South Bismarck Volcanic Arc, and vertically beside Bougainville. At depths of less than 100 km in this section, most earthquake solutions are dip-slip overthrust, but strike-slip solutions are also obtained for north Solomon Sea earthquakes. The solution to the earthquake (No. 22) in the central Solomon Sea beneath the southwest or Solomon Sea side of the Bougainville Trench is dip-slip normal. No strike-slip solutions have been obtained for Bougainville earthquakes, but strike-slip solutions are obtained for earthquakes southeast of Bougainville along the Solomon Island chain.

The tensional stress axes derived from the overthrust solutions for New Britain and Bougainville earthquakes tend to dip steeply, and the compressional stress axes tend to be horizontal and orthogonal to New Britain and Bougainville.

The plunge of the compressional stress axis is roughly parallel to the dip of the Benioff zone in only one of five deep-focus earthquake solutions (earthquake No. 9, beneath the northern tip of Bougainville). The compressional stress axis derived from the deep-focus New Britain earthquake solution (No. 33) is horizontal.

Three solutions have been obtained for earthquakes occurring at a depth of about 200 km beneath Long Island, on the South Bismarck Volcanic Arc: two are dip-slip overthrust, with near-vertical tensional stress axes and horizontal north-south compressional stress axes (Nos. 4 and 26); the other is strike-slip with northeast compressional stress axis (No. 38).

Eastern New Guinea experiences earthquakes with (a) strike-slip solutions which are sinistral if the northwest-trending nodal planes sub-parallel to the Ramu Markham Lineament are the fault planes, (b) dip-slip overthrust solutions, and (c) dip-slip solutions in which one nodal plane is vertical and the other is near-horizontal. Two of the last types (Nos. 2 and 7) occurred at depths of 171 and 99 km; their tensional stress axes plunge about 45° west. More solutions for earthquakes at depths exceeding 100 km in northern New Guinea are required to establish whether the seismicity of the region relates to a Benioff zone, and if subduction is occurring beneath New Guinea.

Solutions for shallow earthquakes in northern New Guinea and Irian Jaya are both dip-slip overthrust and strike-slip. Solutions for shocks along the Bismarck Sea seismic lineation (Nos. 19, 40, 47, and 48) are strike-slip (one of the two possible solutions to No. 17 is also strike-slip), and the motion is sinistral if the nodal planes parallel to the lineation are the fault planes.

The solution for the earthquake (No. 8) on the West Melanesian Arc at Mussau Island is strike-slip, but as its quadrants are reversed it differs from the earthquakes with strike-slip solutions along the Bismarck Sea seismic lineation; thus if its nodal plane trending northwest is the fault plane, the motion is dextral.

ACKNOWLEDGEMENTS

The co-operation of the Director of the World Data Centre, and of the directors of seismograph stations which supplied information, is gratefully acknowledged.

REFERENCES

BESSONOVA, E.N., GOTSADZE, O.D., KEILIS-BOROK, V.I., KIRILLOVA, I.V., KOGAN, S.D., KIKHITKOVA, T.I., MALINOVSKAYA, L.N., PAVLOVA, G.I., & SORSKII, A.A., 1960—INVESTIGATION OF THE MECHANISM OF EARTHQUAKES. Soviet research in geophysics, Vol. 4. *Akad. nauk SSR, geofiz Inst. (English translation by Amer. Geophys. Un.).*

DENHAM, D., 1969 — Distribution of earthquakes in the New Guinea-Solomon Islands region. *J. geophys. Res.*, 74, 4290-9.

HODGSON, J.H., & STEVENS, A.E., 1964 — SEISMICITY AND EARTHQUAKE MECHANISM. Research in geophysics, Vol. 2. *Cambridge, (Mass.), MIT Press*, 27-59.

HODGSON, J.H., & STOREY, R.S., 1953 — Tables extending Byerley's fault-plane techniques to earthquakes at any focal depth. *Bull. seismol. Soc. Amer.*, 43, 49-61.

ISACKS, B., & MOLNAR, P., 1971 — Distribution of stresses in the descending lithosphere from a global survey of focal mechanism solutions of mantle earthquakes. *Rev. Geophys.*, 9, 103-74.

JOHNSON, T., & MOLNAR, P., 1972 — Focal mechanisms and plate tectonics of the southwest Pacific. *J. geophys. Res.*, 77, 5000-32.

MCKENZIE, D.P., 1969 — The relation between fault plane solutions for earthquakes and the directions of the principal stresses. *Bull. seismol. Soc. Amer.*, 59, 591-601.

RITSEMA, A.R., 1957 — Earthquake-generating stress systems in southeast Asia. *Bull. seismol. Soc. Amer.*, 47, 267-79.

RITSEMA, A.R., 1967 — Mechanisms of European earthquakes. *Tectonophys.*, 4, 247-59.

SYKES, L.R., 1968 — Deep earthquakes and rapidly running phase changes; a reply to Dennis & Walker. *J. geophys. Res.*, 73, 1508-10.

THOMPSON, J.E., 1967 — A geological history of eastern New Guinea. *APEA J.*, 7 (2), 83-93.

WICKENS, A.J., & HODGSON, J.H., 1967 — Computer re-evaluation of earthquake mechanism solutions. *Publ. Dom. Obs. Ottawa*, 33 (1).

TABLE 1: NEW GUINEA/SOLOMON ISLANDS EARTHQUAKES WHOSE FOCAL MECHANISM SOLUTIONS HAVE BEEN RECOMPUTED BY WICKENS & HODGSON (1967)

Ref.	*Date*			*Origin Time*						
No.	*Yr*	*mn*	*dy*	*Hr*	*min*	*sec*	*Lat.°(S)*	*Long.°(E)*	*Depth (km)*	*Mag. (M)*
38	36	06	10	08	23	21	5.5	147	160	6.9
42	37	04	05	06	56	41	1	133	100	6.9
47	38	02	01	19	04	21	5	131.5	33	8.2
53	38	08	31	17	45	13	4	151.5	350	6.7
72	41	09	04	10	21	44	4.5	154	100	7.1
86	43	11	06	08	31	34	5.7	134	33	
89	43	12	01	06	04	55	4.5	144	100	7.2
92	44	03	31	02	51	44	5.5	131	50	7
93	44	04	26	01	54	11	0.7	133.5	33	
94	44	04	27	14	38	03	1	133	33	
99	46	01	17	09	39	36	6.2	147.7	100	
105	47	05	27	05	58	52	1.7	135.5	33	7.2
166	50	09	19	20	29	48	2	138.5	33	6.9
175	50	11	08	02	18	12	9.7	159.5	33	7.2
178	50	12	04	16	28	01	5	153.5	100	7
188	51	02	17	21	07	09	7	146	225	7.2
294	52	11	06	19	47	20	5	145.5	33	7.3
295	52	11	28	21	01	27	6.5	155.5	100	6.7
298	52	12	24	18	39	38	5.5	152	33	7
306	53	04	06	00	36	16	7.3	131	33	
307	53	04	23	16	24	17	4	154	33	7.6
334	53	12	02	04	24	51	2.7	141.5	33	6.7
343	54	03	03	06	02	55	5.5	142.5	33	7.2
354	54	06	06	16	50	40	3	135.5	33	7
355	54	06	07	10	15	33	3.5	152.5	475	6.7
391	55	08	16	11	46	58	6	155	220	7.2
392	55	08	21	17	33	58	3	137.5	33	6.7
395	55	09	15	12	30	27	5	134.5	33	6.7
396	55	10	13	09	26	44	9.5	161	33	7
406	56	01	31	09	17	11	4	152	400	7.1
415	56	05	22	12	36	12	4	152.5	540	6.7
449	57	03	23	05	12	31	5.5	131	100	7
461	57	06	22	23	50	23	1.5	137	33	7.2
504	59	03	01	16	49	13	0.5	134.5	100	7
548	60	10	07	15	18	31	7.4	130.7	45	6.7
550	60	10	22	08	22	01	10.3	161.2	93	6.5
554	61	01	05	15	53	56	4.1	143	108	6.7
585	62	06	18	23	42	31	4.8	151.8	47	6.7
591	62	07	30	17	16	44	3.3	143.9	25	7

TABLE 2: THE WICKENS & HODGSON (1967) FOCAL MECHANISM SOLUTIONS FOR THE EARTHQUAKES LISTED IN TABLE 1.

An asterisk draws attention to the earthquakes with more than one possible solution. The cone and eccentricity columns indicate the solid-angle of uncertainty involved

	PLANE A				*PLANE C*				*B Axis*				*P Axis*		*T Axis*			
Ref. No.	*Azimuth*	*Dip*	*Cone*	*Ecc.*	*Azimuth*	*Dip*	*Cone*	*Ecc.*	*Azimuth*	*Plunge*	*Cone*	*Ecc.*	*Azimuth*	*Plunge*	*Azimuth*	*Plunge*	*Total Variation*	
1	2	3	4	5	6	7	8	9	10	11	12	13	14	15	16	17	18	19
38	23.3	65.2	18	.70	282.3	67.6	10	.90	335.5	55.5	6	.67	243.2	1.6	152.2	34.5	34	
42	316.9	69.9	9	.67	225.3	85.7	14	.08	303.7	69.4	8	.64	182.7	11.0	89.3	17.2	31	*
42	129.8	83.2	31	.59	36.6	65.4	17	.20	54.0	64.3	27	.68	170.7	12.2	265.7	22.3	75	*
47	314.2	72.1	1	.94	223.2	86.9	6	.40	303.5	71.9	2	.96	179.8	10.3	87.1	14.7	9	
53	39.6	68.4	2	.25	306.5	82.3	6	.89	18.1	66.9	7	.85	264.9	9.5	171.2	20.8	15	
72	12.5	72.1	10	.14	273.3	63.6	8	.33	312.6	57.3	8	.43	51.3	5.6	144.8	32.1	26	
86	298.0	73.8	38	.75	80.1	20.2	49	.85	24.5	11.7	98	.39	135.0	59.4	288.2	27.8	185	*
86	309.1	82.6	41	.50	53.0	28.3	62	.78	35.3	27.2	87	.56	156.8	45.5	286.5	32.1	190	*
89	264.8	89.8	7	.24	354.9	82.5	2	.90	353.2	82.5	2	.92	129.5	5.4	220.0	5.2	11	
92	269.9	47.0	41	.87	5.8	83.7	14	.05	282.4	46.3	40	.88	147.4	34.1	40.0	23.9	95	
93	69.6	86.0	8	.13	338.3	72.5	8	.19	352.0	72.0	8	.07	112.7	9.4	205.2	15.2	24	*
93	116.9	48.8	11	.99	23.7	86.3	1	.62	109.5	48.6	18	.98	347.9	24.8	241.9	30.7	30	*
93	47.3	89.0	4	.48	316.7	58.6	25	.95	318.9	58.5	18	.97	87.5	20.9	186.5	22.4	47	*
94	223.7	85.3	10	.49	130.8	58.8	17	.29	141.3	58.3	12	.64	263.0	18.0	1.8	25.2	39	*
94	271.0	65.6	37	.77	88.3	24.4	45	.84	0.6	1.0	93	.32	270.2	20.6	93.3	69.4	175	*

99	81.9	72.7	17	.19	187.4	49.5	52	.86	154.1	44.4	47	.89	306.1	42.0	49.5	14.4	116	
105	134.6	17.7	50	.87	321.3	72.4	35	.74	50.7	1.9	98	.51	144.4	62.5	319.7	27.4	183	
166	216.8	81.9	13	.03	121.1	55.2	37	.88	138.1	54.0	37	.87	254.1	17.7	354.8	30.2	87	
175	318.6	60.2	12	.98	59.7	71.5	4	.83	357.0	53.9	28	.89	192.3	35.1	97.1	7.3	42	*
175	290.2	84.9	4	.73	20.5	86.3	16	.75	326.3	83.7	8	.93	155.4	6.2	65.3	1.0	28	*
175	113.9	83.8	2	.48	207.0	63.2	10	.41	191.9	62.4	7	.95	337.2	23.3	73.4	14.0	19	*
178	15.2	86.6	3	.52	106.0	77.0	4	.39	90.6	76.5	2	.21	239.7	11.6	331.1	6.7	9	
188	270.4	83.9	2	.10	2.2	73.5	1	.71	340.8	72.3	1	.68	135.2	16.1	227.3	7.2	4	*
188	232.7	69.6	32	.62	64.2	20.8	43	.79	144.1	3.8	70	.44	45.8	65.2	235.8	24.5	145	*
188	92.4	27.2	50	.63	250.0	64.6	46	.56	164.4	9.0	75	.18	50.3	68.8	257.5	19.0	171	*
294	141.5	75.7	79	.91	46.6	71.6	18	.42	87.0	66.4	60	.95	183.4	2.8	274.6	23.4	157	
295	11.5	74.4	16	.75	155.7	19.0	32	.94	98.5	10.6	64	.74	206.8	59.2	2.6	28.6	112	
298	243.8	88.8	6	.58	333.9	86.7	2	.67	313.5	86.5	4	.86	108.8	3.2	198.9	1.5	12	*
298	250.2	85.7	7	.69	157.0	53.1	34	.99	165.9	52.8	61	.96	287.7	21.8	30.2	28.5	102	*
306	296.9	62.8	11	.13	84.5	31.4	36	.89	19.4	14.4	33	.90	148.8	68.0	285.1	16.3	80	
307	343.1	82.5	2	.94	252.5	85.4	13	.35	311.2	81.2	3	.96	207.9	2.0	117.6	8.6	18	
334	93.3	75.8	1	.64	358.9	73.4	6	.85	41.8	67.8	3	.94	135.8	1.6	226.5	22.1	10	*
334	128.2	89.9	6	.07	38.2	90.0	5	.33	109.9	89.9	5	.29	353.2	0.1	263.2	0.1	16	*
343	5.0	76.5	2	.62	96.8	82.4	3	.41	35.6	74.4	2	.77	231.6	15.0	140.5	4.1	7	
354	166.8	47.3	9	.99	70.8	83.5	1	.25	154.0	46.6	8	.99	36.6	23.5	289.5	34.0	18	
355	280.5	15.1	46	.84	165.5	83.5	42	.80	253.9	13.6	104	.18	153.4	37.1	0.5	49.7	192	*
355	293.1	23.5	64	.69	158.0	72.9	56	.60	243.1	15.6	100	.24	145.2	26.1	0.7	58.9	220	*
391	69.6	81.9	2	.69	337.9	77.8	3	.11	12.6	75.3	2	.66	113.5	2.9	204.3	14.4	7	*
391	356.7	82.1	0	.50	261.1	55.1	1	.98	277.7	54.0	1	.99	34.1	17.9	134.8	30.1	2	*
392	166.2	53.6	8	.99	61.3	70.8	1	.75	129.2	47.3	15	.97	27.3	10.8	287.9	40.7	24	
395	70.8	37.1	70	.47	243.5	53.2	64	.37	156.2	3.5	88	.15	43.0	81.2	246.7	8.1	222	
396	71.1	42.4	45	.63	252.3	47.7	40	.54	341.7	0.6	66	.20	251.7	2.7	84.4	87.3	151	
406	91.7	45.9	28	.81	261.6	44.6	25	.76	176.8	5.1	58	.18	349.5	84.9	86.7	0.7	111	
415	148.9	67.9	75	.47	8.1	27.7	78	.52	65.5	14.8	108	.10	161.8	21.1	301.5	63.2	261	
449	123.9	22.1	33	.90	261.6	73.3	29	.87	175.9	14.0	91	.21	61.2	59.2	273.2	26.9	153	*
449	134.9	29.3	34	.92	268.8	68.6	3	.88	186.6	19.1	12	.99	58.0	61.0	284.2	21.0	49	*
461	231.1	89.5	3	.22	321.1	83.0	4	.14	317.0	83.0	3	.33	95.9	5.3	186.3	4.6	10	
504	196.4	88.9	6	.21	106.0	65.9	9	.65	108.8	65.9	10	.56	238.5	16.0	333.7	17.6	25	*
504	357.3	60.1	11	.19	262.6	81.8	7	.46	338.8	58.8	8	.56	223.4	14.6	125.8	26.9	26	*
504	59.1	36.5	28	.86	226.3	54.2	23	.80	140.8	6.1	61	.31	231.8	8.9	16.8	79.2	112	*
548	149.3	58.7	2	.94	42.8	65.0	2	.92	101.8	48.0	7	.25	7.4	3.9	273.9	41.7	11	
550	47.5	57.1	17	.96	137.6	89.8	2	.65	47.9	57.1	10	.99	277.5	22.8	177.6	22.4	29	
554	175.7	66.6	9	.73	84.4	86.9	4	.13	167.3	66.4	8	.76	42.4	14.0	307.6	18.6	21	*
554	269.8	87.9	1	.21	36.6	3.5	11	.99	359.7	2.8	12	.99	92.7	47.0	267.1	42.8	24	*
585	227.7	65.4	5	.86	136.1	86.4	2	.06	218.3	65.1	4	.87	94.5	14.5	359.2	19.8	11	
591	193.4	75.8	6	.86	100.5	78.6	2	.48	153.0	71.7	4	.93	57.2	1.9	326.5	18.2	12	*
591	73.2	34.6	28	.73	239.6	56.2	22	.59	153.9	6.4	43	.36	245.1	10.9	33.9	77.3	93	*
591	235.1	47.2	51	.37	57.6	42.8	44	.16	146.3	1.2	55	.26	236.3	2.2	27.7	87.5	150	*

TABLE 3: HYPOCENTRES OF INTERMEDIATE AND DEEP-FOCUS NEW GUINEA/SOLOMON ISLANDS EARTHQUAKES WHOSE FOCAL MECHANISM SOLUTIONS HAVE BEEN COMPUTED BY ISACKS & MOLNAR (1971)

No.	*Month*	*Day*	*Year*	*Epicentre* *Lat.° (S)*	*Long.° (E)*	*Depth (km)*
1	Aug.	5	1966	11.1	162.6	52
2	Jan.	7	1968	5.1	153.9	118
3	Aug.	13	1964	5.5	154.3	392
4	July	6	1965	4.5	155.1	506
5	Dec.	26	1965	5.4	151.6	74
6	Jan.	14	1964	5.2	150.8	169
7	Jun.	18	1962	5.0	152.0	103
8	Jun.	13	1967	5.6	148.1	213
9	Sep.	1	1967	5.6	147.2	182
10	Nov.	14	1967	5.4	147.1	201
11	Feb.	26	1963	7.6	146.2	182
12	Apr.	24	1964	5.1	144.2	98
13	Sep.	12	1964	4.4	144.1	107
14	Dec.	14	1966	4.9	144.1	80

TABLE 4: THE ISACKS & MOLNAR (1971) FOCAL MECHANISM SOLUTIONS FOR THE EARTHQUAKES LISTED IN TABLE 3

The format is that adopted by the authors in their publication.

No.	*Axis of Compression (P)* *Trend*	*Plunge*	*Axis of Tension (T)* *Trend*	*Plunge*	*Null Axis (B)* *Trend*	*Plunge*	*Pole of 1st Nodal Plane* *Trend*	*Plunge*	*Pole of 2nd Nodal Plane* *Trend*	*Plunge*
1	206	05	079	82	296	08	031	40	198	49
2	065	03	328	71	157	18	048	45	261	40
3	282	76	056	10	149	10	044	54	244	34
4	157	64	004	24	269	10	175	21	023	66
5	174	40	308	40	060	25	330	00	240	65
6	154	35	334	55	064	00	334	10	154	80
7	169	05	349	85	079	00	349	40	169	50
8	181	24	059	50	286	30	024	14	137	55
9	357	01	090	68	267	22	018	42	157	40
10	189	15	077	56	288	30	033	24	154	50
11	105	41	249	41	355	20	085	00	175	70
12	083	55	264	35	172	01	093	10	269	80
13	215	43	035	47	125	00	035	02	215	88
14	032	15	212	75	122	00	212	30	032	60

TABLE 5: HYPOCENTRES OF NEW GUINEA/SOLOMON ISLANDS EARTHQUAKES WHOSE FOCAL MECHANISM SOLUTIONS HAVE BEEN COMPUTED BY JOHNSON & MOLNAR (1972)

No.	*Date*	*Lat.°* (*S*)	*Long.°* (*E*)	*Depth* (*km*)
1	9 Mar. 69	4.1	135.5	14
2	13 Apr. 63	3.4	135.6	69
3a	6 Nov. 63	2.6	138.3	0
4	27 Apr. 67	1.8	138.7	33
5	12 June 70	2.9	139.1	30
6	8 Sep. 68	3.7	142.9	29
7	14 Dec. 66	4.8	143.9	74
8	18 Sep. 67	5.9	146.6	39
9	30 July 62	3.4	143.7	33
10	10 Dec. 66	3.6	145.4	33
11	17 Mar. 67	3.6	150.9	33
12	16 Apr. 69	3.5	150.9	39
13	13 Aug. 67	4.4	152.5	29
14	28 Jan. 63	2.6	149.9	32
15	23 Dec. 66	7.1	148.3	43
16	27 Feb. 63	6.1	149.2	57
17	31 Jul. 64	6.1	149.4	63
18	17 Nov. 64	5.7	150.7	45
19	19 Nov. 64	6.0	150.8	3
20	7 Dec. 64	5.4	151.3	54
21	22 Feb. 66	5.4	151.5	28
22	5 Aug. 65	5.3	151.7	47
23	12 Sep. 67	5.5	151.7	50
24	3 Mar. 65	5.5	151.9	44
25	25 Feb. 65	5.5	152.0	35
26	12 Aug. 65	5.3	152.2	41
27	30 Apr. 64	4.6	153.2	78
28	25 Dec. 67	5.3	153.7	64
29	4 Oct. 67	5.7	153.9	52
30	9 Oct. 67	5.7	154.0	41
31	6 Mar. 64	6.1	154.4	74
32	17 Apr. 64	6.6	154.9	85
33	10 Apr. 67	7.3	155.8	30
34	10 Apr. 67	7.4	155.7	30
35	17 Oct. 65	8.0	155.9	93
36	8 Jun. 68	8.7	157.5	33
37	19 Jan. 68	9.4	158.4	33
38	27 Nov. 65	9.7	158.7	31
39	17 Jul. 65	9.7	159.8	33
40	13 Feb. 63	9.9	160.7	30
41	15 Jun. 66	10.4	160.8	31
42	13 Jan. 67	10.6	161.4	32
43	28 Sep. 67	6.6	153.4	44
44	8 Oct. 67	9.5	148.8	17

TABLE 6: THE JOHNSON & MOLNAR (1972) FOCAL MECHANISM SOLUTIONS FOR THE EARTHQUAKES LISTED IN TABLE 5

The format is that adopted by the authors in their publication.

Ref. No.	*Nodal-Plane Pole*		*Nodal-Plane Pole*		*Type*
	Azimuth	*Plunge*	*Azimuth*	*Plunge*	
1	46	6	136	0	SS
2	183	0	—	—	Th
3a	211	16	—	—	Th
4	202	10	22	80	Th
5	172	36	26	50	Th
6	2	32	258	20	SS
7	210	26	46	64	Th
8	196	40	40	40	Th
9	4	10	276	40	SS
10	92	4	2	0	SS
11	22	0	112	20	SS
12	305	5	236	6	SS
13	114	0	24	2	SS
14	112	0	24	6	SS
15	333	60	174	26	Th
16	3	30	146	64	Th
17	6	34	194	56	Th
18	356	34	176	56	Th
19	324	14	144	76	Th
20	318	36	109	60	Th
21	334	30	154	60	Th
22	314	40	114	48	Th
23	355	10	175	80	Th
24	358	30	224	50	Th
25	353	30	168	60	Th
26	340	22	160	68	Th
27	15	34	195	56	Th
28	22	44	202	46	Th
29	35	50	215	40	Th
30	40	30	220	60	Th
31	42	45	222	45	Th
32	37	40	217	50	Th
33	32	20	200	71	Th
34	51	30	217	60	Th
35	24	30	226	58	Th
36	42	2	222	88	Th
37	355	19	262	12	SS
38	78	10	258	80	Th
39	12	38	198	52	Th
40	56	16	236	74	Th
41	132	6	25	70	Th
42	88	22	268	66	Th
43	220	57	52	32	N
44	128	32	358	46	N

N — normal fault
SS — strike-slip fault
Th — thrust fault

TABLE 7: HYPOCENTRES OF THE EARTHQUAKES FOR WHICH FOCAL MECHANISM SOLUTIONS WERE OBTAINED IN THIS STUDY

No.	*Yr*	*Mn*	*Dy*	*Hr*	*Mi*	*Sec*	*h (km)*	*Lat.°S*	*Long.°E*	*M*
1	63	01	28	12	12	19.0	33	2.8	149.8	6.4
2	63	02	26	20	14	08.7	171	7.5	146.2	7.2
3	63	02	27	04	30	00.8	52	6.0	149.4	5.4
4	64	01	12	11	13	19.4	227	5.4	146.8	5.7
5	64	02	14	16	29	45.3	58	5.1	151.8	6.1
6	64	04	17	05	59	58.9	74	6.6	155.0	6.0
7	64	04	24	05	56	09.8	99	5.1	144.2	6.8
8	64	06	28	12	51	35.0	7	1.8	149.7	6.2
9	64	08	13	00	31	15.0	392	5.5	154.3	6.5
10	64	11	17	08	15	41.1	60	5.7	150.7	7.3
11	64	12	07	08	58	45.0	70	5.4	151.2	5.9
12	64	12	24	18	45	44.0	78	4.4	153.1	6.1
13	65	07	06	18	36	47.3	509	4.5	155.1	6.2
14	65	09	22	20	01	50.0	62	5.4	151.5	5.9
15	65	12	07	22	19	16.0	118	6.4	146.3	6.4
16	66	02	22	05	02	40.7	59	5.4	151.6	6.7
17	66	12	10	18	08	14.4	33	3.6	145.4	6.2
18	66	12	23	15	50	21.3	46	7.1	148.3	7.2
19	67	03	17	11	24	46.4	33	3.6	150.8	5.7
20	67	03	18	19	15	35.6	101	6.0	146.3	5.8
21	67	04	10	15	02	44.5	47	7.3	155.8	6.1
22	67	09	28	04	56	56.3	44	6.6	153.4	6.4
23	67	10	04	17	21	20.7	52	5.7	153.9	6.7
24	67	10	08	18	08	18.1	70	5.6	154.0	5.7
25	67	11	01	18	56	54.8	14	4.8	135.7	6.3
26	67	11	14	05	28	36.9	201	5.4	147.1	6.0
27	67	12	25	01	23	33.6	64	5.3	153.7	7.0
28	68	01	07	09	56	40.3	118	5.1	153.9	6.1
29	68	01	19	06	04	38.2	33	9.4	158.4	6.5
30	68	02	12	05	44	47.6	74	5.5	153.2	7.2
31	68	03	07	13	22	16.6	39	5.9	151.1	6.0
32	68	03	09	03	19	23.7	86	5.6	154.0	6.0
33	68	04	24	13	59	14.5	565	4.6	149.4	5.9
34	68	04	25	17	14	27.7	419	7.1	156.2	5.3
35	68	05	11	15	33	41.2	76	6.4	147.3	5.8
36	68	05	28	13	27	18.7	65	2.9	139.3	6.7
37	68	06	02	08	18	36.2	35	8.1	158.6	5.8
38	68	06	03	09	17	46.2	190	5.4	147.0	5.9
39	68	07	02	18	40	10.1	62	2.7	138.9	6.3
40	68	07	21	05	52	10.4	5	3.2	150.7	6.1
41	68	08	18	18	38	30.6	538	10.1	159.9	6.2
42	68	09	08	15	12	23.8	29	3.7	143.0	6.2
43	68	09	16	13	55	36.1	59	6.1	148.7	6.3
44	68	09	27	19	06	42.2	7	3.7	143.3	6.4
45	68	10	23	21	04	41.3	12	3.3	143.3	6.8
46	68	11	28	16	30	32.1	169	6.8	156.2	5.9
47	68	12	07	04	57	49.0	15	3.4	145.9	6.3
48	68	12	22	15	27	18.9	33	3.4	148.8	5.4

TABLE 8: P-WAVE POLARITIES RECORDED AT SEISMOGRAPH STATIONS FOR THE EARTHQUAKES LISTED IN TABLE 7

where 0 compression, short-period and long-period
1 compression, short-period
2 compression, long-period
3 compression obtained from questionnaire only
4 dilatation, short-period; compression, long-period
5 compression, short-period; dilatation, long-period
6 dilatation obtained from questionnaire only
7 dilatation, long period
8 dilatation, short-period
9 dilatation, short-period and long-period
( ) polarity is not completely clear owing to either microseisms or a poor quality seismogram

	Earthquake No.					*Earthquake No.*			
Stn	*1*	*2*	*3*	*4*	*Stn*	*1*	*2*	*3*	*4*
ADE	0	0	7	8	MAT	2	2	2	7
AFI	(7)	9	0	1	MAW	(1)	1		
ALQ		(8)			MIN		6		
BAG		3		(1)	MUN	7	0	0	1
BKS		8			NHA	2	0	0	
BRS	3	8	6	8	NOU				1
CAN	3	6			PMG	0	0	9	9
CHG				1	QUE	2	0	2	1
COL	1	8	3		RAB	0	2	0	8
CTA	3	5	6	9	RIV	3	9	9	0
DUG		8			SBA				1
GUA				7	SEO				8
HNR	4	6	2	0	SHL				1
JER		3			SPA		0	0	
KIP		9	2	1	TAU	1	1		1
KIR		3			TOO	0	0	1	
KOU	(1)		8		TUC		6		
LAH	2	0	0		WEL	0	6	9	0
MAN	3	3		(2)	WIL	8	2		

	Earthquake No.					*Earthquake No.*			
Stn	*5*	*6*	*7*	*8*	*Stn*	*5*	*6*	*7*	*8*
ADE		2	0		MAT				7
AFI	2		9		MAW				8
ALQ	4	1	7	8	MUN	2	9	2	
ANP	2		0	2	NDI	0	0	2	0
BAG	4	0	0		NHA		0	2	
BKS	8	1	9	0	NOU		1		
BRS		8	8	8	PMG	9	8	0	9
CHG	0	1	0	0	QUE	0	1	4	
COL	0	0	9	2	RAB		0	9	0
CTA	9		9	9	RIV	7	1	9	
DUG				1	SBA	2	1	7	(7)
GSC	0	1			SEO	2	1	9	7
GUA	0		9	7	SHI	2			
HKC	0	2	0	0	SHL	0	1	0	0
HNR	5	0	9		SPA		1	9	
HOW	2				TAU			2	
KIP			9		TOO			8	8
LAH	2		2		WEL	2	0	7	7
LUG		1			WIL			2	7
MAN	0	0	2						

Stn	Earthquake No. 9	10	11	12	Stn	Earthquake No. 9	10	11	12
ADE	9	6	0		MAT		3		
AFI	0	0	4		MAW		3		
ALQ	9		0		MIN		3		
ANP	8	0	2		MUN	9	0	0	0
BAG		3	0	0	NDI	9	0	0	0
BKS	7	3			NHA	9	0	2	2
BOZ			0		PMG	1	9	9	9
BRS	8	6			POO			0	0
BUL	8				POP			7	7
CHG	9	0	0	0	PPT		0		
COL	9	3	0	1	PVC	1	6		
CTA		6	7	9	QUE	9		0	0
DAV			0	2	RAB		6	7	0
GSC	9		1		RIV	9		(2)	0
GUA	9	0	2	2	SBA	8	0	2	0
HKC	9	0	4	0	SEO	7	0	0	0
HNR	9	6	9	5	SHI	9	0		1
HOW		0	2	2	SHL	8	0	0	0
KIP	2	1	1		SPA	9		1	1
KOD		0	0		TAU		8	0	0
LAH	7	0			TPN			7	
LEM			4	2	TUC		3		
LUG		6			WEL	9	3		
MAN			0	0	WIL		3		

Stn	Earthquake No. 13	14	15	16	Stn	Earthquake No. 13	14	15	16
ADE	6		0	0	MSH				2
AFI	7		9	2	MUN	9	8	0	0
ALQ	8	8		0	NDI				0
ANP	0		7	2	NHA		2		0
BAG	3	3	9	0	NOU			8	8
BKS	9		8	0	PEL			1	
BOZ		1	8		PMG	0	9	0	0
BRS	8	1	1	1	POO			9	0
BUL		8			POP		7		
CAN			1		PPT	6		8	
CHG	0	0	9	0	PVC				1
COL	0	2	9	0	QUE		2	9	0
CTA	0	9	0	9	RAB		8	9	9
DAV				0	RAR				0
DNG				2	RIV	9		0	1
DUG	8	1			SBA	9	2		0
GSC		1	8	0	SDB	9			
GUA	0	2	8	0	SEO	0	2	9	0
HKC	0	0	9	0	SHI			9	2
HNR	3		9	9	SHK				0
KIP			0	0	SHL	0	0	9	1
KIR		3			SNG			9	0
KOD	0	2		1	SPA				(0)
KOU			8	8	STU			8	
LAH		2	9	2	TAB				1
LEM				0	TAU			0	1
LUG			8	8	TOO	8	1		
MAN	3	3		0	TPN	2		2	2
MAT	2	2	7	0	TRN			8	
MAW		1	1		TUC	6			
MCQ	6				WEL	9	2	3	2
					WIL	6	2	0	

Stn	Earthquake No. 17	18	19	20	Stn	Earthquake No. 17	18	19	20
ADE		0	2	1	MAN		7		
AFI	0	1			MAT	0	9	1	
ALQ		0			MSH		0		
ANP	2	(7)	2		MUN		0		1
BAG	2	9	0	1	NDI	2	0	0	8
BKS		0			NOU		1		
BRS		8	1	1	PMG	1	9		0
CHG	2	0	0	8	POO	1	0		
COL	5	4	0	8	PVC	5	1	1	
CTA	2	9	0	2	QUE	0	0		
DAV	2	7	2		RAB	2	9	0	1
GSC	1				RIV	2	0	2	
GUA	0	9	0	8	SBA		0	2	
HKC		9	0	8	SEO	0	7	0	8
HNR	0	9	1	1	SHI	1	1		
HOW	2				SHK	0	9		
KIP		0			SHL	0	0		9
KLG				1	SNG		0	7	9
KOD	0	0			SPA	1	2		1
KOU	1	8			TAB		0		
LAH	2	7			TAU		0		
LEM		0	9	1	TOO		1		1
LUG	2	1	1		WEL	2	2	2	

Stn	Earthquake No. 21	22	23	24	Stn	Earthquake No. 21	22	23	24
ADE	9	4		8	MAT	0	9	0	2
AFI		(7)	2	2	MAW	8			
ALQ		7	2		MSH		7	0	
ANP	2	7	2	2	MUN		0	2	1
BAG	0	9	0	0	NDI	2	9	0	0
BKS		7	2		NHA		9	2	
BRS		1	1		NOU		8	1	1
BUL		8			PMG	9	0	9	9
CHG		9	0	0	POO	2	7	0	0
COL	0			0	PVC	1	8		1
CTA	9		7	9	QUE		9	0	2
DAV	2	7	0		RAB	5	0	5	9
GUA	2	9	0	0	RAR		(7)	2	
HKC	2	9	0	2	RIV	7	9	0	0
HNR	2	7	1	7	SBA	(8)	9	0	0
HOW	2				SEO	2	9	2	0
KIP			2		SHI		9	2	0
KLG			1		SHK	2	9	2	0
KOD	2	9	0	0	SHL	0	9	0	0
KOU		8	1	1	SNG	2		2	0
LAE		8		8	SPA		9		0
LAH		7	0	0	TAU	9		2	
LEM	1	8	2	0	TOO		8		
LUG			8	8	WEL		7	2	2
MAN	2			0					

Stn	Earthquake No. 25	26	27	28	Stn	Earthquake No. 25	26	27	28
ADE	(1)	9	0	0	MEK			1	
AFI	1	1	0		MSH	0	2	0	2
ALQ	1		2		MUN	0	9	0	0
ANP	7	2	2	2	NDI	0	0		
BAG	9	0	0	0	NOU		1	1	
BKS	1		0	(2)	PMG	0	9	9	9
BOZ		0	4		POO	1	2		0
CHG	0	2	0	0	PVC		1	1	
COL		0	0	0	QUE	0	2	0	2
CTA	0	9	7	0	RAB		0	9	9
DAV	(7)		0	0	RAR		1	2	
ESA			8		RIV		7	0	0
GRK			8	(1)	SBA	1	0	0	0
GSC	0		2		SEO	7	1	0	0
GUA	5		0	0	SHI	0		0	
HKC	7	0	1	0	SHK		2	1	1
HNR	0	0	9	7	SHL	0	0	0	0
KIP	1		2		SNG	0		0	0
KLG			1		SPA	1	0	0	2
KOD	0	2		0	TAB			0	(2)
LAE		8	8	(1)	TAU			1	
LAH	1	2	2	(2)	TBL			8	
LEM	1	1	0	0	TOO		8		
MAN	9				WEL		1	2	0
MAT	7	0	0	0					

Stn	Earthquake No. 29	30	31	32	Stn	Earthquake No. 29	30	31	32
ADE	9	0	7	0	LEM	0	9	2	0
AFI	9		2		MAT	0	2	2	
ALQ	7	2	2		MEK	1			1
ANP	2	7	2		MSH		7		
BAG	0	9	2	0	MUN		9	2	1
BKS	7	2	0		NDI	0	9	2	1
BOZ		0			NOU				1
BRS	8			1	PMG	0	0	9	9
BUL		7		1	POO	0	9	2	0
CHG	0	7	2	0	PPT		7		
COL	0	0	2	1	PVC		8		1
CTA	9	0	9	9	QUE	0	9	2	0
DAV	0	9	2	2	RAB	0	9	0	9
GRK		8			RAR	7			
GSC		0			RIV	7	0	7	1
GUA	0	0	0	0	SBA	9		2	
HKC	0	7	2		SEO	0	0	4	1
HNR	0	9	7		SHI			0	
KIP		0			SHK	0	0	2	
KLG	1		1	1	SHL	0	9	0	0
KOD	0	9	2	1	SPA		2	1	1
KOU				1	TAB	1	2	2	
LAE				8	TOO	8		1	
LAH		7		0	WEL	9	0		1

Stn	Earthquake No. 33	34	35	36	Stn	Earthquake No. 33	34	35	36
ADE	8	1	0	0	LUG			1	
AFI	1		0	0	MAN				2
ALQ				2	MAT	9	(8)	0	0
ANP				0	MAW	8			
BAG	9		0	0	MEK			1	8
BKS				0	MUN		8	0	0
BRS			1	1	NDI			0	2
BUL	1	1	1	0	NOU		1	1	
CHG	8		0	0	PMG	5	9	9	4
COL	1	8	0	0	POO			0	0
CTA	9	0	9	9	PVC			1	
DAV			2	0	QUE	1		0	0
ESA	9	9	0		RAB	5	0	9	0
GRK	1	8	8	8	RAR				2
GSC	1			2	RIV	8	1	2	0
GUA	9	9	8	9	SBA			0	0
HKC	8			0	SEO	8	(8)	0	0
HNR	9	9	2	0	SHI				0
KIP				2	SHK	8	9	0	0
KLG	8	1	1	1	SHL		(8)	0	0
KOD			0	2	SNG			0	
KOU			1		SPA	1	1	0	0
LAE	1		1		TAB				2
LAH				0	TOO	8			
LEM			1	0	WEL	(1)		0	0

Stn	Earthquake No. 37	38	39	40	Stn	Earthquake No. 37	38	39	40
ADE	0	1	1		MAN	4			
AFI	8	1			MAT		9		0
ANP			(8)	2	MEK		8	1	
BAG	0	1	9	9	MUN	1	8	1	8
BKS		(1)	1	2	NDI	1			
BRS	1	1	1		NOU	(1)			
BUL	8				PMG	9	9	0	0
CHG	0	(1)	1	9	PVC	1			
COL	1	1	8	0	QUE	1			7
CTA	0	9	0	0	RAB		0	0	9
DAV				7	RAR	8	1		
GRK	8	1	1		RIV	0		1	2
GUA		9	7	2	SBA	1	1	1	
HNR	9	0	1	2	SEO		8	8	0
KIP		(1)			SHI			1	
KLG		8	1		SHK	2		(8)	0
KOD	4				SHL	1	(1)	1	9
LAH				2	SPA	1	1	1	
LEM		8	1		WEL	2	0		2

Stn	Earthquake No. 41	42	43	44	Stn	Earthquake No. 41	42	43	44
ADE	0	0	0	7	MAW	8			
AFI	4	2	0	(1)	MCQ	1			1
ALQ	9	0	2		MEK	(1)	1	1	
ANP	9	0	2		MSH	9	0	2	
BAG	0	0	0	4	MUN	9	0	0	7
BKS	8				NDI	9	0	2	
BRS		1	8		NOU			1	
BUL		2	2		PMG	1	0	9	0
CHG	9	0	0	2	POO	9	0	2	2
COL	9	0	0	1	PVC			1	
CTA	8	0	9	2	QUE	9	0	2	0
DAV				2	RAB	0	7	4	9
ESA	0		9	2	RAR	0		(1)	
GUA	0	4	0	5	RIV	(2)	2	9	2
HKC	9	0	0	(2)	SBA	5	0	0	
HNR	9	2	0	2	SEO	9	0	0	2
KIP	9		2		SHI		0	1	
KLG		1	1	(1)	SHK	9	0	0	2
KOD	7		2	2	SHL	7	0	2	0
KOU			1		SNG		0	0	2
LAE			8	1	SPA	5	0		1
LAH	7	2	2		TAB	8	0	0	
LEM	9	0	0	7	TBL		8		
LUG			1		WEL	0	0	2	
MAT	7	2	0	2	WEW				8

Stn	Earthquake No. 45	46	47	48	Stn	Earthquake No. 45	46	47	48
ADE	5	8	7		LEM	5	8	5	
AFI	9	9	2		LUG		1		
ALQ	7				MAT	2	9	2	(2)
ANP	(2)		2		MEK		8		
BAG	0	8	0	(2)	MSH	0		2	
BKS	7	(8)			MUN	9	8	9	
BRS		8			NDI	2	9	2	1
BUL		8			PMG	0	0	0	0
CHG	0	9	2	(8)	POO	2	9	2	1
COL	9	9	0	(8)	PVC		1		1
CTA	0	1	5	0	QUE	0	9	2	1
DAR	8			8	RAB	9	0	7	9
DAV	2		2	(1)	RAR	9		2	
ESA	2	7		2	RIV	2	9	2	2
GUA	0	0	2	0	SBA	0	7		2
HKC	0		0	(1)	SEO	2	8	2	
HNR	0	1	0		SHI	(1)			
KIP	7	8			SHK	0		2	
KLG				(1)	SHL	0	9	2	
KOD	0	9	2		SPA	0			
KOU		1		1	TAB	2			
LAE	1	1			TOO	1			
LAH	2	9	2		WEL	0	9	2	0

TABLE 9: FOCAL MECHANISM SOLUTIONS FOR THE EARTHQUAKES LISTED IN TABLE 7

The azimuth of the direction of maximum dip (orthogonal to the strike) and the dip of each nodal plane are tabulated below. Azimuth and plunge of the B, P, and T axes and the approximate solid angle of uncertainty of the B axis are listed in degrees.

	Nodal Planes				*B Axis*			*P Axis*		*T Axis*		
No.	*Az of Dip*	*Dip*	*Az of Dip*	*Dip*	*Az*	*Pl*	*Unc*	*Az*	*Pl*	*Az*	*Pl*	*Type*
1	112	89	202	69	201	69	1 x 1	069	15	335	15	SS
2	090	88	348	12	001	12	33 x 1	100	45	260	45	DS
3	162	58	043	54	101	37	17 x 1	193	03	285	53	DS
4	343	52	214	51	277	28	1 x 1	008	01	099	62	DS
5	see discussion											
6	010	46	239	56	309	26	39 x 1	216	07	113	64	DS
7	259	84	139	13	171	11	NO	067	50	271	38	DS
8	319	80	050	85	349	78	NO	185	11	094	03	SS
9	075	62	221	32	156	14	32 x 33	288	70	061	15	DS
10	see discussion											
11	see discussion											
12	see discussion											
13	238	34	343	80	260	32	26 x 17	130	44	008	27	DS
14	see discussion											
15	068	67	159	87	077	68	NO	297	17	202	14	SS
16	322	41	142	49	053	00	NO	142	04	322	86	DS
17	see discussion											
18	333	59	153	44	063	00	NO	333	04	153	80	DS
19	115	89	205	86	189	86	7 x 2	070	02	340	04	SS
20	283	55	179	69	244	48	NO	047	41	145	09	SS
21	345	25	209	71	293	14	30 x 1	196	24	052	60	DS
22	001	45	230	57	301	26	NO	102	63	208	07	DS
23	035	60	173	38	113	21	1 x 1	018	12	251	63	DS
24	084	44	220	55	148	23	10 x 6	240	06	343	66	DS
25	see discussion											
26	331	48	204	56	273	28	24 x 16	178	05	080	60	DS
27	see discussion											
28	042	65	185	31	124	15	NO	029	18	253	66	DS
29	see discussion											
30	239	85	149	82	181	81	1 x 1	283	02	013	10	SS
31	see discussion											
32	see discussion											
33	309	60	184	46	239	31	1 x 1	334	08	077	59	DS
34	312	84	052	34	038	34	54 x 1	285	30	163	41	—
35	031	46	241	48	317	15	28 x 1	227	01	133	75	DS
36	036	37	213	53	123	01	1 x 1	214	08	036	81	DS
37	312	82	221	79	257	76	1 x 1	087	14	356	02	SS
38	257	67	354	71	300	60	NO	035	03	126	30	SS
39	see discussion											
40	216	89	126	85	141	84	1 x 1	262	03	352	05	SS
41	276	49	154	58	220	52	2 x 2	028	57	127	05	DS
42	056	40	250	51	334	05	44 x 12	245	06	112	81	DS
43	014	38	188	52	100	02	30 x 7	190	07	346	82	DS
44	028	37	242	58	321	16	NO	228	12	102	70	DS
45	102	86	193	80	171	78	8 x 1	058	04	327	11	SS
46	312	52	163	42	235	15	20 x 6	074	75	326	05	DS
47	095	83	185	84	133	81	1 x 1	230	08	320	02	SS
48	296	79	205	86	228	78	10 x 1	071	79	161	85	SS

SS — strike-slip
DS — dip-slip
NO — non-orthogonal

TABLE 10: HYPOCENTRES OF THE EARTHQUAKES FOR WHICH SOLUTIONS WERE ATTEMPTED IN THIS STUDY BUT NOT OBTAINED

Yr	*Mn*	*Dy*	*Hr*	*Mi*	*Sec*	*h (km)*	*Lat.°S*	*Long.°E*	*M*
63	02	14	22	07	54.3	80	5.0	144.6	6.4
64	07	06	10	06	05.0	76	6.3	154.7	5.8
64	11	19	23	35	06.4	3	6.0	150.8	6.7
65	01	10	07	37	35.5	116	5.8	147.3	5.8
65	02	25	04	51	28.2	41	5.4	152.0	6.5
65	03	03	15	14	09.3	33	5.4	151.9	6.7
67	03	22	13	00	23	28	5.4	146.4	5.6
67	11	17	09	19	21.0	60	6.3	154.9	5.4
68	01	29	10	13	16.5	70	5.6	153.9	5.7
68	03	25	17	42	08.7	476	4.5	155.1	5.0
68	09	16	16	00	53.1	71	6.0	148.8	5.9

APPENDIX

SEISMOGRAPH STATION ABBREVIATIONS

ADE	Adelaide	SA
AFI	Afiamalu	Samoa
ALQ	Albuquerque	USA
ANP	Anpu	Taiwan
BAG	Baguio	Philippines
BHA	Kabwe (Broken Hill)	Zambia
BKS	Berkeley	USA
BOZ	Bozeman	USA
BRS	Brisbane	Qld
BUL	Bulawayo	Rhodesia
CAN	Canberra	A.C.T.
CHG	Chiengmai	Thailand
COL	College	Alaska
CTA	Charters Towers	Qld
DAV	Davao	Philippines
DNG	Daru	PNG
DUG	Dugway	USA
ESA	Esa 'ala	PNG
GRK	Goroka	PNG
GSC	Goldstone	USA
GUA	Guam	Marianas
HKC	Hong Kong	
HNR	Honiara	Solomon Is.
JER	Jerusalem	Israel
KIP	Kipapa	Hawaii
KIR	Kiruna	Sweden
KLG	Kalgoorlie	WA
KOD	Kodaikanal	India
KOU	Koumac	N. Caledonia
LAE	Lae	PNG
LAH	Lahore	Pakistan
LEM	Lembang	Java
LUG	Luganville	N. Hebrides
MAN	Manila	Philippines
MAT	Matsushiro	Japan
MAW	Mawson	Antarctica
MCQ	Macquarie Island	
MEK	Meekatharra	WA
MIN	Mineral	USA
MSH	Meshed	Iran
MUN	Mundaring	WA
NDI	New Delhi	India
NHA	Nhatrang	Vietnam
NOU	Noumea	N. Caledonia
PEL	Peldehue	Chile
PMG	Port Moresby	PNG
POO	Poona	India
POP	Popondetta	PNG
PPT	Papeete	Soc. Is.
PVC	Port Vila	N. Hebrides
QUE	Quetta	Pakistan
RAB	Rabaul	PNG
RAR	Rarotonga	Cook I.
RIV	Riverview	NSW
SBA	Scott Base	Antarctica
SDB	Sa Da Bandeira	Angola
SEO	Seoul	Korea
SHI	Shiraz	Iran
SHK	Shiraki	Japan
SHL	Shillong	India
SNG	Songkhla	Thailand
SPA	South Pole	Antarctica
STU	Stuttgart	Germany
TAB	Tabriz	Iran
TAU	Hobart	Tasmania
TBL	Tabele	PNG
TOO	Toolangi	Victoria
TPN	Tapini	PNG
TRN	Trinidad	
TUC	Tucson	USA
WEL	Wellington	NZ
WIL	Wilkes	Antarctica

PLATE I

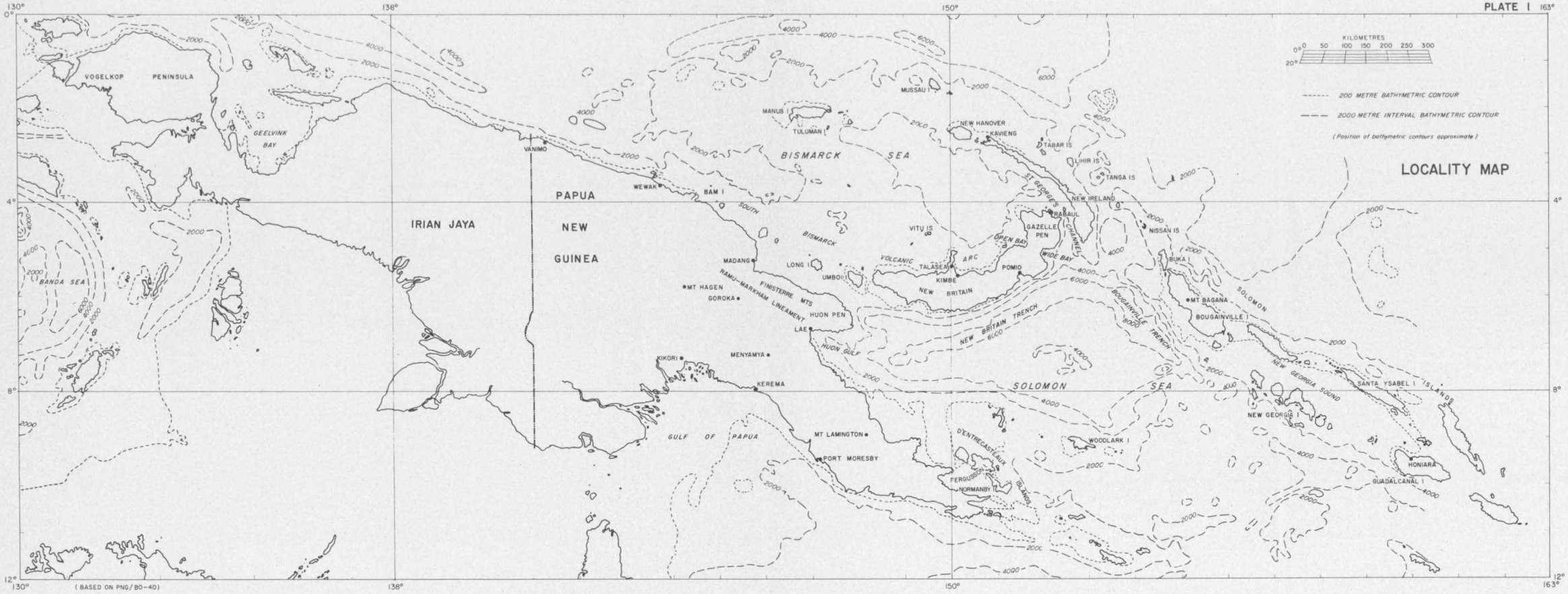

(BASED ON PNG/80-40)

PLACES AND FEATURES MENTIONED IN TEXT

PNG/89-216

PLATE 5

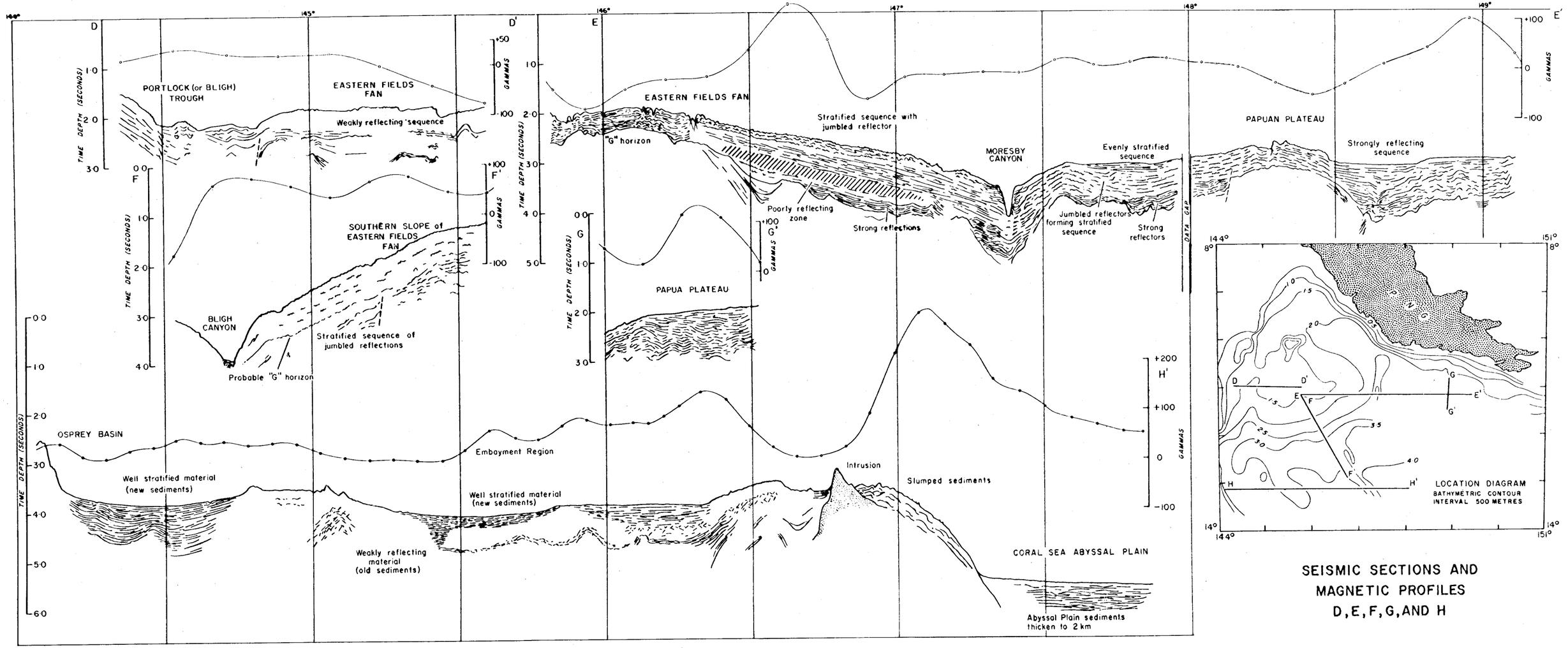

SEISMIC SECTIONS AND MAGNETIC PROFILES D, E, F, G, AND H

PLATE 2

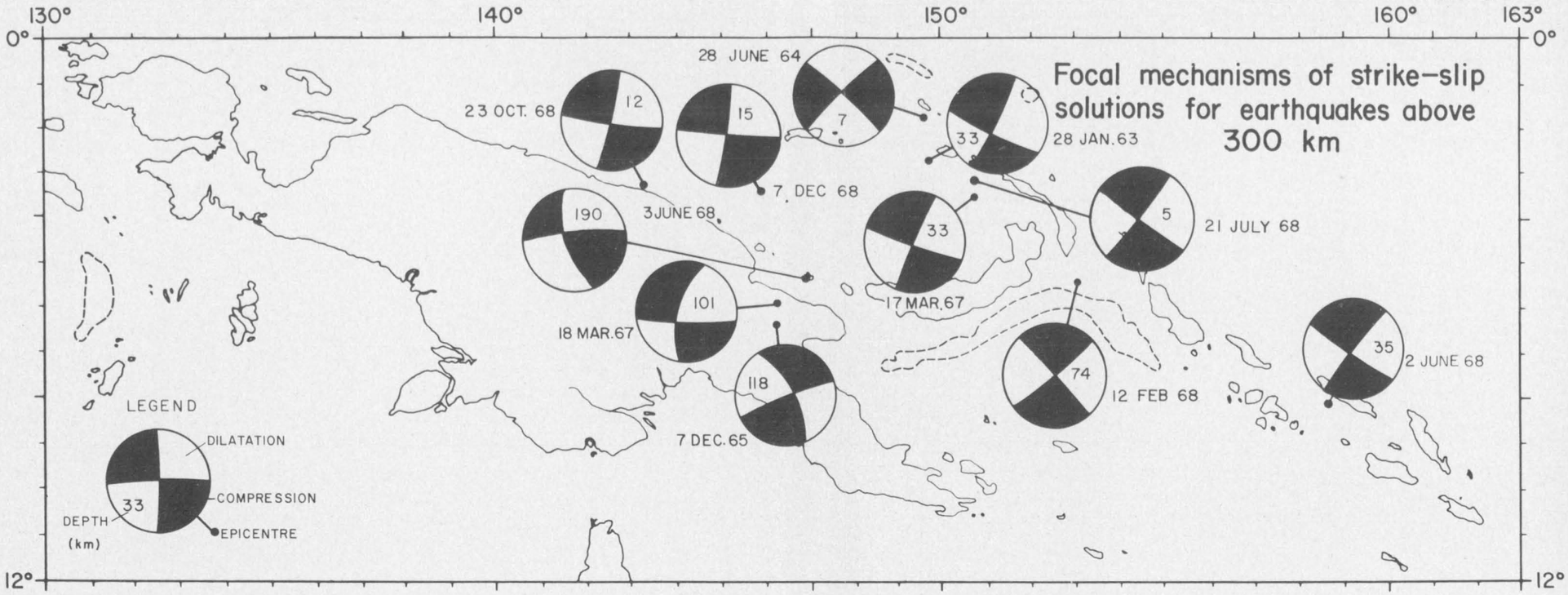

PLATE 3

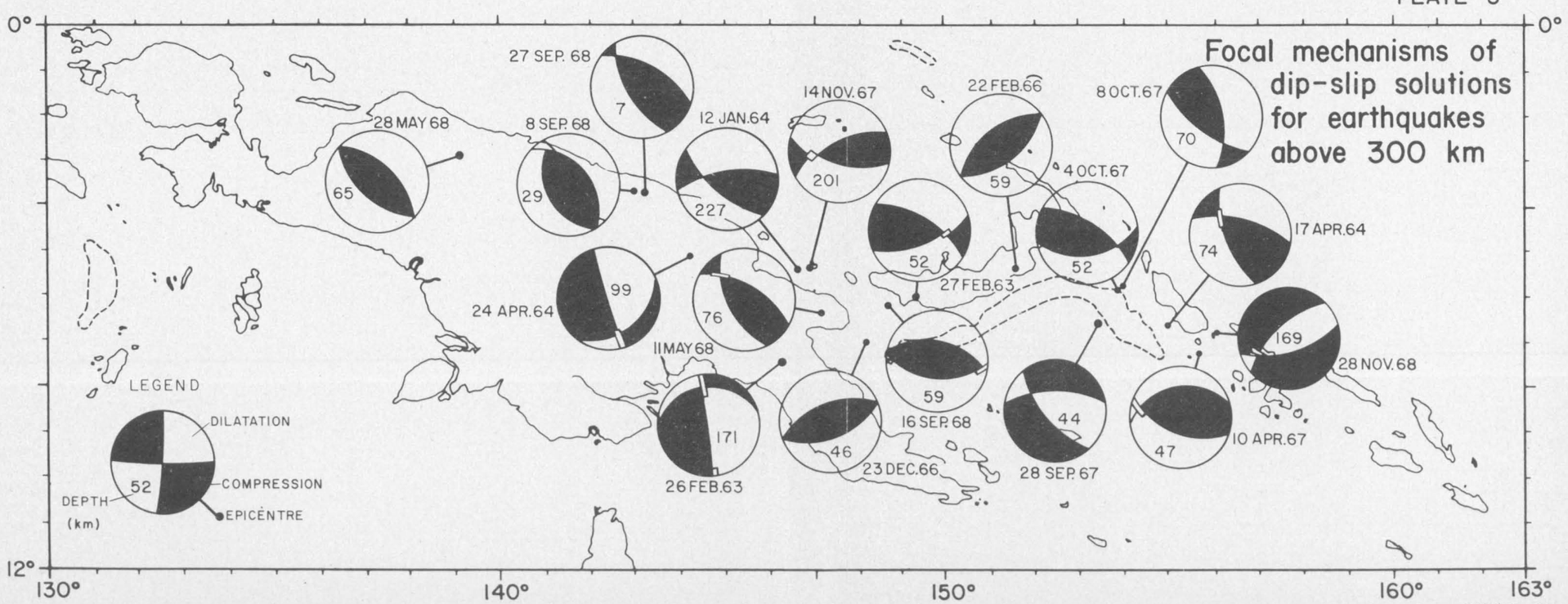

PNG/89-218

130° 140° 150° 160° 163°

0°

12°

Focal mechanisms of solutions for earthquakes below 300 km

24 APR.68

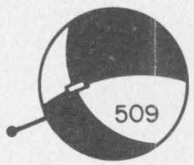

6 JULY 65

13 AUG.64

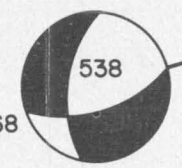

18 AUG.68

LEGEND

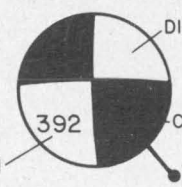

PNG/B9-219